

# A Handbook for Post-Mission Disposal of Satellites Less Than 100 kg



**International Academy of Astronautics**



**Notice:** The cosmic study or position paper that is the subject of this report was approved by the Board of Trustees of the International Academy of Astronautics (IAA). Any opinions, findings, conclusions, or recommendations expressed in this report are those of the authors and do not necessarily reflect the views of the sponsoring or funding organizations. For more information about the International Academy of Astronautics, visit the IAA home page at [www.iaaweb.org](http://www.iaaweb.org).

**Copyright 2019 by the International Academy of Astronautics. All rights reserved.**

The International Academy of Astronautics (IAA), an independent nongovernmental organization recognized by the United Nations, was founded in 1960. The purposes of the IAA are to foster the development of astronautics for peaceful purposes, to recognize individuals who have distinguished themselves in areas related to astronautics, and to provide a program through which the membership can contribute to international endeavours and cooperation in the advancement of aerospace activities.

© International Academy of Astronautics (IAA) May 2019. This publication is protected by copyright. The information it contains cannot be reproduced without written authorization.

Title: A Handbook for Post-Mission Disposal of Satellites Less Than 100 kg

Editors: Darren McKnight and Rei Kawashima

International Academy of Astronautics  
6 rue Galilée, Po Box 1268-16,  
75766 Paris Cedex 16, France  
[www.iaaweb.org](http://www.iaaweb.org)

ISBN/EAN IAA : 978-2-917761-68-7



*Cover Illustration:* credit

# **A Handbook for Post-Mission Disposal of Satellites Less Than 100 kg**

**Editors**

**Darren McKnight**

**Rei Kawashima**



# **A Handbook for Post-Mission Disposal of Satellites Less Than 100 kg**

*Published by*

***International Academy of Astronautics***

*Study Group 4.23*

*May 2019*

*Executed in Coordination with UNISEC-Global*



## TABLE OF CONTENTS

TABLE OF CONTENTS .....	1
LIST OF FIGURES .....	2
LIST OF TABLES .....	6
EXECUTIVE SUMMARY .....	7
List of Contributors .....	8
FOREWORD .....	9
Chapter 1 Overview .....	11
Chapter 2 Debris Mitigation Guidelines and Related Legal Topics .....	17
Chapter 3 Determining the Orbital Lifetime of a Microsatellite .....	29
Chapter 4 Re-entry and Survivability of Microsatellites .....	38
Chapter 5 Using Propulsion and Drag Augmentation to Reduce Orbital Lifetime .....	49
Chapter 6 Using Other Retarding Forces .....	72
Chapter 7 Evaluating Tradeoffs Between PMD Options .....	91
APPENDICES .....	98

## LIST OF FIGURES

Figure 1.1	The cataloged population has grown steadily over time with major fluctuations caused by fragmentation events (additions) and increased solar activity (reductions). Source: NASA .....	11
Figure 1.2	Satellite size families provide a way to differentiate between types of small satellites. ....	13
Figure 1.3	This handbook follows a logical progression through a few simple questions to help guide a designer/operator of microsattellites to understand the issues in order to be compliant with debris mitigation guidelines and aware of related space safety concerns.....	14
Figure 2.1	Debris mitigation is implemented and enforced at the national level by adoption in national legislation of internationally agreed principles, guidelines, norms, and standards. Source: Orbital Debris. C. Bonnal. Belin, 2016.....	20
Figure 2.2	LEO and GEO are protected orbital regions for debris mitigation guidelines. Source: IADC.....	23
Figure 3.1	Atmospheric drag acts first to reduce the apogee of an elliptical orbit. ....	32
Figure 3.2	Atmospheric density in LEO varies exponentially with altitude. [Source: Space Exploration Stack Exchange for US Standard Atmosphere 1976].....	32
Figure 3.3	Coefficient of drag, $C_D$ , varies by altitude in LEO; curve is for a sphere or tumbling flat plate in low solar activity. [4].....	33
Figure 3.4	The solar cycle is not as regular as the name would suggest – it varies in length, shape, and magnitude from cycle to cycle. Source: Australian Government Space Weather Services. ....	34
Figure 3.5	A classic orbital lifetime lookup tool provided by King-Hele [2] for average solar activity and $C_D$ of 2.1. The red and blue horizontal bands show two general families of orbits and satellite configurations that will comply with the 25-year rule. ....	35
Figure 4.1	A microsattellite that has typical mass, construction, and material with a natural re-entry trajectory will pose very little air or ground hazard.....	38
Figure 4.2	The historical re-entry count of tracked orbital objects highlights its dependency on solar activity. (Courtesy of The Aerospace Corporation). ....	39
Figure 4.3	The re-entry process is basically the dismantling of the re-entering object over time; an uncontrolled re-entry would likely have an even longer footprint. (The Aerospace Corporation) .....	41
Figure 4.4	The location of recovered re-entry debris worldwide highlights that recovery requires that a human sees it or found it after the fact. (ESA: <a href="http://www.esa.int/spaceinimages/Images/2017/04/Debris_recoveries">http://www.esa.int/spaceinimages/Images/2017/04/Debris_recoveries</a> , 4 March 2018) .....	41

Figure 4.5	The Tiangong-1 Space Station ground track and atmospheric re-entry area were largely over water; as a result, the “ground” footprint was likely also primarily over the water. (Courtesy of The Aerospace Corporation).....	42
Figure 4.6	This Delta II Second Stage propellant tank survived re-entry. (Photo: NASA, <a href="https://orbitaldebris.jsc.nasa.gov/reentry/">https://orbitaldebris.jsc.nasa.gov/reentry/</a> , 6 March 2018).....	43
Figure 4.7	NASA’s ORSAT Software was used to predict the re-entry breakup of the Upper Atmosphere Research Satellite (UARS) spacecraft identifying elements likely to survive re-entry. (Courtesy of NASA, <a href="https://orbitaldebris.jsc.nasa.gov/reentry/orsat.html">https://orbitaldebris.jsc.nasa.gov/reentry/orsat.html</a> ).....	47
Figure 5.1	The plot of estimated braking $\Delta V$ (m/s) required vs initial orbital altitude highlights the different challenges of orbit circularization to 600 km (i.e., diagonal lines) rather than dropping the perigee to 400 km (i.e., data points in lower right quadrant) to accelerate re-entry.....	52
Figure 5.2	The point at where perigee drop to 400 km is superior to circularizing an orbit to 600 km is about 800 km altitude. ....	54
Figure 5.3	NanoSail-D2 <a href="http://www.nasa.gov/mission_pages/smallsats/11-010.html">http://www.nasa.gov/mission_pages/smallsats/11-010.html</a> .....	55
Figure 5.4	InflateSail comparison of deployed vs. undeployed decay profile. (deployed sail profile from actual TLEs, undeployed decay profile from orbit propagation) [19] .	56
Figure 5.5	Echo II undergoing stress test (image credit NASA) .....	57
Figure 5.6	Global Aerospace GOLD inflatable balloon (Global Aerospace Corporation) .....	57
Figure 5.7	Inflatable Antenna Experiment (image credit NASA).....	57
Figure 5.8	The altitude range from which a satellite can be deorbited when targeting 5, 15, and 25 yr deorbit time, is shown as a function of area-to-mass ratio.....	58
Figure 5.9	Examples of non-catastrophic micrometeoroid impacts accentuates the need to consider the debris environment when considering the use of drag-augmentation devices. The left panel shows a returned solar array from the Hubble telescope. (image credit ESA). The right panel shows an impact on satellite component retrieved during the STS-41C Solar Max repair mission. (image credit NASA) .....	60
Figure 5.10	Various deployment mechanisms with coiled booms are shown to highlight the engineering considerations for using such PMD options. Left: Deployment mechanism of the ESA Gossamer Deorbiter (metal boom version), Middle: DeOrbitSail deployment mechanism (image credit DLR), Right: DLR Boom Deployer that travels along with boom as it extends (image credit DLR).....	62
Figure 5.11	Lunar Flashlight concept design (Complements of NASA) .....	62
Figure 5.12	Lunar Flashlight and NEA Scout sail sub-system (Complements of NASA).....	62
Figure 5.13	Sail deorbit system mass increases linearly as a function of sail area. ....	63
Figure 5.14	Sail deorbit system mass decreases as a percentage of total satellite mass, as sail area increases. ....	63
Figure 5.15	Sail deorbit system stowed volume increases linearly with increasing sail area. ....	64

Figure 5.16	The inflatable sphere stowed volume as a function of projected surface area varies by technology solution.....	64
Figure 5.17	Inflatable sphere system mass increases linearly with increasing projected surface area.....	65
Figure 5.18	Inflatable sphere system mass increases linearly as a percentage of total satellite mass for a CGG inflation system and leads to an unfeasible solution for structures greater than 1 m <sup>2</sup> . Larger inflatable structures will have a mass percentage that decreases as projected area increases.....	65
Figure 5.19	The aerodynamic, solar and gravity gradient torque versus altitude for a 100 kg satellite with 25 m <sup>2</sup> sail is depicted for LEO applications. ....	66
Figure 5.20	The deployment activation state diagram identifies the key operational activities required for fail-safe deployment of a drag sail. ....	67
Figure 5.21	Surrey Space Centre’s InflateSail: carbon-fibre boom tips are suspended from sliding gantry. (Image Credit: Surrey Space Center) .....	68
Figure 6.1	The decomposition of the solar radiation pressure force, FSRP, into the anti-normal, F <sub>n</sub> , and anti-sun, F <sub>s</sub> , parts shows that the more light-absorptive the surface, the larger the anti-sun component of the SRP force.....	73
Figure 6.2	Perturbing forces of atmospheric drag and solar radiation pressure acting on a 5 kg satellite with a 25 m <sup>2</sup> solar sail are depicted. The qualitative behavior observed is AMR-independent and would be the same for any spacecraft with any sail as long as the sail is kept ram-facing or Sun-facing. ....	75
Figure 6.3	The apparent Sun motion in the orbital frame is depicted with the O <sub>z</sub> -axis as the orbit plane normal; the O <sub>x</sub> -axis is along the geocentric radius vector. For a near-circular orbit, the satellite velocity is aligned approximately with the transverse direction (the O <sub>y</sub> -axis). ....	76
Figure 6.4	The orientation of the solar sail normal favorable for SRP-based deorbiting is shown. ....	77
Figure 6.5	SRP force efficiency as a function of the average sail normal cone angle shows the importance of the proper orientation of the sail to achieve desired results.....	78
Figure 6.6	The external torques acting upon a 3 kg satellite with a 25 m <sup>2</sup> solar sail are shown with the assumption of a 13 cm distance between the center of pressure and the center of mass. ....	79
Figure 6.7	The evolution of the orbit altitude for the 900 km dusk-dawn sun-synchronous orbit at mean solar activity is depicted for a 3 kg satellite with a 25 m <sup>2</sup> solar sail.....	80
Figure 6.8	The principle of operation of an electrodynamic tether (EDT) leverages Earth’s magnetic field. ....	83
Figure 6.9	The deorbit profile for 3U and 1U cubesats using nanoTerminator Tape™ (i.e., TT) follow similar general trends. [21].....	85
Figure 6.10	CubeSat nanoTerminator Tape is shown mounted on a 3U cubesat structure (left) [4] and a 1U cubesat (right). [21].....	85

Figure 6.11	Required deorbit time as a function of altitude are shown for a 70 kg satellite at various orbital inclinations with a tape tether of 900 m in length and 25 mm in width, and electron emitter of 0.04 A. ....	86
Figure 6.12	The deorbit time profile for a 70 kg satellite an 800 km SSO with a 900 m tether and electron emitter of 0.04 A. ....	86
Figure 6.13	The deorbit time profile for a 70 kg satellite an 800 km SSO with a 900 m tether, with and without electron emitter of 0.04 A. ....	87
Figure 6.14	The orbital altitude evolution of seven microsattellites after deployment is depicted highlighting the potential effectiveness of an EDT system. [14] .....	88

## LIST OF TABLES

Table 3-1	Using STELA to determine orbital lifetimes for a 1U cubesat with and without a drag-augmentation device hints at the benefit of such a PMD device to limit orbital lifetime. ....	36
Table 4-1	Material properties for several common spacecraft materials shows why beryllium, glass, and titanium are more likely to survive re-entry. [5].....	44
Table 5-1	The $\Delta V$ requirement for circularizing 625 km and 650 km orbits to 600 km versus AMR shows that an object with a smaller AMR requires a greater propulsive maneuver.....	51
Table 5-2	The $\Delta V$ requirement to drop a satellite's perigee to 400 km versus AMR is not highly dependent on AMR. ....	51
Table 5-3	The comparison of $\Delta V$ (m/s) for the two de-orbiting strategies highlights the utility of dropping the perigee to 400 km for the higher altitude LEO orbits.....	53
Table 5-4	The collision scenarios for parts of a drag sail satellite are speculated to highlight potential operational considerations for such PMD options; the actual damage is very difficult to determine without significant testing. ....	59
Table 6-1	The deorbit time for the sun-synchronous orbits of different altitudes are determined assuming a 5 m x 5 m sail at high, mean, or low solar activity (SA). The ranges reflect the variation of the deorbit time across the orbits with different local times of the ascending node. ....	81
Table 6-2	The advantages and disadvantages of EDT provide insights into the utility of an EDT as a viable PMD option. ....	84
Table 7-1	The pros and cons of potential PMD strategies highlight the key issues a microsatellite designer/operator must address. ....	92
Table 7-2	A quantitative comparison of PMD approaches for four representative mission scenarios shows that there is not a single perfect one-size-fits-all PMD solution. ....	95

## EXECUTIVE SUMMARY

Activities in space are accelerating with a rapid increase in the growing number of countries building and operating satellites. The actual number of satellites being deployed to orbit is increasing even more quickly. Many of these are likely to be small satellites possibly deployed in large constellations.

The purpose of this handbook is to provide guidance to the designers, developers, and operators of these micro satellites (microsatellites) and smaller satellites (i.e., less than 100 kg) deployed to low Earth orbit, LEO (i.e., below 2,000 km altitude). Tradeoffs on ways to select and implement post-mission disposal (PMD) solutions for these microsatellites in compliance with international space debris mitigation guidelines and ISO 24113 are provided. This handbook is intended to be informative and not normative; it does not provide sufficient detail to assure compliance to national and international directives which may be applicable. This handbook strives to make the fairly complex and difficult process of selecting an appropriate PMD strategy straightforward. The process summarized in this handbook has a similar objective to both (1) ESA's Debris Risk Assessment and Mitigation Analysis (DRAMA) suite of tools, specifically Orbital SpaceCraft Active Removal (OSCAR) and Survival And Risk Analysis (SARA) and (2) NASA Technical Standard 8719.14A, *Process for Limiting Debris*, and executed via the Debris Assessment Software (DAS).

It must be noted that changes to spacecraft manufacturing, debris mitigation guidelines, the debris environment, etc. may all change the landscape for debris mitigation over time. As a result, it is important to take this handbook as a snapshot in time of useful tools, insights, standards, and procedures; these may change quickly so be diligent in keeping abreast of the most up-to-date advancements in these areas. Other publications are also being created regularly providing support to this mission.

The tradeoff study in the last chapter provides performance results comparing viable PMD options with each other and how well they may comply with existing debris mitigation guidelines and ISO 24113. The potential capability of PMD options assessed have to be considered in tandem with their previous operational usage (i.e., technology readiness level) due to the 90% PMD success rate requirement. Propulsive maneuver is shown to be the only option that works reliably for all LEO orbits but it carries with it a large size, weight, and power (SWAP) burden. However, a propulsion system also provides the proven ability to conduct collision avoidance maneuvers and controlled re-entry.

Drag-augmentation devices are only viable below 800-1,000 km altitude and they impose a low to moderate SWAP penalty. However, as the altitude approaches 1,000 km the size of the drag-augmentation device may pose a significant collision hazard on its own accord. Solar sails provide a slow deorbiting capability above 1,000 km and transition to behave like a drag sail below 800 km, though this has not been proven yet in low Earth orbit (LEO). Electrodynamic tethers (EDT), while not yet demonstrated in orbit, hold promise for deorbiting effectiveness at altitudes as high as 1,000 km.

## List of Contributors

### Editors

Darren McKnight, Centauri Corporation  
Rei Kawashima, UNISEC-Global

### Primary Authors

Darren McKnight, Centauri Corporation	Chapter 1&3
Christophe Bonnal, CNES	Chapter 2
Daniel Oltrogge, AGI	Chapter 2
Martha Mejía-Kaiser, IISL	Chapter 2
Alim Rüstem Aslan, Istanbul Technical University	Chapter 3
David B. Spencer, Penn State University	Chapter 4
Fabio Santoni, Sapienza University of Rome	Chapter 5
Norman Fitz-Coy, University of Florida	Chapter 5
Lourens Visagie, Stellenbosch University	Chapter 5
Alfred Ng, CSA	Chapter 5
Aaron Q. Rogers, SSL	Chapter 5
Satomi Kawamoto, JAXA	Chapter 6
Sergey Trofimov, KIAM RAS	Chapter 6
Juan-Carlos Dolado Perez, CNES	Chapter 7
Marlon Sorge, The Aerospace Corporation	Chapter 7

### Reviewers

Vladimir Agapov, Keldysh Institute of Applied Mathematics RAS  
Alex da Silva Curiel, SSTL  
George A Danos, Cyprus Space Exploration Organisation (CSEO)  
Laurent Francillout, CNES  
Livio Gratton, Colomb Institute  
Akira Kato, JAXA  
Toshiya Hanada, Kyushu University  
Scott Hull, NASA Goddard Space Flight Center  
Mohammed Khalil Ibrahim, Cairo University  
Heiner Klinkrad, TU Braunschweig  
Rene Laufer, Baylor University  
Peter Martinez, Secure World Foundation  
Barnaby Osborne, ESA  
Mikhail Ovchinnikov, Keldysh Institute of Applied Mathematics RAS  
Luca Rossettini, D-Orbit  
Rainer Sandau, IAA  
Hanspeter Schaub, University of Colorado  
Thomas Schildknecht, University of Bern  
Klaus Schilling, Julius-Maximilians-University Wuerzburg  
Craig Underwood, University of Surrey  
Benjamin Bastida Virgili, ESA/ESOC  
Carsten Wiedemann, TU Braunschweig  
Tetsuo Yasaka, iQPS Inc.

## FOREWORD

The Space Age began more than 60 years ago, with small satellites. Sputnik had a mass of 83.4 kg and Explorer 1 with a mass of 13.6 kg. In the years that followed, satellites increased steadily in mass, complexity, capability, and cost. Satellites of several hundred kg to over 1000 kg became common. These factors restricted satellite building to a fairly small number of space agencies and large companies that could afford the development and test facilities to carry out such programmes.

Then, in the early 1980s, developments in electronics, sensors, and computers started to allow the development of smaller and smaller satellites. Initially these so-called *microsatellites* with masses under 100 kg were not able to match the capabilities of their larger cousins, but gradually the capability gap reduced, and by the 1990s, small satellites with mass under 100 kg were accomplishing tasks previously possible only on much larger satellites. With more technical possibilities, lower development costs and shorter development timeframes, the entry barrier to participation in space activities was substantially lowered and many more actors were able to enter the space arena. These included many academic institutions, which started to develop training programmes in satellite engineering.

Satellites continued to reduce in size and mass, eventually dropping under 10 kg and shrinking down in size to dimensions of a few tens of centimetres. These came to be known as *nanosatellites*. Then, in the early 2000's, the cubesat standard was defined by the academic community. Initially, this was meant to facilitate the development of nanosatellites for teaching and research applications. Several small companies started to produce commercial off-the-shelf components in the cubesat form factor to meet the growing demand for such components from the academic and scientific community. With growing interest by more actors, the pace of development (and capabilities) of small satellites grew rapidly. It did not take long for the commercial sector to start taking an interest in nanosatellites and this has fueled the dramatic growth in the number of small satellites launched into space. These nanosatellites are now being launched by the dozens each year for a variety of applications. In the last few years, there have been a number of private sector proposals to build small satellite constellations in low Earth orbit that might see as many as 16,000 new small satellites (less than 500 kg) introduced into Earth orbit during the next 10-15 years.

All of these small satellites hold great promise of bringing the benefits of space activities to many millions of people around the world. At the same time, they are raising concerns about the increasing congestion of the Earth's orbital environment. This environment contains over 23,000 objects larger than 10 cm, the smallest size that can be consistently tracked. Of these 23,000 objects, only about 1,800 are operational satellites; the remainder are defunct satellites, upper stages, and a variety of debris fragments. In addition to the trackable population, there are a much larger number of objects that are too small to track. Objects smaller than 10 cm are not consistently tracked and may number as many as 900,000 objects around 1 cm in size and perhaps as many as 100,000,000 fragments 1 mm and smaller.

This is the congested orbital environment into which satellites are being introduced. Users of the space environment have a responsibility to ensure that their space activities do not worsen the already serious debris situation in space. This includes the developers and operators of small satellites. One of the most significant means to ensure that small satellites do not add to the debris problem is to implement a post-mission disposal (PMD) strategy that reduces the amount of time that a satellite stays in orbit beyond the end of its mission. This is best addressed during the design and development phase of the satellite.

But, given the characteristics of a small satellite, and given its operational orbit, what are the specific measures that a satellite designer should take to reduce the satellite's post-mission orbital lifetime? How does one sift through all the available literature on PMD options to select a particular PMD strategy? Is there a broadly accurate guide or principle, based on experience or practice, that a satellite designer could use to identify potentially useful PMD options or to exclude unfruitful ones? This is exactly what this Handbook provides.

This Handbook on post-mission disposal for small satellites provides practical guidance to those involved in the design, development, authorization, and supervision of small satellite projects on ways and means of ensuring that these satellites do not pose a long-term debris risk in orbit, long after the end of their operational missions.

The Handbook, compiled by 39 leading international experts under the auspices of the IAA Permanent Committee on Space Debris and the IAA Permanent Committee on Small Satellites, contains the latest knowledge on space debris and information on post-mission disposal concepts, distilled to its essentials and collected in a convenient and accessible form for the designers of small satellites.

The Handbook is not meant to be a comprehensive treatment of every aspect of the debris problem, or the theory of astrodynamics in the extended Earth atmosphere in low Earth orbit. Instead, it provides pragmatic guidance on how to work through a design trade space of possible PMD solutions. The Handbook is structured in such a manner that the reader can easily determine an optimal path through the book to access the information most relevant to a given satellite.

I congratulate the Academy and the authors of this very timely book for providing an excellent, highly accessible guide on post-mission disposal for the designers of small satellites and I encourage everyone planning or developing a small satellite mission to read this book.

Peter Martinez  
Executive Director  
Secure World Foundation

# CHAPTER 1 OVERVIEW

## Introduction

The space arena is currently experiencing a period of rapid and dramatic change. In the early decades of the space age this domain was dominated by a few space powers and most space actors were governmental entities that carried out national civil and military space programs. Nowadays, there is a much larger number and diversity of space actors. The global commercial space economy has grown from a fledgling enterprise to now exceeding many civil and military space investments. The number of spacefaring countries exceeds 90 depending how you define a spacefaring country: as of this writing (February 2019) over 90 countries have operated a satellite in space, 92 countries are represented in the United Nations Committee on Peaceful Uses of Outer Space (UN COPUOS), more than 50 countries can manufacture satellites, and citizens from over 40 countries have been in space. This increasing growth in the number of space actors has been facilitated by advances in space technology that have also greatly lowered the barriers to entry for new space actors, especially from the private sector. This, in turn, has accelerated the pace of technological development, further lowering entry barriers for emerging space actors.

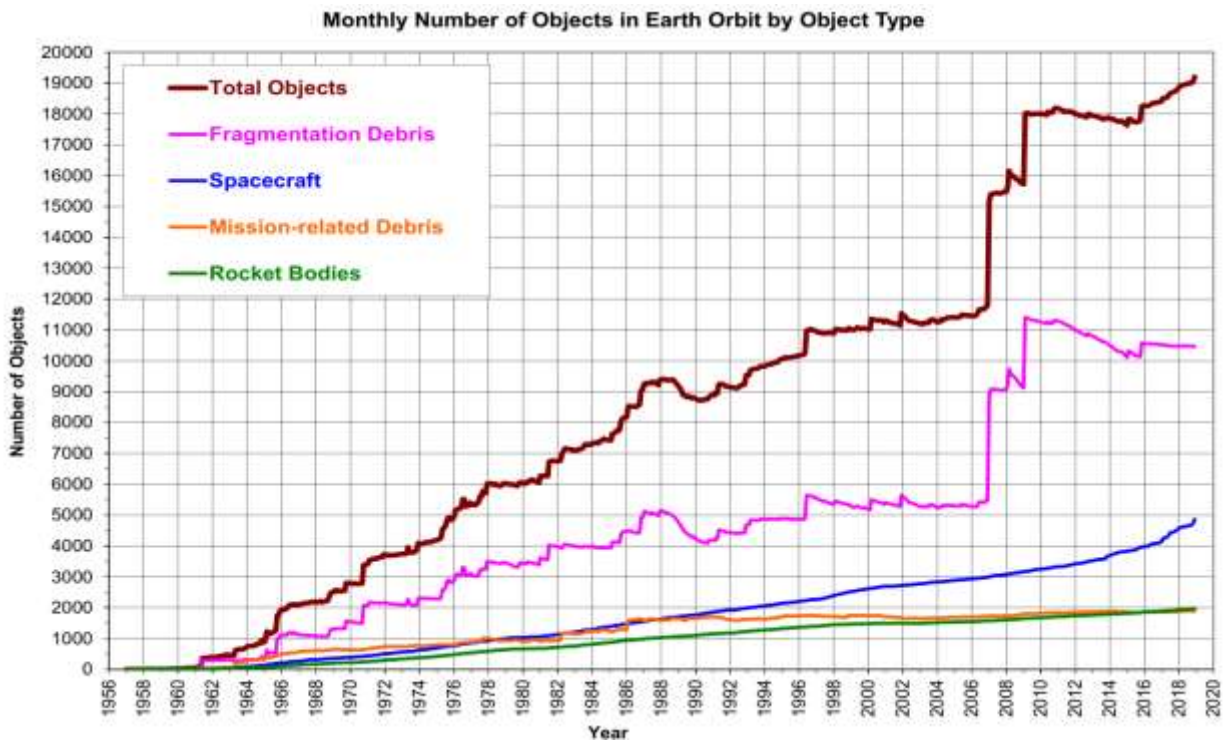


**Figure 1.1** The cataloged population has grown steadily over time with major fluctuations caused by fragmentation events (additions) and increased solar activity (reductions). Source: NASA

All of these activities have produced scientific advancements, enhanced nation-state capacity building, and improved the quality of life for many global citizens. However, these positive outcomes have been at the cost of a growing threat from orbital debris in Earth orbit. More than

19,000 objects are cataloged and tracked in Earth orbit; Figure 1.1 shows this accumulation by object type. Only about 8% of these are operational satellites; the remaining 92% of the trackable population is debris from over 5,000 space launches and nearly 300 satellite fragmentations over the last 60 years. Despite a concerted international effort, the growth of debris being deposited in Earth orbit has not slowed. International debris mitigation guidelines were agreed upon in the mid-1990's that have been followed to varying levels of compliance over the years; these debris mitigation guidelines will be covered in Chapter 2 .

Given the risks posed by space debris to the safety and sustainability of space activities, it is the responsibility of every space operator who wants to leverage the space environment to act prudently so that generations to come have the same luxury of high reliability access to space. One way to do this is to develop and implement reliable post-mission disposal (PMD) strategies compliant with debris mitigation guidelines. In a more pragmatic construct this encourages us all to “leave no footprints” or, possibly, leave where you visit as clean as you found it.

## **Objective**

The purpose of this handbook is to provide guidance to the designers, developers, and operators of micro satellites (microsatellites) and smaller satellites (i.e., less than 100 kg) deployed to low Earth orbit (LEO) below 2,000 km altitude on ways to implement PMD approaches for these microsatellites, to be compliant with the space debris mitigation guidelines. This handbook is intended to be informative and not normative; it does not provide sufficient detail to assure that you are compliant with national and international directives which may be applicable to your mission. However, it does expose the reader to all aspects relevant to the possible requirements for mission authorization. It should be noted that we have limited this handbook to LEO missions where the debris risk is greatest at this time.

This handbook explains the debris mitigation guidelines that may affect satellite design and operations and provides insights to help satellite designers and operators to select the most appropriate PMD strategy for their particular space mission. If you are developing or operating a microsatellite, and you want to find the best PMD strategy for your mission, this handbook is for *you!* It has been compiled by international experts in space debris, small satellites, and PMD; it represents the current state-of-the-art of knowledge in this field.

The handbook provides step-by-step guidance on how to examine your space mission from a PMD perspective. This examination may require no change at all to your space system. Alternatively, you may have to adjust the deployment altitude, modify the configuration of the satellite itself, change planned operational processes, or all of these.

This handbook provides observations regarding potential unintentional consequences of compliance and best practices that transcend simple adherence to guidelines and standards. It

should be noted that these guidelines are equally applicable to launch vehicle operators and their hardware.

This handbook is not meant to be an exhaustive depiction of orbital debris issues. Rather, it is intended to be a concise and pragmatic guide for the responsible conduct of small satellite missions with regard to space and ground safety issues from debris. It has been written to be useful not only for university microsatellite project leaders but also for commercial microsatellite deployers, policy makers, regulators, and insurance personnel.

Figure 1.2 standardizes terminology to be used in this study. It should be noted that whenever the term microsatellite is used it comprises all satellites up to 100 kg in mass. Note also that this handbook is relevant to individual microsatellites. When such satellites are deployed as part of a constellation there may be additional issues that must be addressed as part of a holistic PMD strategy for an operational constellation.

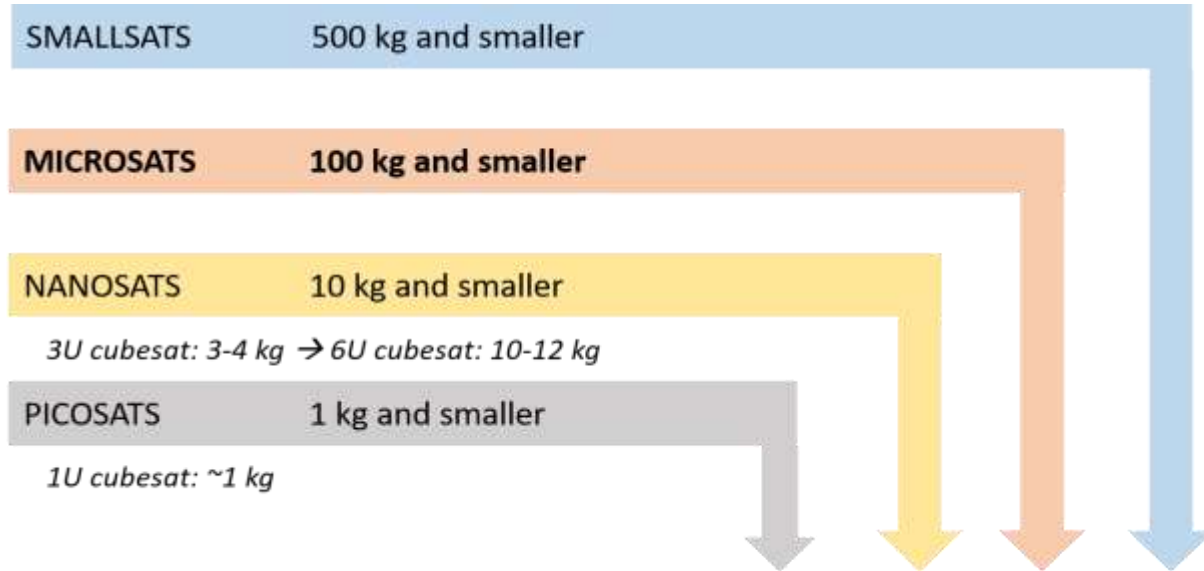


**Figure 1.2** Satellite size families provide a way to differentiate between types of small satellites based on their mass.

This handbook complements other activities related to smallsats by the International Academy of Astronautics that have highlighted the emerging applications for smallsats empowered by new space technologies. Two recent publications of note are:

- The recently released (2017) International Academy of Astronautics (IAA) study titled “Definition and Requirements of Small Satellites Seeking Low-Cost and Fast-Delivery.”<sup>1</sup>
- The newest version of ISO/TS 20991, *Space Systems – Requirements for Small Spacecraft* was released in 2018.<sup>2</sup>

<sup>1</sup> <http://iaaweb.org/iaa/Scientific%20Activity/cost.pdf>

<sup>2</sup> <http://iaaweb.org/iaa/Scientific%20Activity/Study%20Groups/SG%20Commission%204/sg418/sg418finalreport.pdf>

## Organization of Handbook

Figure 1.3 depicts the approach of this handbook and provides a roadmap to guide the reader through the material contained within it.

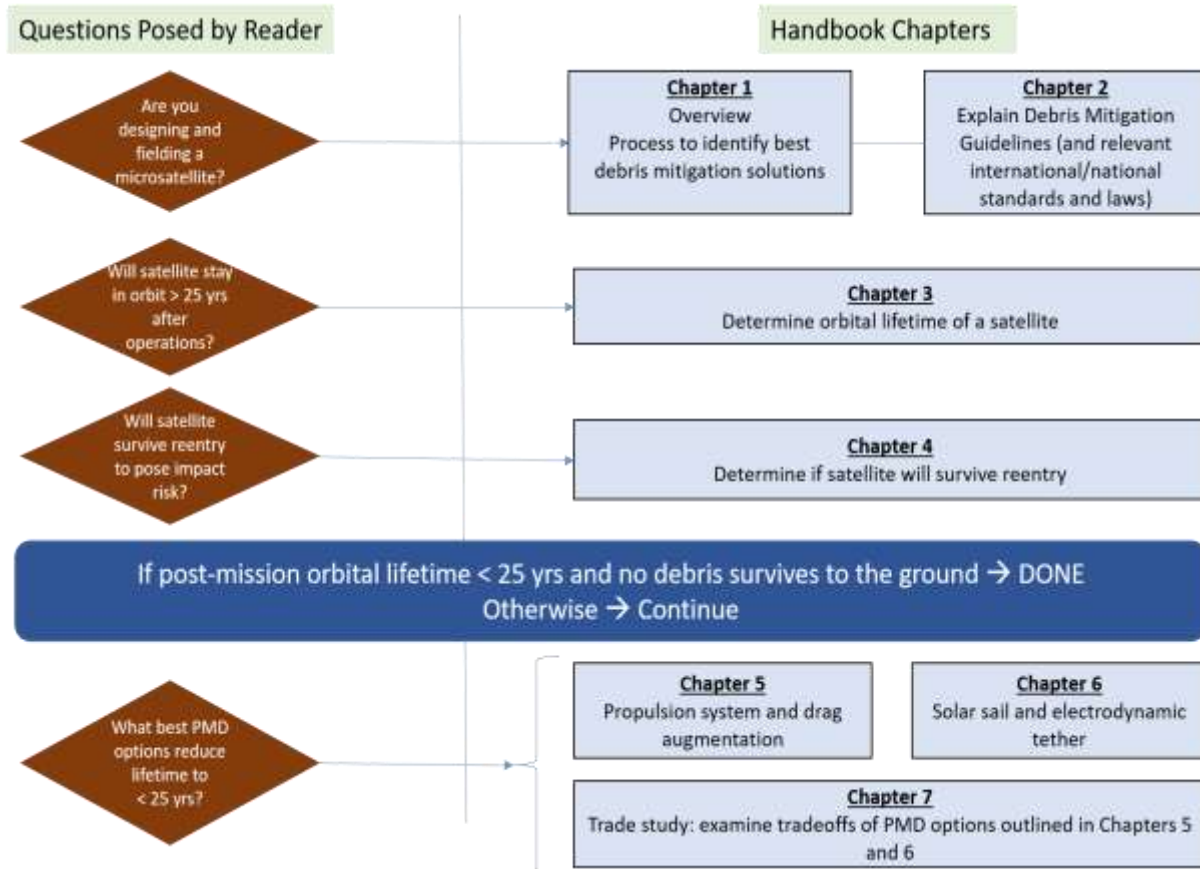


**Figure 1.3** This handbook follows a logical progression through a few simple questions to help guide a designer/operator of microsatellites to understand the issues in order to be compliant with debris mitigation guidelines and aware of related space safety concerns.

Chapter 2 reviews orbital debris mitigation guidelines. This includes the various international forms of these guidelines plus relevant standards, regulations, and laws. At a high level, debris mitigation guidelines call space actors to minimize the generation, the extended presence of debris in orbit, and the hazard of re-entering orbital debris to people and property on the ground.

Chapter 3 explains how to determine the orbital lifetime of a satellite; this is a critical component of the debris mitigation guidelines and minimizes collision risk to others. While a maximum of 25 yr orbital lifetime after mission completion is currently the standard, this chapter will provide sufficient tools to allow you to design a system to re-enter within a much shorter time, if desired. The reader is introduced to both a simplified process of orbital lifetime estimation and tools to determine a satellite's lifetime analytically. The simplified look-up table process helps the reader to better understand the importance of individual physical parameters relevant to orbital lifetime

calculations. However, more accurate lifetime calculations will require more computationally-intensive tools identified in the text.

Chapter 4 examines technical considerations for re-entry survival. For the satellite systems applicable to this handbook (i.e., satellites under 100 kg), it is unlikely that any mass will make it to the ground to pose a hazard to people and property unless very nontraditional materials, or especially robust component designs, are used.

Chapter 5 and Chapter 6 provide the means to determine how to reduce the orbital lifetime of a space system to adhere to debris mitigation guidelines. The effectiveness, operational maturity, and engineering cost (i.e., size, weight, and power) of various PMD options are explained.

Chapter 5 explains how an impulsive force may be used to reduce orbital lifetime. This includes both a propulsive maneuver and the natural force from atmospheric drag via some drag-augmentation device or strategy. The explanation of how an impulsive propulsive maneuver changes a satellite's orbit to reduce its lifetime will be leveraged in describing how drag forces act on a satellite; drag is simply a continuous force from the atmosphere that acts in the opposite direction to the satellite's motion, similar to a propulsive maneuver in the opposite direction of the velocity vector.

Chapter 6 explains how to leverage other retarding forces such as solar radiation pressure via a solar sail or the Lorentz force through an electrodynamic tether. In contrast to drag forces that always act opposite the velocity of the satellite, these retarding forces may be more complicated to model since the direction and magnitude of these forces vary with respect to the spacecraft's orientation and position relative to the Sun and Earth's magnetic field, respectively.

Chapter 7 examines tradeoffs between potential PMD approaches described in Chapter 5 and Chapter 6 to adhere to debris mitigation guidelines. This chapter also highlights other short-term and long-term issues related to specific PMD strategies as a function of effectiveness, operational maturity, and engineering cost (i.e., size, weight, and power).

Each of the chapters begin with a KEY POINTS section providing the highlights of the associated chapter to give the reader a clear indication of the relevancy of that chapter to their situation.

Appendix A contains a list of tools useful for complying with debris mitigation guidelines and related sources for each. Appendix B contains a list of acronyms used in the handbook.

## **Summary**

The intent of this handbook is to make the fairly complex and difficult process of selecting an appropriate PMD strategy as straightforward as possible and to make space safety simple to achieve. This handbook is meant to be informative, not normative. The process summarized in this handbook has a similar objective to both (1) ESA's Debris Risk Assessment and Mitigation

Analysis (DRAMA) suite of tools, specifically Orbital SpaceCraft Active Removal (OSCAR) and Survival And Risk Analysis (SARA) and (2) NASA Technical Standard 8719.14A, *Process for Limiting Debris*, and executed via the Debris Assessment Software (DAS): <https://orbitaldebris.jsc.nasa.gov/mitigation/das.html>.<sup>3</sup>

It must be noted that changes to spacecraft manufacturing, debris mitigation guidelines, the debris environment, etc. may all change the landscape for debris mitigation over time. As a result, it is important to take this handbook as a snapshot in time of useful tools, insights, standards, and procedures; these may change quickly, so the reader is advised to be diligent in keeping abreast of the most up to date advancements in these areas.

---

<sup>3</sup> Appendix A contains a list of tools relevant to debris mitigation compliance.

## CHAPTER 2 DEBRIS MITIGATION GUIDELINES AND RELATED LEGAL TOPICS

---

### KEY POINTS

In general, all the space debris mitigation guidelines and standards, such as the IADC<sup>4</sup> or ISO<sup>5</sup> standard 24113, apply to any spacecraft, whatever its size. These various sets of guidelines have the following general four elements in common:

1. Passivate energetic sources, such as batteries, and vent excess propellant.
2. Eliminate creation of debris; this includes avoiding explosions and collisions.
3. Ensure that all objects left on-orbit are re-entered within 25 years after the end of their operational life (EOL) or moved to an acceptable graveyard orbit.
4. Suggest to limit the re-entry casualty risk to humans to less than  $10^{-4}$  per re-entry event.

This handbook primarily focuses on the third and fourth requirements.

---

### Introduction

Orbital debris was first identified as a concern as early as 15 years after the maiden orbital launch of Sputnik in October 1957. One of the first warnings of a potential collision in Earth orbit was made in 1971 by late Nagatomo and his colleagues. The word “space debris” was not used at that time and collision probability was calculated among the 2,000 objects on-orbit hinting for the first time the possible necessity of Space Traffic Control. [1]

The first analysis of the orbital environment identified micrometeoroid fluxes as the primary risk, but by 1974 there were already concerns about man-made Earth-orbiting objects potentially presenting risks of collision with operational satellites. Several publications from that period [2-4] raised the question of the potential evolution of the space debris population in Earth orbit and identified the risks linked to hypervelocity collisions. Although there were only 3,700 cataloged objects by that time, representing a mass of 900 tons, these pioneers did set in place the first collision models, the initial development of the EVOLVE tool (i.e., long-term debris evolution model), the first debris propagation models, the first orbital spatial density models, and the comparison with the natural micrometeoroid population. However, none of the early studies addressed debris mitigation directly, nor did they make any recommendations in this regard.

---

<sup>4</sup> IADC is Inter-Agency Space Debris Coordination Committee

<sup>5</sup> ISO is International Organization for Standardization

The first publication which presented a long-term assessment of orbital debris growth was the now-famous article by Donald Kessler and Burton Cour-Palais describing the potential self-sustaining sequence of collisions leading to a proliferation of orbital debris and the long-term creation of a debris belt around the Earth. [5] This article not only identified the potential cascading effect but was the first one to give clear recommendations on how to mitigate the number of space debris. “The most effective way would be to keep the number of large objects as small as practical”; “this could be accomplished by retrieving objects in orbit which no longer serve a useful function”; “Every effort should be made to prevent [the production of debris] in space, either by explosion or by collision”. This fundamental publication did describe the key bases of today’s mitigation rules: limit the number of objects in orbit, avoid their explosion, and avoid their collisions. By the time this article was published in 1978, there were 5,200 cataloged objects, with a total mass of 1,400 tons in orbit.

These initial ideas were disseminated globally during the following decade through numerous dedicated conferences. In 1982, Bob Reynolds and colleagues presented the NASA debris evolution model, a fundamental tool for every spacecraft designer. [6] Recommendations were issued for the operations of spacecraft in LEO [7] with a special focus on the future Space Station. [8] It was also at that time that Europe started reacting to the growing orbital debris risk through an ad hoc inter-agency working group leading to the first report presenting general recommendations. [9] By then, 1988, the number of cataloged objects had increased to 6,300, with 1,600 tons in orbit.

The first major synthesis compiled in Europe on the topic was the study “Safe” conducted under the leadership of Walter Flury; it covered various kinds of launcher and spacecraft missions, while providing detailed recommendations for what were to become the “classical” debris mitigation guidelines. [10] This led to the publication in September 1988 of the first standards and requirements for debris mitigation. [11] Unfortunately, these first requirements were too theoretical and impractical to be implemented.

The first standard solely devoted to space debris was published by NASA in 1995, [12] soon followed by the one from the Japanese space agency (JAXA) in 1996, [13] and then by another from the French space agency (CNES) in 1998. [14] In 1995, the catalog contained 9,000 objects representing a total mass of 3,800 tons in orbit. Numerous other “national” standards have been published since, such as the one from the German Space Agency (DLR) [29] and others still under development such as from the Russian Space Agency.

In parallel, at the international level, national space agencies started gathering regularly to exchange research and findings on the space debris situation and to prepare internationally agreed-upon guidelines. The IADC (Inter-Agency Space Debris Coordination Committee [15]) initially met informally in 1987 as a coordination group between NASA and ESA, with the first official meeting of the IADC being held in Moscow in 1993.

The IADC has met 36 times to date (through the end of 2018) and currently includes 12 national space agencies as well as the European Space Agency (ESA). Its flagship production to date is the “IADC Space Debris Mitigation Guidelines”, initially published in 2002 after five years of negotiations among partners; it was revised in 2007 [16] and a new revision is expected in 2019. By the time of the initial publication of the IADC guidelines, there were 11,000 cataloged objects with a total mass of 4,900 tons of man-made debris in orbit.

These guidelines were presented to UN COPUOS and discussed within the members for five years. As a result, UN COPUOS Scientific and Technical Sub-Committee (STSC) issued their own guidelines [17] in February 2007, very similar in principle to the ones from IADC, even though less demanding in some aspects.

In parallel, efforts were also led in Europe to harmonize the various standards among the major space agencies. These efforts led to the EDMS (European space Debris Mitigation Standard), finalized in July 2002 (at the same time as the IADC Guidelines), then to the ECOC (European Code of Conduct for Orbital Debris), approved and signed by the five main European space agencies in July 2004. [18] This text, although limited to Europe, turned out to be of significant importance as it was used as the basis for the ISO 24113 standard.

ISO 24113, [19] first published in 2010 and now planning for third version in September 2019, is the highest level standard at the international level dealing with space debris mitigation. It is complemented by second-tier standards, dealing with dedicated topics such as lifetime evaluation of an orbital object, re-entry risk management, collision avoidance, or requirements devoted more precisely to spacecraft or launchers. At the time this ISO standard was issued in 2010 there were 17,500 cataloged objects with a total mass of 6,000 tons in orbit. The next version of ISO 24113 is due for finalization in 2019.

These ISO standards are important as they represent requirements, which may turn out to be compulsory for designers and operators, when included in contracts. If such internationally-approved requirements, are indeed shared by everyone, it would guarantee that every government, academic, and industrial satellite developer or operator plays by the same rules and acts efficiently to control and reduce the threat posed by space debris.

Several countries and organizations have already adopted ISO 24113 as their baseline, such as European Space Agency (ESA) through an ECSS adoption notice [20] or have national regulation closely derived from it, rendered applicable by law, as is the case of the French Space Operations Act. [21] Figure 2.1 shows the interplay of commercial actors, governments, and intergovernmental organizations in the development and codification of debris mitigation standards, regulations, and principles. While academia is not explicitly included in Figure 2.1, academia serves a valuable global role as a generator of new debris mitigation concepts and as a non-political venue for discussions on the potential evolution of debris mitigation principles, guidelines, norms, and standards.

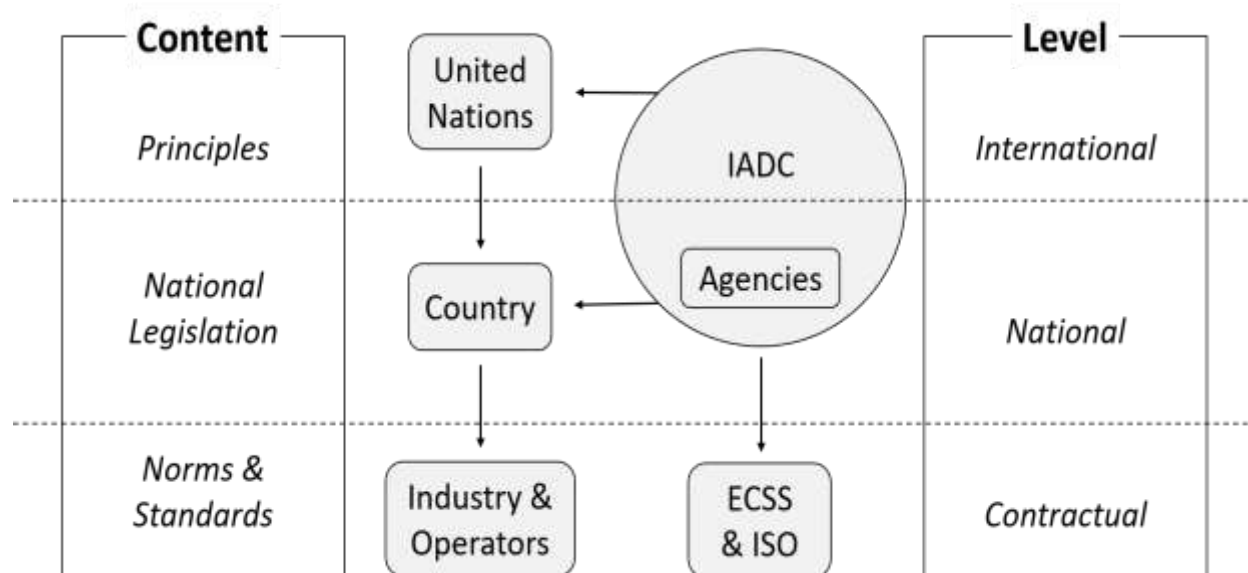


**Figure 2.1** Debris mitigation is implemented and enforced at the national level by adoption in national legislation of internationally agreed principles, guidelines, norms, and standards. Source: Orbital Debris. C. Bonnal. Belin, 2016.

### International and National Legislation

International space law treaties have set a legal basis for space activities. According to Article I (a) of the Liability Convention, [22] any man-made objects in space and their component parts are considered ‘space objects’. This is relevant for satellite components that may survive re-entry and cause damage on the surface of the Earth or to aircraft in flight. Damage is “[...] loss of life, personal injury, or other impairment of health; or loss of or damage to property of States or of persons, natural or juridical, or property of international intergovernmental organizations.” (Liability Convention Art. 1(a)). The State that launches; procures the launch; or provides its territory or facilities for the launch of a satellite bears the absolute liability to compensate other State or international intergovernmental organization in case of damage. The word ‘procure’ can include “[...] placing an order for launch”.<sup>6</sup>

States are responsible for their national space activities relative to other States and international intergovernmental organizations, which includes space activities performed by governmental and non-governmental entities and international intergovernmental organizations of which the State is a member (Article VI, Outer Space Treaty [23]). The operation of a satellite belonging to a governmental institution or to a non-governmental institution (e.g., a private company or university) is attributed to the States where the institution is incorporated or located or from whose territory it is launched.

<sup>6</sup> Smith and Kerrest, “Article I (Definitions) Liability Convention”, in *Cologne Commentary on Space Law 2*, eds. Hobe, Schmidt-Tedd and Schrogl (Cologne: Heymanns, 2013), 114.

Given that States have this responsibility towards other States and international intergovernmental organizations, the introduction of the IADC Space Debris Mitigation Guidelines and following standards of ISO, ECSS, and others, has led a growing number of States to establish national legislation that requires the owner/operator of a satellite to obtain permission (e.g., license, authorization) to launch and operate a satellite. These States set requirements for the design and operation of satellites. Based on this legislation, States may impose specific requirements for the permissions they grant to an owner/operator to launch and operate a given satellite. Below are examples of States that have enacted legislation or/and regulations<sup>7</sup> that entail the application of space debris mitigation measures:

- Austria, Outer Space Act, § 5; [24]
- Belgium, Law of Activities of Launching, Flight Operation or Guidance of Space Objects, Article 8; [25]
- Canada, Licensing of Space Stations, Article 3.3.3; [26]
- Denmark, Outer Space Act, Part 3, Article 6. (1)(4); [27]
- Finland, Act on Space Activities, Section 5(3) and Section 10; [28]
- France, Technical Regulations, Article 34; [21]
- Germany, Administrative Provision on Satellite Systems, Part B, Article 5.7; [29]
- Ukraine, Ordinance on Space Activity, Article 9 [30] and Industrial standard URKT-11.03; [31]
- The United Kingdom, The Outer Space Act, Article 5; [32]
- The United States, Code of Federal Regulations, Title 47, § 25.114 (14); [33] and
- Japan, Act on the Launching and Control of Spacecraft, Article 22 [34].

Designers, developers, and operators of microsatellites are advised to comply with all applicable requirements of the State from whose territory the satellite is launched, or which has jurisdiction over the launching system or platform, and of the State of which they are nationals or where their institution is incorporated. States, which have no specific legislation on space activities and on space debris mitigation measures, may nevertheless impose requirements and restrictions for space activities performed by their nationals based on general domestic legislation, like safety and security rules. Care needs to be taken that some domestic space legislation is compulsory not only for legal persons (e.g., private companies), but also for natural persons with nationality of the State (for instance Denmark, Finland), when they engage in the operation of a space system in another country than that of their nationality.

### **Space Debris Mitigation Guidelines – A synopsis of international best practices**

As was discussed in the previous section, our knowledge of what needs to be done to mitigate orbital debris effectively has been evolving for more than 30 years now. These practices are codified in various principles and guidelines, codes of conduct, national “laws”, “standards”,

---

<sup>7</sup> A list of National Space Legislation can be found at [https://www.esa.int/About\\_Us/ECSL\\_European\\_Centre\\_for\\_Space\\_Law/National\\_Space\\_Legislations#EUROPE](https://www.esa.int/About_Us/ECSL_European_Centre_for_Space_Law/National_Space_Legislations#EUROPE)

“requirements”, and “specifications” which are all coherent thanks to the regular cooperation among orbital debris teams throughout the world.

The guidance contained in these various instruments can be summarized in the following seven points, which, though not corresponding exactly to the formulation found in any specific instrument, represent the essence of international best practice distilled from all of these sources:<sup>8</sup>

1. Spacecraft and launch vehicles shall be designed and operated in such a way that there is no release of orbital debris during their mission. This implies, of course, that it is forbidden to fragment intentionally a spacecraft or a stage in orbit. The various texts include some details on this requirement, mainly in case of a launch where a dedicated structure is left in orbit in addition to the upper stage, or where very small debris (i.e., smaller than 1 mm) are released through the use of solid propulsion or pyrotechnics.
2. The accidental fragmentation of a spacecraft or an upper stage shall be avoided during its mission. The probability of such an event shall be lower than  $10^{-3}$  until the EOL. This directive imposes requirements for both system design and operations.

System design and operational actions shall include systematic passivation of objects left in orbit, i.e., removal of any stored energy such as propellant, pressurant, kinetic energy from fly wheels, electrical energy from batteries, etc. Additionally, it is common sense that the potential for accidental breakup caused by collisions with resident space objects shall be minimized.

Collision avoidance tools and techniques are the subject of detailed discussions at the international level, and it is proposed that a spacecraft that operates in GEO shall have a maneuvering capability enabling collision avoidance and EOL disposal. It is also specified that a spacecraft operating in LEO, when equipped with a propulsion system, shall be able to perform collision avoidance maneuvers.

3. A spacecraft or launch vehicle upper stage operating in the LEO protected region (see Figure 2.2) shall be disposed of in such a way that it leaves this region within 25 years after the EOL, and if it operates above LEO, it does not re-enter within 100 years after the EOL. The LEO protected zone is defined as the shell that extends from the surface of Earth up to an altitude of 2,000 km.

---

<sup>8</sup> For a complete exposition of guidelines, the reader is referred to the text of the IADC Space Debris Mitigation Guidelines [[https://www.iadc-online.org/index.cgi?item=docs\\_pub](https://www.iadc-online.org/index.cgi?item=docs_pub)], the UN COPUOS Space Debris Mitigation Guidelines [[http://www.unoosa.org/oosa/oosadoc/data/documents/2006/aac.105c.11/aac.105c.11.284\\_0.html](http://www.unoosa.org/oosa/oosadoc/data/documents/2006/aac.105c.11/aac.105c.11.284_0.html)], and ISO 24113 [<https://www.iso.org/standard/57239.html>].

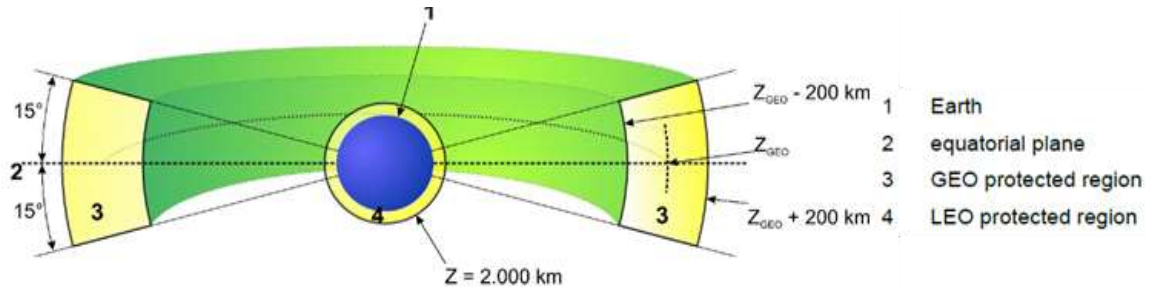


**Figure 2.2** LEO and GEO are protected orbital regions for debris mitigation guidelines. Source: IADC

4. If the casualty risk associated with the atmospheric re-entry of a spacecraft or launch vehicle upper stage operating in LEO is higher than  $10^{-4}$  per mission<sup>9</sup>, then a controlled re-entry shall be considered as baseline approach, aiming at an uninhabited area such as the South Pacific Ocean.<sup>10</sup>
5. If a space object operating in LEO presents a re-entry casualty risk lower than  $10^{-4}$  and cannot be deorbited in a controlled way, then its final orbit, after end-of-life maneuvers, shall be such that it re-enters the atmosphere less than 25 years starting from:
  - a. the orbit injection period, if the object has no capability to perform collision avoidance maneuvers<sup>11</sup> or, otherwise,
  - b. the end of operational life (EOL) epoch.
6. A spacecraft or launch vehicle upper stage operating in the vicinity of GEO shall be transferred to an orbit in such a way that it does not enter the GEO protected region within 100 years of its operational end-of-life. The GEO protected zone is defined as the segment of a spherical shell with an altitude of geostationary altitude  $\pm 200$  km and a latitude sector within  $15^\circ$  South and  $15^\circ$  North (i.e., trapezoidal torus).
7. The probability of successful disposal of a spacecraft shall be at least 90% through EOL; that of a launch vehicle upper stage shall be at least 90%.<sup>12</sup>

### Specifics for Microsatellites

In legal terms, there is no distinction between satellites on basis of size or mass; all have equal status as space objects. The question of applicability of these guidelines for microsatellites was raised officially in the IADC in 2000 through the IADC Action Item AI 18.4 “Small satellites.” Its goal was to assess the impact of small satellites (and small satellite constellations) on the long-

<sup>9</sup> This is the value included in several existing guidelines/regulations and is under discussion at the international level.

<sup>10</sup> Principle of such calculation is described in ISO 27875.

<sup>11</sup> Requirement considered in ISO 24113, not yet approved, under discussion at international level.

<sup>12</sup> In late 2018, discussions have occurred about raising this to 95% and even possibly higher (i.e., 99%) if satellite is part of a constellation.

term evolution of the space environment in LEO, and to discuss disposal practices for small satellites. A study on the evolution of the orbital population was done prior to this action and was reported in AI 15.1 in 2000. Several hypotheses were then made concerning the small satellite launch scenarios, including constellations of 1000 picosatellites (1 kg each) at 600 km or 800 km altitude, and 100 nanosatellites (10 kg each) at the same altitudes.

The study, conducted by nine agencies, was very comprehensive, taking into account expected operational lifetime as a function of the size of the spacecraft. Results showed that the more objects in orbit, the more critical the long-term situation becomes. The conclusion of the study, adopted unanimously among the IADC members, was that any small satellite remains a satellite, and that all the space debris mitigation requirements identified in the various regulatory documents should be applicable, but not more.

An examination of the above existing guidelines leads to the following findings:

The point related to the non-generation of orbital debris (larger than 1 mm) during the launch and operational phases of a mission is fully applicable. General examples are: there should be no retainer bolts released in orbit following deployment of solar arrays or antennas, and there should be no clamp bands left in orbit following launcher separation. In case of an optical payload, the optical cover should not be jettisoned in orbit. If a small satellite is equipped with solid propulsion, it should not leave aluminum slag, or equivalent, in orbit at the end of combustion.

Any satellite should be properly passivated at the end of mission; this impacts the propulsion system, if any, but also the batteries and, more generally, any equipment potentially leading to accidental generation of debris after end-of-life.

Any satellite deployed in the LEO protected region (meaning whose perigee becomes lower than 2000 km altitude within 100 yr following its launch) should re-enter the atmosphere within 25 yr (see IADC guideline 5.3.2 for more details).

If the satellite presents a casualty risk upon re-entry higher than  $10^{-4}$ , then it performs a controlled re-entry (which implies a significant level of propulsion and control until re-entry). Typically, spacecraft with a mass larger than 500 kg present a risk above this threshold, but much smaller spacecraft may turn out to be dangerous if their design includes a lot of refractory material, such as titanium, in compact (i.e., densely-packed hardware) components.

For the common case of a microsatellite presenting no casualty risk, it should re-enter Earth's atmosphere within 25 yr starting from:

- a. The orbit injection period, if the object has no capability to perform collision avoidance maneuvers or
- b. The end of operational life (EOL) epoch.

This means that if a microsatellite has no propulsion on-board with a thrust level and control sufficient to perform collision avoidance maneuvers, then it should be injected into an orbit compliant with the 25-year rule. This is required even if it is equipped with a post-mission disposal device to reduce the orbital lifetime. Such an altitude, depending on the characteristics of the spacecraft, is in the 600-625 km range (the reader is referred to ISO 27852 [36] and Chapter 3 of this handbook).

A satellite which has no on-board propulsion system should not operate in the GEO protected region as it cannot perform collision avoidance maneuvers nor post-mission disposal.

If a microsatellite is equipped with a significant propulsion capability aimed at lowering its final orbit in order to comply with the 25-year rule, then such a maneuver should have a probability of success better than 90%. Otherwise, if there is no propulsion system on-board, the initial injection orbit of the small satellite should naturally comply with the 25-year rule, i.e., be lower than 600-625 km altitude.

## **Summary**

In general, all the space debris mitigation rules, such as ISO 24113, apply to any spacecraft, whatever its mass or size. If a microsatellite is equipped with a propulsion system with thrust and reactivity sufficient to enable collision avoidance maneuvers and end-of-life orbit altitude modification, it should (1) comply with the protected region rules in GEO and (2) comply with the 25-year rule in LEO.

The demonstrated probability of success of such end-of-life maneuvers should be higher than 90%. The satellite should also be passivated at EOL. If its structure is such that it may present a casualty risk on ground, then it should be deorbited in a controlled way to guarantee a safe disposal.

If a microsatellite has no capability to perform collision avoidance maneuvers, even if it is equipped with a PMD device, it should not be operated in GEO. In LEO, it should be injected into an orbit naturally compliant with the 25-year rule if it does not have collision avoidance capability even if it is equipped with a PMD device. The satellite should also be passivated at EOL (i.e., safe batteries, capacitors, etc.) and all efforts must be taken to eliminate creation of all debris greater than 1mm, this includes preventing explosions and avoiding collisions.

## **References**

1. Makoto Nagatomo, Hiroki Matsuo and Kuninori Uesugi, "Some Consideration on Utilization Control of the Near Earth Space in Future", Proc. 9<sup>th</sup> ISTS, Tokyo 1971, pp 257-263
2. Brooks, Gibson, Bess, Predicting probability that Earth-orbiting spacecraft will collide with man-made objects in space, IAF-A74-34, Sept. 1974.
3. Brownlee, Tomandl, Hodge, The flux of meteoroids and orbital debris striking satellites in Low Earth Orbit, Nature 323, pp136-138, 1974.

4. Bess, Mass distribution of orbiting man-made space debris, NASA TN-D8108, Dec. 1975.
5. Kessler, Cour-Palais, Collision frequency of artificial satellites: the creation of a debris belt, *Journal of Geophysical Research*, June 1st, 1978, Vol 83, No A6.
6. Reynolds, Fisher, Edgecombe, A model for the evolution of the on-orbit man-made debris environment, *Proceedings of the NASA/JSC Orbital Debris workshop*, NCP2360, pp102-132, 1982.
7. Kessler, Reynolds, Anz-Meador, Orbital debris environment for spacecraft designed to operate in Low Earth Orbit, NASA TM 100 471, 1988.
8. Kessler, Orbital debris environment for Space Station, JSC 20001, 1984.
9. ESA-SP-1109, The report of the ESA Space Debris Working Group, Nov. 1988.
10. Safe Disposal of orbiting systems and spacecraft including the prevention of debris creation, ESA-contract N°.9024/90/NL/PM(SC).
11. ESA-PSS-01-40 Issue 2, System safety requirements for ESA space systems, Sept. 1988.
12. NSS 1740.14, NASA Safety Standard, Guidelines and assessment procedures for limiting orbital debris, Oct. 1995.
13. NASDA STD-18, Space debris mitigation standard, March 1996; now converted to JMR-003 in JAXA.
14. CNES MPM-51-00-12, Exigences de sécurité, débris orbitaux, April 1999.
15. <https://www.iadc-online.org>
16. IADC-02-01 Revision 1, IADC Space debris mitigation guidelines, May 2002, revised Sept. 2007.
17. A/AC.105/890, Space debris mitigation guidelines of the Scientific and Technical Subcommittee of the Committee on the Peaceful Uses of Outer Space, Feb.2007.
18. European Code of Conduct for Space Debris Mitigation, Issue 1.0, 28 June 2004.
19. ISO 24113, Space systems, Space debris mitigation requirements, July 2010; 2<sup>nd</sup> version in 2011.
20. ECSS-U-AS-10C, Adoption notice of ISO 24113: Space Systems – Space debris mitigation requirements, Feb.2012.
21. France, Arrêté du 11 juillet 2017 modifiant l'arrêté du 31 mars 2011 relatif à la réglementation technique en application du décret n° 2009-643 du 9 juin 2009 relatif aux autorisations délivrées en application de la loi n° 2008-518 du 3 juin 2008 relative aux opérations spatiales [Technical Regulations to the French Space Operations Act, revised in 2017], <https://www.legifrance.gouv.fr/affichTexte.do?cidTexte=JORFTEXT000035367295&categorieLien=id>
22. Convention on International Liability for Damage Caused by Space Objects (Liability Convention), March 29, 1972, entered into force Sep. 1, 1972; 24 UST 2389; TIAS 7762; 961 UNTS 187. <http://www.unoosa.org/oosa/en/ourwork/spacelaw/treaties/introliability-convention.html>. As of Jan. 1, 2018, 95 States have ratified this treaty. Status of International Agreements Relating to Activities in Outer Space as at 1 January 2018. LSC 57th Session. UN Doc. A/AC.105/C.2/2018/CRP.3, Apr. 9, 2018,

[http://www.unoosa.org/res/oosadoc/data/documents/2018/aac\\_105c\\_22018crp/aac\\_105c\\_22018crp\\_3\\_0\\_html/AC105\\_C2\\_2018\\_CRP03E.pdf](http://www.unoosa.org/res/oosadoc/data/documents/2018/aac_105c_22018crp/aac_105c_22018crp_3_0_html/AC105_C2_2018_CRP03E.pdf)

23. Treaty on Principles Governing the Activities of States in the Exploration and Use of Outer Space, Including the Moon and Other Celestial Bodies (Outer Space Treaty), Jan. 27, 1967, entered into force Oct. 10, 1967; 18 UST 2410; TIAS 6347; 610 UNTS 205. <http://www.unoosa.org/oosa/en/ourwork/spacelaw/treaties/introouterspacetreaty.html> . As of Jan. 1, 2018, 107 States have ratified this treaty. Status of International Agreements, [22].
24. Austria, Bundesgesetz über die Genehmigung von Weltraumaktivitäten und die Einrichtung eines Weltraumregisters. (2011). [Federal Law on the Authorization of Space Activities and the Establishment of a Space Register - Austrian Outer Space Act]. Bundesgesetzblatt [Federal Gazette] I Nr. 132/2011, Dec. 27, 2011.
25. Belgium, Law of 17 September 2005 on the Activities of Launching, Flight Operation or Guidance of Space Objects (revised on Dec. 1, 2013), Belgian Official Journal of 15 January 2014, [http://www.belspo.be/belspo/space/doc/beLaw/Loi\\_en.pdf](http://www.belspo.be/belspo/space/doc/beLaw/Loi_en.pdf)
26. Canada, Licensing of Space Stations, Canadian Client Procedures Circular CPC-2-6-02, Issue 4, June 201, <http://www.ic.gc.ca/eic/site/smt-gst.nsf/eng/sf01385.html#s3.3>
27. Denmark, Lov om aktiviteter i det ydre rum [Outer Space Act]. (2016). Act no. 409, May 11, 2016, entered into force on July 1, 2016. Unofficial translation into English: <https://ufm.dk/en/legislation/prevaling-laws-and-regulations/outer-space/outer-space-act.pdf>
28. Finland, Act on Space Activities (2018). Jan, 2018, <https://tem.fi/en/spacelaw>
29. Germany, Verwaltungsvorschrift für die Anmeldung, Koordinierung und Notifizierung von Satellitensystemen im deutschen Namen und für die Übertragung der Orbit- und Frequenznutzungsrechte (VVSatSys) (July 5, 2018). [Administrative provision for the registration, coordination and notification of satellite systems in the German name and for the transfer of rights to use orbits and frequencies (in accordance with the Telecommunications Act § 56, as amended on Oct. 30, 2017)], [https://www.bundesnetzagentur.de/SharedDocs/Downloads/DE/Sachgebiete/Telekommunikation/Unternehmen\\_Institutionen/Frequenzen/SpezielleAnwendungen/Satellitenfunk/VerfahrenAnmeldungSatSysteme\\_pdf.pdf?\\_\\_blob=publicationFile&v=3](https://www.bundesnetzagentur.de/SharedDocs/Downloads/DE/Sachgebiete/Telekommunikation/Unternehmen_Institutionen/Frequenzen/SpezielleAnwendungen/Satellitenfunk/VerfahrenAnmeldungSatSysteme_pdf.pdf?__blob=publicationFile&v=3)
30. Ukraine, Ordinance of The Supreme Soviet of Ukraine On Space Activity (1996). Law of Ukraine of Nov. 15, 1996, last amended 2015.
31. Ukraine, Industrial standard URKT-11.03 “Limitation of the Near-Earth Orbital Debris Making at Operation of Space Technical Equipment”, entered into force in on 19 July 2006. A brief description of this Industrial standard is in Ukraine, Space Debris Mitigation Standards, National Mechanisms, [http://www.unoosa.org/documents/pdf/spacelaw/sd/Ukraine\\_updated20170110.pdf](http://www.unoosa.org/documents/pdf/spacelaw/sd/Ukraine_updated20170110.pdf)
32. The United Kingdom, The Outer Space Act 1986, Chapter 38, (Revised) as of 2018, <https://www.legislation.gov.uk/ukpga/1986/38/contents>
33. The United States, Code of Federal Regulations. US Government Printing Office, cite US 47CFR25, Title 47 – Telecommunication, as of 2018, <http://www.ecfr.gov/cgi-bin/text->

[idx?SID=f0e96087ff1ac46ccb6ac590e4969acb&mc=true&tpl=/ecfrbrowse/Title47/47cfr25\\_main\\_02.tpl](#)

34. Japan, Act on the Launching and Control of Spacecraft, Act. No. 76 of 2016, [https://www8.cao.go.jp/space/english/activity/documents/space\\_activity\\_act.pdf](https://www8.cao.go.jp/space/english/activity/documents/space_activity_act.pdf). Other supporting documents: <https://www8.cao.go.jp/space/english/activity/application.html36>.

## CHAPTER 3 DETERMINING THE ORBITAL LIFETIME OF A MICROSATELLITE

---

### KEY POINTS

The orbital lifetime of a space object entirely operating in low Earth orbit (LEO), without any manual intervention, will be driven by atmospheric drag. For a typical microsatellite, the orbital lifetime will be less than 25 years if it is placed into a circular orbit below approximately 600-625 km. If it is placed into an elliptical LEO orbit, the lifetime will be less than 25 years as long as its perigee is below approximately 400 km.<sup>13</sup>

---

### Introduction

Gravity imposes a force on a satellite that causes it to continue to orbit the Earth. If this were the only force acting on a satellite, it would stay in orbit forever. However, the interaction between Earth's atmosphere and the orbiting satellite decreases the satellite of its energy causing it to eventually reach such a low altitude that it can no longer remain in orbit. At this point, it ceases to pose a risk to other orbital assets, however, this re-entering object still has the potential for posing an impact risk to aircraft in flight [1] and people & property on the Earth. For microsatellites, there is little chance that any material will make it to the ground unless the satellite contains some very unique materials with high melting temperatures (e.g., glass, titanium, etc.) or possibly densely-packed components such as batteries and momentum wheels. This will be covered in detail in Chapter 4 .

The density of the atmosphere decreases exponentially with rising altitude and increases with solar activity and (in a less predictable way) with geomagnetic activity. The solar activity parameter that correlates best with atmospheric density variations is the F10.7 cm solar flux which oscillates on roughly an 11-year cycle. As a result, the effects of drag can vary significantly over time and altitude, making determining an object's orbital lifetime non-trivial.<sup>14</sup>

There are analytic models that can be used to calculate the orbital lifetime from the contraction of the orbit due to atmospheric drag such as Analytical Graphics, Inc. (AGI) Systems Tool Kit (STK). There is also a semi-analytic orbital propagator called STELA<sup>15</sup> (Semi-analytic Tool for End-of-Life Analysis) procured by CNES for lifetime computation in support of the French Space

---

<sup>13</sup> If a satellite is placed into an elliptical orbit with an apogee well outside of LEO and a perigee inside LEO, the lifetime may also be strongly affected by luni-solar perturbations and solar radiation pressure so a detailed, mission-specific analysis would be required.

<sup>14</sup> Note: the *operational lifetime* of a satellite is how long it functions properly in space while *orbital lifetime* is how long it physically remains in orbit.

<sup>15</sup> STELA software is freely downloadable from <https://logiciels.cnes.fr/en/content/stela>.

Operation Act. The OSCAR tool inside DRAMA<sup>16</sup> also provides the capability to compute the orbital lifetime using a semi-analytic propagator, with the possibility to analyze post-mission disposal options and their effect. Any of these tools provide an accurate and responsive way to determine the orbital lifetime of a satellite in orbit. This chapter shows a simplified method to examine orbital lifetimes using a lookup chart taken from a classic book on determining orbital lifetimes to help illustrate the tradeoffs between physical parameters relevant for determining the orbital lifetime of a satellite. [2] However, results from STELA are provided for quantitative comparisons and it is suggested that some sort of high-fidelity orbital lifetime tool such as STELA be used to calculate the orbital lifetime for your respective microsatellite.

### Factors in Determining Orbital Lifetime

The deceleration exerted by atmospheric drag on a satellite is given by:

$$a = \left(\frac{1}{2}\right) C_D \left(\frac{A}{M}\right) \rho V^2 \quad \text{Equation 1}$$

where  $C_D$  = coefficient of drag, no units

$A$  = projected satellite area (normal to velocity vector),  $m^2$

$M$  = mass of satellite, kg

$\frac{A}{M}$  = area to mass ratio, AMR,  $m^2/kg$

$\rho$  = atmospheric density,  $kg/m^3$

$V$  = velocity through the ambient atmosphere  $\approx$  orbital velocity, m/s

Orbital velocity (approximately 7.6 km/s) varies only slightly in low-LEO<sup>17</sup> where drag affects orbital lifetimes measurably. Conversely, the coefficient of drag varies between 2 to 3 as a function of object shape and altitude. [3] As a result, the four primary variables that determine the orbital lifetime of a satellite are (1) area-to-mass ratio, (2) altitude, (3) coefficient of drag, and (4) solar activity. We will look at each term individually before examining how to use them for determining orbital lifetime.

*Area-to-Mass ratio:* The area-to-mass ratio (AMR) can be calculated by dividing the area that the satellite presents in its direction of motion by the mass of the satellite. The larger the AMR, the more atmospheric drag will affect the orbit. So, simply speaking, a satellite with a larger AMR will be removed more quickly from orbit than one with a smaller AMR value at the same altitude

<sup>16</sup> DRAMA software is freely downloadable from <https://sdup.esoc.esa.int>

<sup>17</sup> Low-LEO in this handbook is considered as orbital altitudes below 1,000 km.

and same time. Later in this handbook, we will examine how increasing AMR can be used to reduce orbital lifetime.

Interestingly, an AMR value between 0.003-0.03 m<sup>2</sup>/kg (with the typical value of approximately 0.01 m<sup>2</sup>/kg) covers most spacecraft from small 1U cubesats to large commercial communication satellites deployed in GEO. This commonality is due to the physical limitations of how much circuitry can be packed into a payload bus. It is fairly simple to calculate the AMR of a specific satellite, but do not be surprised if it is not in this general range.

If you would like to be conservative, you can use the smallest possible cross-section as the area term. This will produce the largest possible orbital lifetime so if you can meet the 25-year rule with that minimum value it provides you some extra confidence that you will be compliant. However, as you will soon find out, there are other factors in the calculation of the orbital lifetime of a satellite that may have even a greater influence on the final value for orbital lifetime.

A 1U cubesat has a minimum cross-sectional area of 0.01 m<sup>2</sup> since one face of the bus is 10 cm × 10 cm = 0.1 m × 0.1 m = 0.01 m<sup>2</sup>. The actual average cross-sectional area for a tumbling 1U cubesat is 0.015 m<sup>2</sup>. The mass of a typical 1U cubesat is about 1 kg so the AMR is easily determined by 0.01 m<sup>2</sup> ÷ 1 kg = 0.01 m<sup>2</sup>/kg (or 0.015 m<sup>2</sup> ÷ 1 kg = 0.015 m<sup>2</sup>/kg for a tumbling 1U cubesat). Some 1U cubesats can be as heavy as 1.5 kg which would produce an AMR of 0.007 m<sup>2</sup>/kg or 0.01 m<sup>2</sup>/kg, respectively.

A 3U cubesat has a minimum cross-sectional area of 0.01 m<sup>2</sup> and a mean cross-sectional area of 0.03 m<sup>2</sup> (without any deployable appendages). As a result, for the roughly 3-6 kg 3U spacecraft, the AMR ranges from approximately 0.002-0.01 m<sup>2</sup>/kg. If the 3U cubesat has a fixed orientation so that the area exposed to the atmosphere is constantly 0.03 m<sup>2</sup> (i.e., travels with broadside in the direction of the satellite's motion) and it has a mass of 6kg then its AMR is 0.005 m<sup>2</sup>/kg.

*Altitude:* Generally speaking, a satellite's orbit is elliptical: the altitude above the Earth is not constant and the extremes in altitude of a satellite are provided by two parameters, apogee and perigee.<sup>18</sup> Apogee is the highest altitude that the satellite reaches above Earth's surface during an orbit while perigee is the lowest altitude. If a satellite is in a circular orbit, apogee and perigee are identical and the satellite remains at same altitude throughout its orbit. It should be noted that if a satellite is in an elliptical orbit (i.e., not a circular orbit), drag will first circularize the orbit. That is to say, it will act on the satellite more at the lower altitudes of the orbit; the drag that acts primarily at and around perigee will first largely produce a lowering of the apogee, as shown in Figure 3.1.

---

<sup>18</sup> Alternatively, the two parameters of eccentricity and semi-major axis may be used. Eccentricity, *e*, is the "ellipticity" of the orbit shape. For example, *e* = 0 is a circular orbit and 0 < *e* < 1 for an elliptical orbit. The semi-major axis, *a*, is roughly the average distance between the center of the Earth and the altitude of the orbiting object. For example, a satellite in an 800 km circular altitude has a semi-major axis of 7,178km since the radius of the Earth is 6,378km.

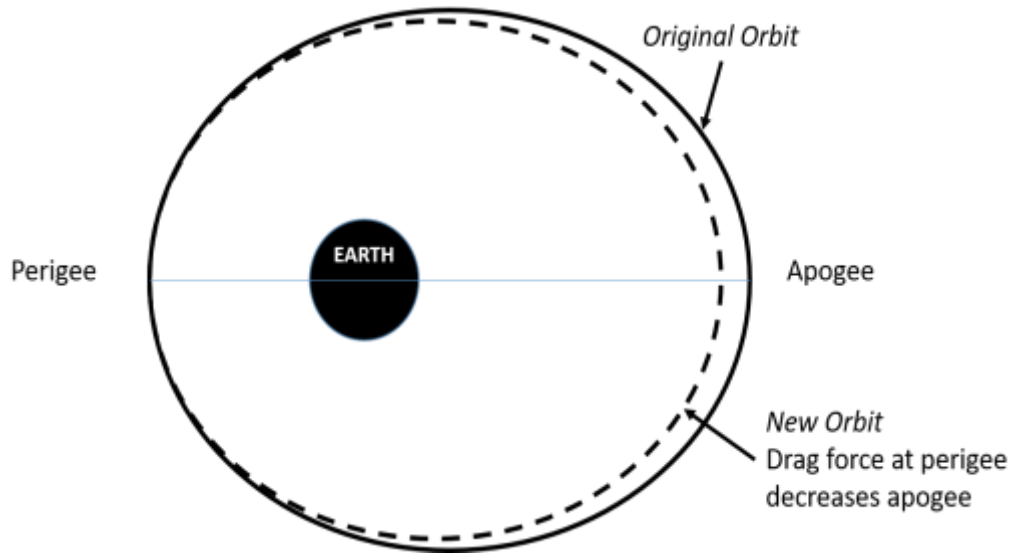


**Figure 3.1** Atmospheric drag acts first to reduce the apogee of an elliptical orbit.

The reason that altitude is so important is that atmospheric density decreases exponentially with increasing altitude, as shown in Figure 3.2.

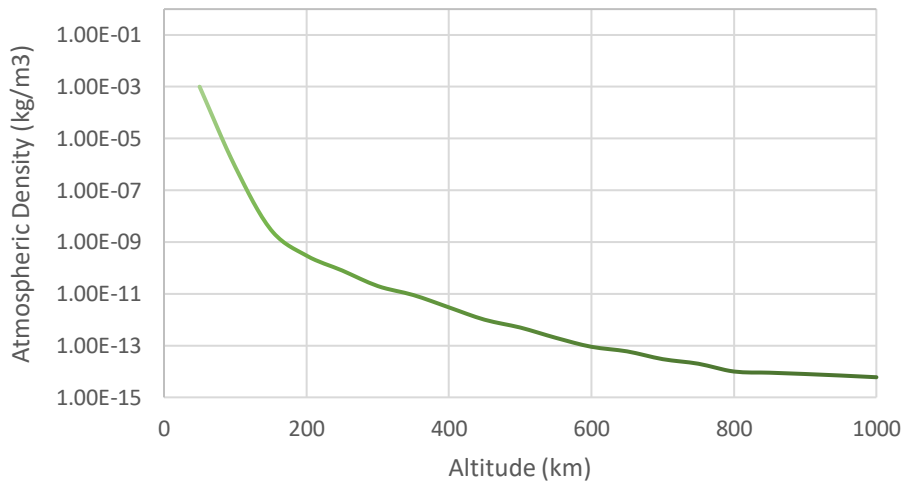


**Figure 3.2** Atmospheric density in LEO varies exponentially with altitude. [Source: Space Exploration Stack Exchange for US Standard Atmosphere 1976]

The atmospheric density may drop by a factor of 100 as altitude increases from 200 km to 400 km. However, going from 600 km to 800 km altitude (i.e., another 200 km increase in altitude), there may only be a factor of 10 reduction in atmospheric density. Above 1,000 km, drag has almost a negligible effect except for objects with very large AMR values; if needed to consider drag at these altitudes, it is advisable to use an analytical model such as STELA.

Coefficient of Drag ( $C_D$ ): The coefficient of drag may vary between roughly 2 to 3 in LEO depending on the altitude, solar activity, and shape of the object. For objects closer to their EOL (i.e., at 200-400 km)  $C_D$  is fairly consistent at 2.0-2.2 (i.e., average of 2.1). However, as altitude rises to near 1400 km the  $C_D$  rises to values approaching approximately 3. Figure 3.3, provided as part of the STELA application, depicts the average  $C_D$  for LEO assuming a general sphere or tumbling plate.

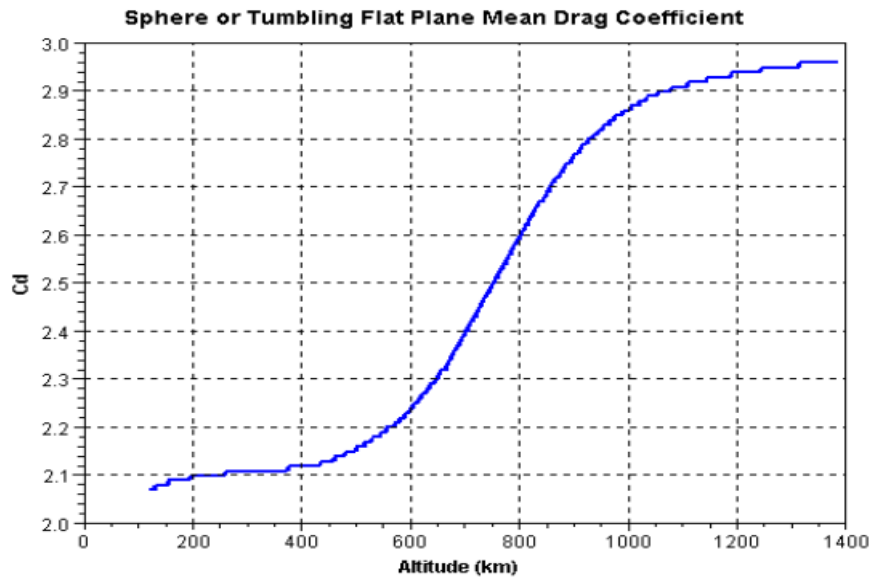


**Figure 3.3** Coefficient of drag,  $C_D$ , varies by altitude in LEO; curve is for a sphere or tumbling flat plate in low solar activity. [4]

Solar Activity: The calculation of a satellite’s orbital lifetime is complicated by continual variations in solar activity that lead to changes in atmospheric density in LEO. Radio emissions from the Sun with wavelength of 10.7 cm have been found to correlate most closely with changes in atmospheric density; this is called the F10.7 cm solar flux.

The solar cycle is neither exactly 11 yr nor does it follow exactly the same pattern of activity during each cycle. Figure 3.4 shows the sunspot number (which correlates directly to the F10.7 cm solar flux<sup>19</sup>) over several centuries highlighting the variability over time. Clearly, there are significant variations over time in both shape and amplitude (i.e., the maximum level and minimum level). Notice how the solar maximum in 2014/2015 (the latest solar maximum on plot) was significantly lower than the previous solar maximum in 2002/2003. Such protracted lower solar activity levels will cause orbital lifetimes to be systematically under-estimated.

The uncertainty in solar activity will contribute significantly to possible mismatches between predicted and actual orbital lifetimes. Atmospheric drag effects can easily vary by factors of 2-4 between high and low solar activity in comparison to the average values shown in Figure 3.4. In

<sup>19</sup>  $F_{10.7} \approx 0.9 \text{ sunspot number} + 59.6$

other words, during periods of high solar activity the drag effects (for the same object for same altitude) can be 2-4 times larger than average; the reverse is true during periods of low solar activity. The OSCAR tool implements different methods providing a forecast of solar and geomagnetic activity as recommended by recent standards. For estimation of orbital lifetime, five different methods may be used to generate future solar and geomagnetic activity data which serves as input for the orbit propagation. The methods are based on recommendations by ISO, ECSS as well as a method which has been implemented within the French Space Operations Act.

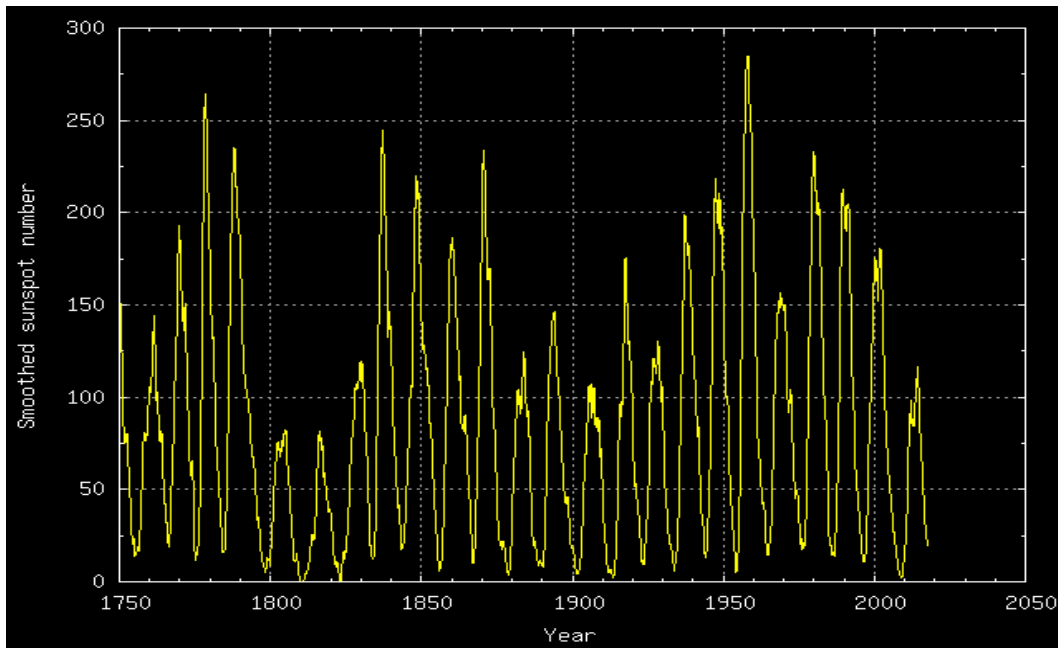


**Figure 3.4** The solar cycle is not as regular as the name would suggest – it varies in length, shape, and magnitude from cycle to cycle. Source: Australian Government Space Weather Services.

### King-Hele Orbital Lifetime Lookup Chart

The benefit of examining the empirical lookup chart provided by King-Hele in his book on determining the orbital lifetime of satellites is that it is simple and helps the reader to see the interdependency of terms contained in the deceleration of a satellite from atmospheric drag (i.e., Equation 1).

The drawback of this approach is that it is not as accurate as numerical models that use real-time solar activity reporting, altitude-dependent  $C_D$ , and a time-varying area exposed to the atmosphere. Figure 3.5 is the lookup chart provided by King-Hele in his classic book, *Satellite Orbits in An Atmosphere Theory and Applications*, for average solar activity and  $C_D$  of 2.1. However, as noted earlier, the changing amplitudes over the centuries makes determining an “average” solar cycle very difficult.

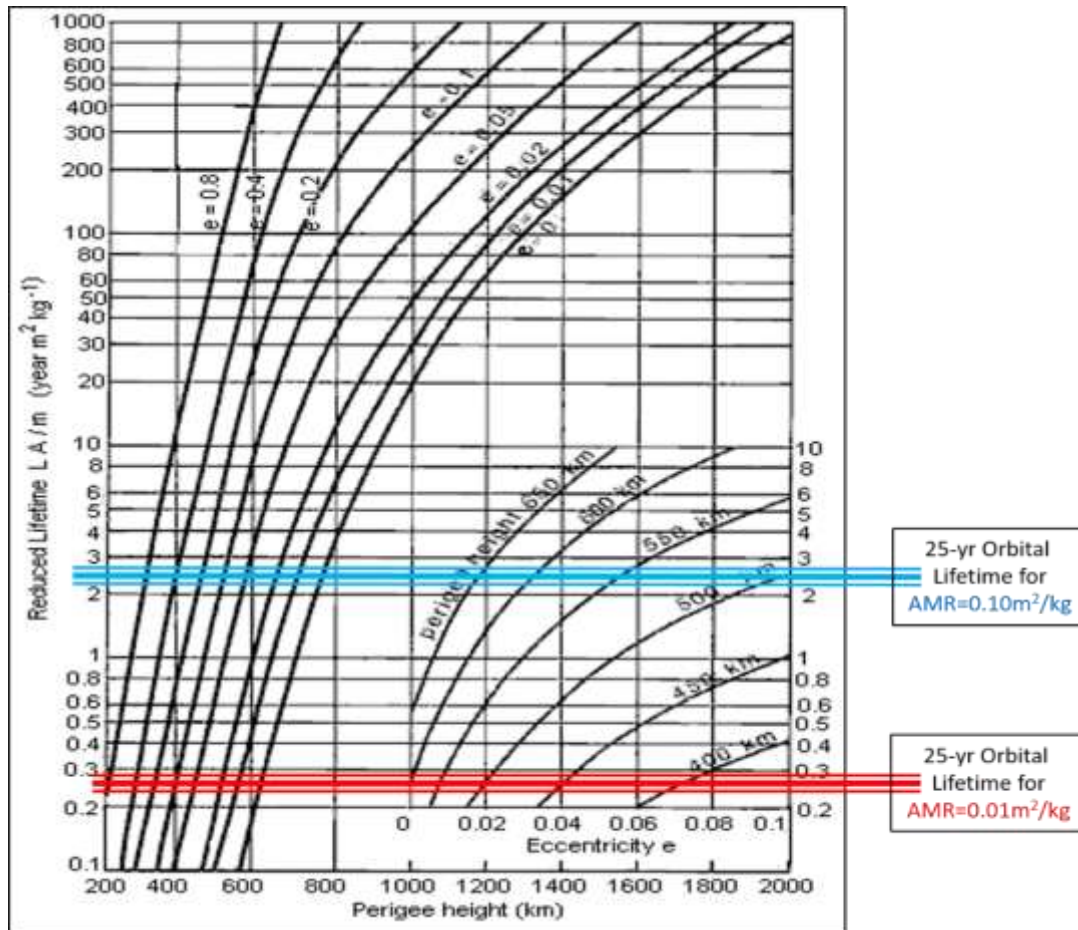


**Figure 3.5** A classic orbital lifetime lookup tool provided by King-Hele [2] for average solar activity and  $C_D$  of 2.1. The red and blue horizontal bands show two general families of orbits and satellite configurations that will comply with the 25-year rule.

The basic chart is annotated with lines for a 25 yr orbital lifetime using a nominal AMR of  $0.01 \text{ m}^2/\text{kg}$ . This thick red line shows that as long as a LEO microsatellite has a perigee below 400 km or has a circular orbit with an altitude of below around 600-625 km, the orbital lifetime will not exceed 25 yr. Similarly, if the AMR is increased by a factor of ten (i.e.,  $\text{AMR} = 0.1 \text{ m}^2/\text{kg}$ ), as it might be altered with a drag-augmentation device, to produce a 25 yr lifetime is provided when the perigee is dropped to 500 km or the circular orbit is no higher than 800 km.

### STELA Orbital Lifetime Calculations

STELA is the Semi-analytic Tool for End-of-life Analysis that has been procured by *CNES* (The French Space Agency) to support the *French Space Operations Act*. STELA is available for download from <https://logiciels.cnes.fr/en/content/stela>. Table 3-1 provides outputs for several microsatellite missions assumed to start in 2018 (for solar activity values) using STELA highlighting the importance of AMR and altitude on orbital lifetime.

**Table 3-1** Using STELA to determine orbital lifetimes for a 1U cubesat with and without a drag-augmentation device hints at the benefit of such a PMD device to limit orbital lifetime.

Scenario	Parameters	STELA Output
<i>1U in 800 km circular orbit</i>	Assume 1 kg tumbling 1U cubesat (AMR = 0.015 m <sup>2</sup> /kg) with an inclination of 90°	92 yr
<i>1U in 600 km x 800 km orbit</i>		24 yr
<i>1U in 400 km x 1000 km orbit</i>		5 yr
<i>1U in 600 km circular orbit</i>		8 yr
<i>1U in 800 km circular orbit</i>	Assume 1 m <sup>2</sup> drag-augmentation device and 2 kg microsatellite (AMR = 0.5 m <sup>2</sup> /kg) with an inclination of 90°	2 yr
<i>1U in 600 km x 800 km orbit</i>		7 mo
<i>1U in 400 km x 1000 km orbit</i>		50 dy
<i>1U in 600 km circular orbit</i>		70 dy

The examination of the key parameters that affect orbital lifetime identifies the engineering terms available to manage orbital lifetime: altitude and cross-sectional area (which may also vary over time). However, the derived term of coefficient of drag (i.e., based largely on the altitude and shape of a space object) and the dynamic solar environment contribute significantly to the final orbital lifetime and uncertainty in these calculations.

### Summary

This chapter has identified STELA as a viable means to determine the orbital lifetime of a space system. Alternatively, ISO 27852 (Space Systems - Estimate of Orbit Lifetime)<sup>20</sup> or other tools like OSCAR or STK can be used to calculate orbital lifetime. However, it is important to remember that the variability of actual solar activity still persists and contributes to the uncertainty in any long-term orbital lifetime calculation, no matter which tool is used. In addition, elliptical orbits with apogees above LEO will definitely require analytic means to estimate orbital lifetimes as solar-lunar perturbations become relevant and significant.

Figure 3.5 provides the high-level insights from this chapter; one can reduce the orbital lifetime of a satellite by reducing the altitude of the satellite's orbit and/or increasing the satellite's area

<sup>20</sup> <https://www.iso.org/standard/68572.html>

exposed in the velocity direction of the microsatellite (Chapter 5 ) and/or introducing a force from other sources such as solar radiation pressure or the Lorentz Force (Chapter 6 ).

## References

1. Matteo Emanuelli and Tobias Lips, "Risk to Aircraft from Space Vehicles Debris," UN COPUOS Scientific and Technical Subcommittee: 2015 Fifty-second session 6 February 2015.
2. Desmond King-Hele, *Satellite Orbits in an Atmosphere - Theory and Applications*, Blackie [Glasgow, 1987].
3. G.E. Cook, "Satellite Drag Coefficients," *Planet. Space Sci.* 13. 929 (1965); FA Herrero, "The Drag Coefficient of Cylindrical Spacecraft in Orbit at Altitudes Greater Than 150 km: NASA, *Technical Memorandum* 85043 (Goddard Space Flight Center. Greenbelt, MD. 1983).
4. STELA Technical Note on Calculating the Coefficient of Drag, March 2011, <https://logiciels.cnes.fr/sites/default/files/Stela-User-Manual.pdf>.

## CHAPTER 4 RE-ENTRY AND SURVIVABILITY OF MICROSATELLITES

---

### KEY POINTS

This chapter demonstrates how to determine whether a satellite is likely to survive re-entry and pose an impact risk to aircraft in flight or people and property on the ground.

There are four primary characteristics that determine whether a given satellite will survive re-entry, as shown in Figure 4.1. Microsatellites will pose little air or ground impact risks as long as they comply with the following three characteristics:

- Material: aluminum and circuit boards
- Mass: under 100 kg
- Construction: no hardened or especially densely-packed components

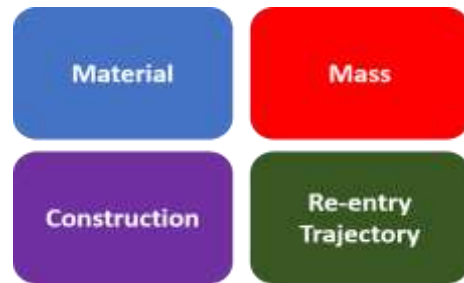


**Figure 4.1** A microsatellite that has typical mass, construction, and material with a natural re-entry trajectory will pose very little air or ground hazard.

The probability of demise of the hardware also depends on the re-entry trajectory.

The use of materials with high melting points (e.g., steel, titanium, glass, beryllium, etc.) and very densely-constructed devices should be avoided as much as possible. If the use of such materials and components cannot be avoided, an analysis tool such as ORSAT, SCARAB, SARA, or DEBRISK, should be used to evaluate the probability that objects may survive re-entry to cause damage to property and/or people.

---

### Introduction

Small satellites are generally fragile objects. Yet, when their orbits decay and the satellite re-enters the atmosphere, there remains a question as to whether parts of the satellite will survive to the ground, and if so, what kind of risk might that hardware pose to population and their property.

Two types of re-entries can occur: controlled and uncontrolled. A controlled re-entry is generally a more complex process and is reserved for missions such as human spacecraft and very large spacecraft with both robust attitude control and propulsion systems. Most re-entry events are uncontrolled re-entries of spacecraft, rocket bodies, and fragmentation debris. Some of these objects can pose a risk of injury to people on the ground or aircraft in flight due to the unpredictability of their trajectories and exactly where and when they will re-enter and, should parts survive re-entry, where they will land. Since a controlled re-entry is much more difficult and

expensive to execute than an uncontrolled re-entry, this chapter will focus on the technical issues surrounding uncontrolled re-entry.

The space object population is made up of operational payloads, defunct payloads, rocket bodies, crewed platforms, mission-related objects, and fragmentation debris. Orbiting objects below 800-1,000 km in altitude have a finite lifetime in orbit due to the interaction with Earth's atmosphere. Atmospheric drag, even with an extremely small atmospheric density, will slowly cause orbiting objects to move to lower orbits. As an object's orbit gets lower and lower, the increasing air density acts upon it until it can no longer maintain its orbit and it follows a ballistic re-entry trajectory.

Figure 4.2 shows the historical trend of tracked re-entering objects. It is easily seen that most of the re-entering objects are (fragmentation and mission-related) debris.

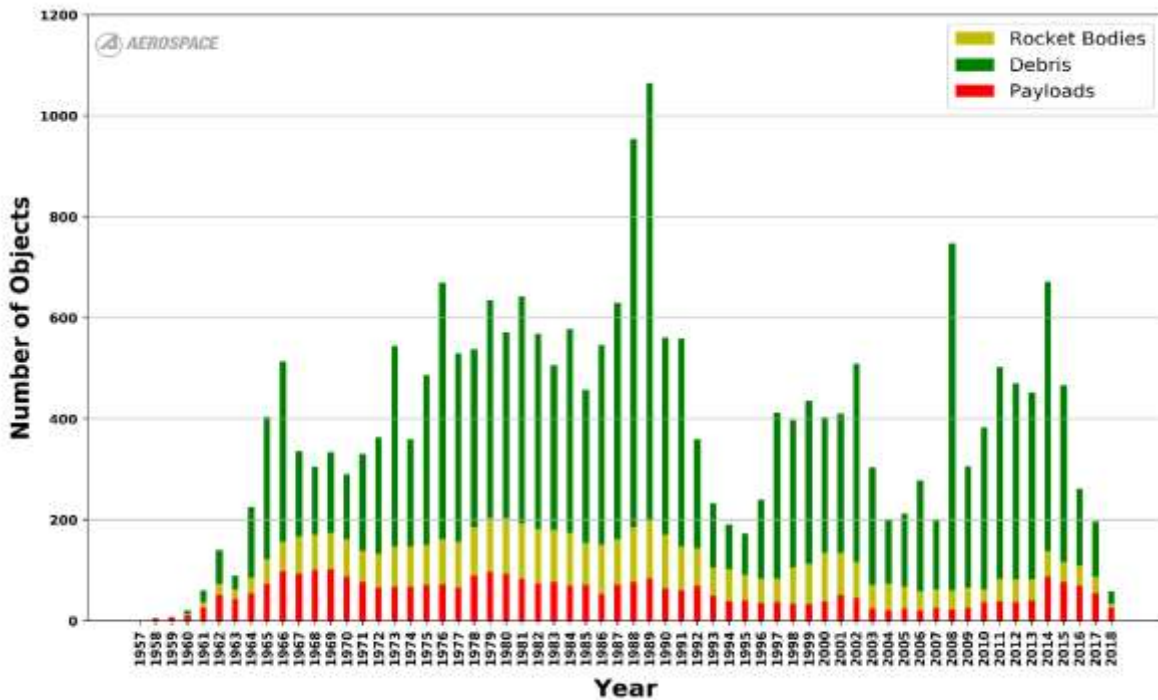


**Figure 4.2** The historical re-entry count of tracked orbital objects highlights its dependency on solar activity. (Courtesy of The Aerospace Corporation).

The general assumption that objects burn up and disintegrate when they re-enter is true for many components of a space object. However, there are scenarios where parts of a spacecraft survive to the ground relatively intact (and recognizable). As was introduced in Chapter 3, the shape, size, and mass of a re-entering object determines its orbital lifetime; these same characteristics drive re-entry survivability calculations. For example, solar panels, which are typically light and flexible (and relatively fragile), are unlikely to survive re-entry to the ground. Larger and more sturdy parts made from higher melting point materials (such as stainless steel or titanium) have a greater chance of surviving intact to the ground or to pose a risk of collision with aircraft in flight.

Common objects that survive re-entry are propellant tanks due to their material, structure, and shape.

### **Aerodynamic Heating**

The energy of a space object is a combination of kinetic and potential energies. An object re-entering Earth's atmosphere goes from having orbital velocity (kinetic energy) and altitude (potential energy) to essentially zero energy.<sup>21</sup> Energy is converted to heat and work of the drag force during the re-entry phase. If the heat of ablation (i.e., required to cause melting) for a given material used in a satellite is less than the heat dissipated during re-entry, the material melts. [1] However, not all of the kinetic and potential energy gets transferred to heating. The amount of energy that goes into heating is a function of entry angle, shape, dynamics, and material composition of the re-entering object.

There are two types of drag that decelerate re-entering objects: pressure and friction. Pressure drag occurs when high pressure at the leading edge of the object generates large forces on the object. Friction drag occurs when the heated atmospheric gasses flow in the same direction as the object's surface in the various boundary layers of the gasses. Higher pressure drag objects transfer more of this dissipative energy to the atmosphere and less to the object itself. An object under high friction drag transfers more of this energy to itself rather than the atmosphere.

Objects that are more aerodynamically sleek, such as flat plates (e.g., solar panels), have more friction drag than pressure drag. As a result, they have a greater heat buildup and are more likely to burn up during re-entry. Blunt objects, such as tanks, have more pressure drag and less friction drag, resulting in a lower energy-conversion fraction so are more likely to survive re-entry.

### **Anatomy of a Re-entry Breakup**

Gradually, an object in a low altitude orbit (under 800-1,000 km) decays due to atmospheric drag. Should the object be in an elliptical orbit with a perigee altitude that dips down into the upper atmosphere, that drag-induced energy dissipation will cause the apogee of the orbit to drop, ultimately making the intermediate orbit more circular, as discussed in Chapter 3 and shown in Figure 3.1. Because of the continual interaction with the atmosphere, the orbit follows a spiral trajectory where it increases its rate of decay until the final re-entry plunge takes place. By the time a LEO object re-enters, it has contracted to a circular orbit. As the object begins its final re-entry, it starts to heat up. Fragile parts of the object (such as solar panels) break off due to heating and aerodynamic loading. As the object moves further into the atmosphere, it begins to shed more components and further breaks apart. As this process continues, each piece disintegrates (either partially or completely). Those objects that do not demise will follow their own re-entry trajectory.

---

<sup>21</sup> There is still potential energy due to its position on Earth's surface as a result of its displacement from the center of the Earth but this is not relevant for orbital discussions.

As the pieces that survive re-entry reach the ground, they create what is known as a footprint. This process is depicted in Figure 4.3.

Since around 70% of the Earth's surface is covered by water, a sizable percentage of objects that survive re-entry will land in the water and will consequently likely never be recovered. However, the remaining 30% will land on the ground, where they are often recovered. Figure 4.4 shows the locations of recovered objects that survived re-entry. Most of the pieces that reach the ground are small (and unlikely to be recovered), while others are larger and may remain in a recognizable form.

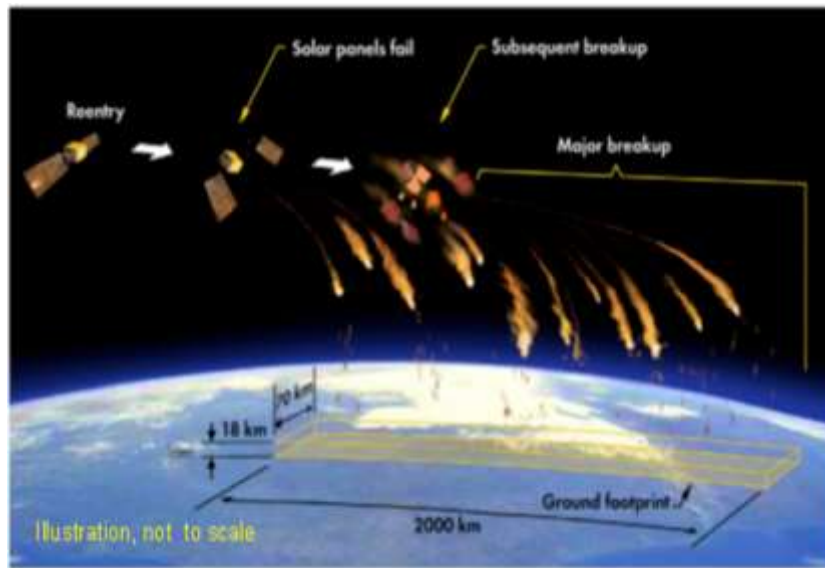


**Figure 4.3** The re-entry process is basically the dismantling of the re-entering object over time; an uncontrolled re-entry would likely have an even longer footprint. (The Aerospace Corporation)

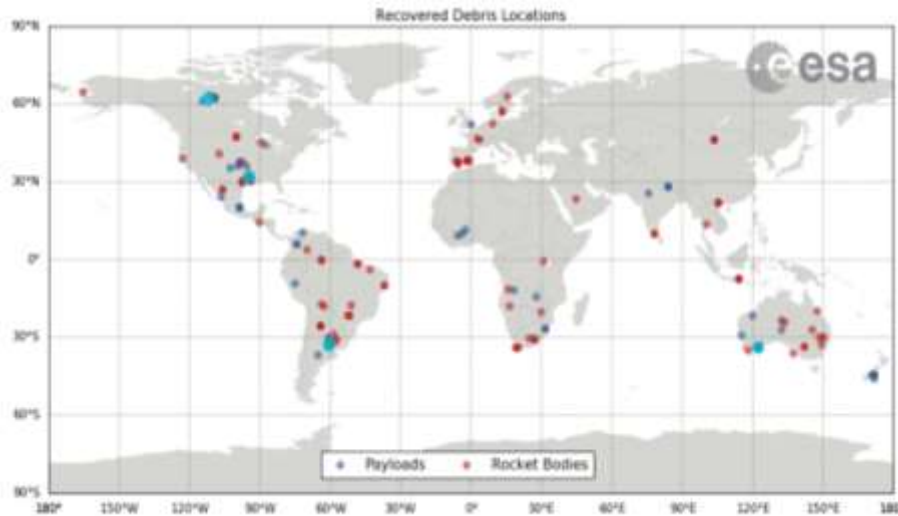


**Figure 4.4** The location of recovered re-entry debris worldwide highlights that recovery requires that a human sees it or found it after the fact. (ESA: [http://www.esa.int/spaceinimages/Images/2017/04/Debris\\_recoveries](http://www.esa.int/spaceinimages/Images/2017/04/Debris_recoveries), 4 March 2018)

## Re-entry Prediction Capability

In late February 2018, the Chinese Space Station, Tiangong-1, was predicted to re-enter the Earth's atmosphere in early April 2018. When this prediction on the re-entry time was made, the error bars on when Tiangong-1 would re-enter were  $\pm 1$  week. This prediction assumed that an uncontrolled re-entry would take place. It was determined that pieces of the space station would likely survive re-entry due to the size, material, and shape of Tiangong-1. Orbital mechanics tells us that since the Tiangong-1 has an orbital inclination of  $42.7^\circ$ , the station will fly over regions between latitudes of  $42.7^\circ$  North and  $42.7^\circ$  South. Any debris that survives re-entry will land within this latitude band.

Figure 4.5 shows the likely "ground" footprint of the Tiangong-1 space station debris. It was unknown where along its flight path the Tiangong-1 would land even days before eventual re-entry. Experience shows that good predictions are subject to a 10%-20% error of the "time to go" prediction. For example, if we predict that an object will re-enter within 10 days, or about 150 orbits, our prediction is accurate to  $\pm 1-2$  days or approximately 15-30 orbits.

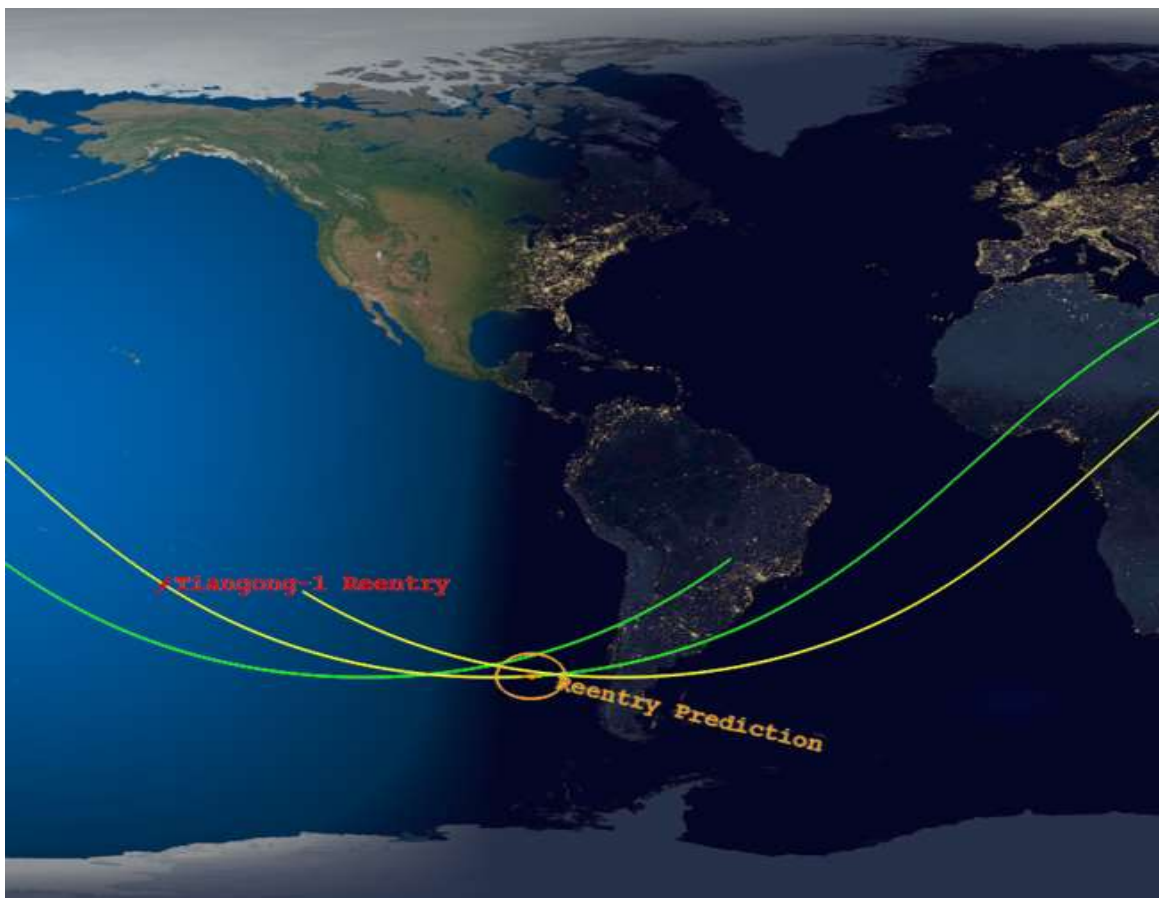


**Figure 4.5** The Tiangong-1 Space Station ground track and atmospheric re-entry area were largely over water; as a result, the "ground" footprint was likely also primarily over the water. (Courtesy of The Aerospace Corporation).

It appears that all objects from Tiangong-1 that might have made it to Earth's surface harmlessly splashed in the Pacific Ocean just to the west of South America; this was very near the maximum likelihood zone identified early in the prediction process.

### **Casualty Risk to the Population**

While no one has yet been injured or killed from re-entries, even for massive objects such as space stations and rocket bodies, the probability of such an event is not inconsequential. In January 1997, the first confirmed case of someone on the ground being hit with a piece of re-entering debris occurred in Oklahoma (U.S.). Lottie Williams was walking and felt something brush her shoulder. The object that struck her weighed less than a soda can and was a small piece of woven metal that was thought to have come from a rocket launched the previous year. Later that same evening, a 250 kg nearly intact fuel tank, shown in Figure 4.6, landed near a Texas (U.S.) farmhouse. The fuel tank ruptured upon impact. Had there been residual hazardous propellant (such as hydrazine, a common propellant used in spacecraft) remaining in that tank, there might have been a spill that could have been potentially dangerous for people nearby. Likewise, had the tank fallen on a house or on a person, it certainly would have caused damage to a house or injury or death to a person.

According to the International Academy of Astronautics (IAA) Space Debris Situation Report, the cumulative expected value of the number of people on the ground to have been struck and killed by a falling piece of debris now exceeds one. [3] This is reflective of both the large number of massive objects that have re-entered and the growing global population.



**Figure 4.6** This Delta II Second Stage propellant tank survived re-entry. (Photo: NASA, <https://orbitaldebris.jsc.nasa.gov/reentry/>, 6 March 2018)

Internationally, a 1 in 10,000 probability threshold for an impact casualty risk from an uncontrolled re-entry is a commonly accepted risk level by space agencies and nations around the world. [4]

### Recommended Design Practices for Minimizing Satellite Survivability Upon Re-entry

A microsatellite that is re-entering is unlikely to pose a significant risk to a person on the ground or aircraft in flight. However, to further reduce the risk posed to someone on the ground, a satellite designer can choose materials and design features for the satellite that will increase the likelihood that the satellite and its components will melt during re-entry; this is called design for demise.

The physical characteristics of several common satellite materials are shown in Table 4-1. The lower the melting temperature and heats of ablation, the more likely it is that the material will burn up during re-entry. Note that the melting point (i.e., temperature at which material becomes a liquid) is related to the material’s heat of ablation (i.e., measure of the effective heat capacity of an ablating material, numerically the heating rate input divided by the mass loss rate which results from ablation.). As a result, for objects to survive re-entry, they should have a high melting point, high specific heat, and a high heat of ablation. Conversely, it is best to have lower melting temperatures and lower heats of ablation to insure disintegration during re-entry.

**Table 4-1** Material properties for several common spacecraft materials shows why beryllium, glass, and titanium are more likely to survive re-entry. [5]

Material	Melting/Softening Temperature (°K)	Specific Heat (J/kg°C)	Heat of Ablation (kJ/kg)	Heat of Ablation (kJ/m <sup>3</sup> )
Graphite/Epoxy	700	720	350	550
Aluminum	850	897	900	2,400
Stainless Steel	1,700	490	900	7,250
Titanium	1,940	523	1,600	7,050
Zerodur Glass	2,000	800	1,400	3,550
Beryllium	1,557	1,020	4,100	7,550

Materials such as aluminum and graphite/epoxy composites have very low heats of ablation and will readily demise during re-entry. Components made of materials such as titanium, glass, and beryllium have very high heats of ablation, and are more likely to survive re-entry. Many variants of glass-ceramics are used in high-temperature applications, such as cooktops, stoves, and fireplaces, so it shouldn’t be surprising that they are more likely to survive exposure to high temperatures.

However, there are likely applications where some of these high-temperature materials must be used. Therefore, there are some design practices that can be implemented to reduce the likelihood of them surviving re-entry or reducing the casualty risk on the ground.

First, if the designer can change the aerodynamic characteristics of the object one might encourage disintegration on re-entry. For example, decreasing the blunt edges and making the object less like a ball will decrease the probability of survival.

Second, by bundling objects that would likely survive re-entry the number of survivable objects may be reduced. For instance, a spacecraft with several batteries that each would likely survive re-entry could be redesigned to put those batteries in a survivable box on the spacecraft. Due to a reduced casualty cross-section, the single survivable box thus poses a lower risk than multiple survivable batteries. This technique may be useful if the material is known to be re-entering over a populated area where fewer lethal pieces making it to the ground would be better. However, generally speaking, it is best to separate objects as soon in the re-entry process as possible to maximize the chances for the material to disintegrate.

Assessing the survivability of a re-entering object is a complex process, but if your spacecraft is a microsatellite or smaller and is constructed of typical spacecraft materials such as aluminum and graphite/epoxy (used for circuit boards) there is a low probability that any material will survive to the ground.

If it is deemed necessary to perform this complex demise modeling, several predictive software models are available. While we are not advocating using one organization's model over another, we would like to show some capability of ORSAT (Object Re-entry Survival Analysis Tool) to illustrate the utility of such analytic re-entry breakup and survivability models used in the technical community.

Another very powerful tool is SCARAB (Spacecraft Atmospheric Re-Entry and Aerothermal Break-Up). SCARAB is a software tool that analyzes mechanical and thermal destruction of spacecraft and other objects during re-entry (controlled or uncontrolled). It is an integrated software package (flight dynamics, aerodynamics, aero thermo-dynamics, thermal-, and structural analysis) used to perform re-entry risk assessments (quantify, characterize and monitor surviving fragments during re-entry). SCARAB has been validated with in-flight measurements and re-entry observations, and it has been compared to other re-entry prediction tools of the international community. Similarly, CNES has developed the DEBRISK [6] tool with the same analytic objective.

## **ORSAT, Object Re-entry Survival Analysis Tool**

NASA developed ORSAT (The Object Re-entry Survival Analysis Tool) to predict the re-entry survivability of an object re-entering Earth's atmosphere. A simplified version of ORSAT is available on-line as part of the Debris Assessment Software (DAS).<sup>22</sup>

The DAS software can be used to help understand the physics of re-entry but for strict compliance to debris mitigation guidelines ORSAT, SCARAB, SARA (part of DRAMA [8]), or DEBRISK should be used.

ORSAT includes numerically integrated trajectory analysis, along with atmospheric, aerodynamic, aerothermodynamic, and thermal/ablation models to assess the impact risk for re-entering objects. This physics-based model is able to compute surface temperatures and determine what happens to individual components of a re-entering spacecraft.

NASA's Upper Atmosphere Research Satellite (UARS) re-entered in 2011 and had a mass of about 6,000kg. While UARS is not a typical microsatellite system, the analysis of its re-entry provides a good example to describe the technical aspects of ORSAT (and really any re-entry survivability tool).

Based on a component analysis of this satellite, Figure 4.7 shows the re-entry breakup analysis of this spacecraft. This analysis shows that most of the lightweight and odd-shaped pieces (e.g., solar array drive, honeycomb structure, etc.) will likely melt (or demise) in the atmosphere between 40 and 80 km altitude.

The model predicts that several heavy parts (e.g., reaction wheels, fuel tanks, bulkhead fitting, etc.) made from high strength materials (titanium, stainless steel, and beryllium) will survive re-entry and impact the Earth. However, there were no reports of pieces from this re-entry being found.

---

<sup>22</sup> <https://www.orbitaldebris.jsc.nasa.gov/mitigation/das.html>

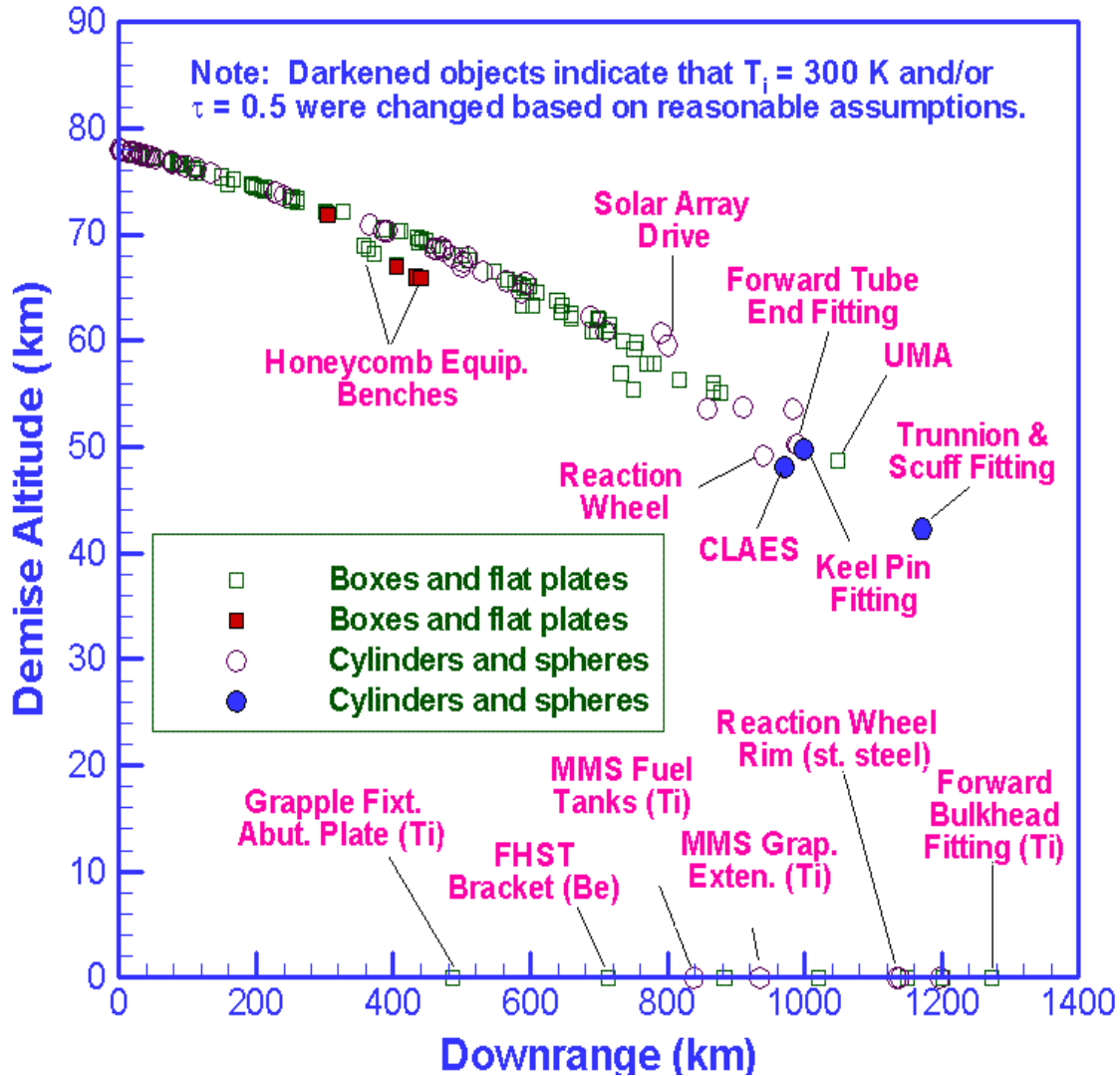


**Figure 4.7** NASA's ORSAT Software was used to predict the re-entry breakup of the Upper Atmosphere Research Satellite (UARS) spacecraft identifying elements likely to survive re-entry. (Courtesy of NASA, <https://orbitaldebris.jsc.nasa.gov/reentry/orsat.html>)

### Summary

While the risk of injury due to re-entering space objects is very small (albeit not zero), microsattellites with parts made from typical materials (e.g., aluminum, graphite, epoxy, phenolics, etc.) are likely to burn up during re-entry and not cause noticeable risk to people on the ground. The use of materials with high melting points (e.g., steel, titanium, glass, beryllium, etc.) should be avoided as much as possible. However, even when care is taken in material selection, there is still the possibility that a densely-constructed device, such as a battery or control moment gyro, may still survive re-entry. [7]

If the use of such materials and components cannot be avoided, it is likely that a program, a re-entry analysis tool such as ORSAT, SCARAB, SARA, or DEBRISK, will have to be used to

evaluate the re-entry risk (i.e., the probability that objects may survive to cause damage to property and/or people).

Spacecraft designers have a lot of control over the materials used to construct their spacecraft, and they should keep in mind the survivability of re-entering debris when choosing the materials to use. It should be noted that attempts to keep the mass of a satellite low by selection of low-density materials will contribute to lowering the risk of intact hardware surviving to the ground. While satellite pieces falling from the sky following a re-entry could injure or kill someone, statistically, a person on the ground is much more likely to be killed by an airplane falling from the sky. However, the risk of damage by surviving components after re-entry may increase with the advent of large constellations, if design for demise measures are not considered carefully.

## References

1. Rainey, L.B., ed., “Space Modeling and Simulation: Roles and Applications Throughout the System Lifecycle”, The Aerospace Press and The American Institute of Aeronautics and Astronautics, 2004 (Chapter 18).
2. Chobotov, V.A., ed., “Orbital Mechanics”, 2<sup>nd</sup> Edition, AIAA Education Series, 1996 (Chapter 10).
3. IAA Space Debris Situation Report on Space Debris, 2017.
4. Casualty Risk Tolerance for Re-entering Debris  
[http://www.esa.int/Our\\_Activities/Operations/Space\\_Debris/Reentry\\_and\\_collision\\_avoidance](http://www.esa.int/Our_Activities/Operations/Space_Debris/Reentry_and_collision_avoidance), date cited 4 March 2018.
5. Wertz, J.R., Everett, D.F., and Puschell, J.J., “Space Mission Engineering” The New SMAD”, Space Technology Library, Microcosm Press, 2011, chapter 30.2.
6. <https://logiciels.cnes.fr/en/content/debrisk>
7. Beck, J., “Death of a Smallsat,” 8<sup>th</sup> European Workshop on Space Debris Modeling and Remediation, Paris, 25-27 June 2018.
8. DRAMA is freely available at <https://sdup.esoc.esa.int>

## CHAPTER 5 USING PROPULSION AND DRAG AUGMENTATION TO REDUCE ORBITAL LIFETIME

---

### KEY POINTS

Post-mission deorbiting of microsattellites may be accomplished either actively or passively. An active approach could be a retrograde thrust to decelerate the satellite and is typically achieved via propulsive devices. The performance of propulsive devices is typically characterized by their capability to change a satellite's velocity (i.e., its  $\Delta V$  capacity) which, in turn, directly changes the satellite's orbit. Passive deorbiting utilizes the natural orbital environment to generate a retrograde "thrust". For LEO satellites at altitudes below 800-1,000 km, the Earth's atmosphere generates a retrograde force (i.e., atmospheric drag) that causes the satellite's orbit to decay along a spiral trajectory toward the Earth. The rate of the decay is dependent on the satellite's cross-sectional area in the direction of motion. Drag-augmentation devices increase cross-sectional area to passively reduce the post-mission orbital lifetime of satellites in this region. The increase in area is typically achieved by deploying either a drag sail or a gossamer structure (e.g., inflatable balloon or boom). A propulsion system could also enable collision avoidance and controlled re-entry.

---

### Introduction

Strategies for post-mission deorbiting rely on forces which decelerate the satellite, thereby reducing the orbital altitude and result in a deorbiting scenario. These strategies fall primarily into four categories:

- a) propulsion systems,
- b) drag-augmentation devices,
- c) electrodynamic tethers, and
- d) solar sails.

Propulsion systems and drag-augmentation devices are covered in this chapter. Solar sails and electrodynamic tethers are covered in Chapter 6. Propulsive deorbiting systems rely on a retarding thrust to lower the satellite's altitude. While these systems are straightforward practical solutions, they come at a cost in terms of (i) satellite reliability (i.e., the propulsive system and the attitude determination & control system have to both be functional at the end of the mission) and (ii) require additional launch mass (e.g., a standalone propulsion system and/or additional propellant) that usually does not support the mission's operational objectives directly. However, these systems provide a proven way that reduces an object's orbital lifetime in an expeditious fashion and to perform collision avoidance and controlled re-entry, if needed.

## Propulsive Deorbiting

Retrograde propulsive devices for deorbiting typically utilize two strategies: (i) controlled re-entry where the satellite is guided to an impact point over the ocean or an uninhabited area to reduce risk or (ii) uncontrolled re-entry, where the casualty risk to people on the ground has been met, the satellite is maneuvered to a lower perigee or lower circular orbit for an eventual uncontrolled atmospheric re-entry. Typically, high-thrust propulsive systems (e.g., chemical engines) utilize either a one- or two-impulse Hohmann-type transfer to reduce the orbital altitude. (However, the second impulse is generally unnecessary as the atmosphere completes the deorbit maneuver if the perigee is low enough.) Conversely, low-thrust propulsive systems (e.g., electric engines) typically utilize a continuous burn strategy.

The Hohmann-type maneuver uses an impulse at the higher altitude to maneuver the satellite to an elliptic trajectory toward the desired lower altitude and a second impulse to circularize to the lower orbital altitude. The continuous burn trajectories, employed by low-thrust propulsive devices, continuously remove energy and achieve lower orbital altitudes through a spiral trajectory. However, rather than employing a continuous burn strategy, low-thrust propulsive devices can also utilize a multi-burn strategy to provide the required  $\Delta V$  to lower the orbital altitude. In this scenario, a multi-burn sequence is employed at perigee with each burn generating an elliptical transfer orbit lowering the apogee altitude on each pass which further accelerates the orbital decay. With an assumption of unperturbed two-body orbital motion, the  $\Delta V$  required for a Hohmann transfer (i.e., transfer between circular orbits) can be estimated from

$$\Delta v = \sqrt{\frac{\mu}{R_i} \left( 1 - \sqrt{\frac{2R_f}{R_i + R_f}} \right)} + \sqrt{\frac{\mu}{R_f} \left( \sqrt{\frac{2R_i}{R_i + R_f}} - 1 \right)}, \quad \text{Equation 2}$$

where  $R_i$  and  $R_f$  are, respectively, the radii of the initial and final circular orbits ( $R_i > R_f$ )<sup>23</sup> and  $\mu$  is the Earth's gravitational parameter. Furthermore, the above expression can be used to determine the orbital altitude change for a given  $\Delta V$ . For microsattellites in Earth orbit that “on paper” do not comply with the 25-year rule, active PMD methods must be considered. A direct and expedient approach is that of a propulsive maneuver to reduce the satellite's altitude such that decay can be achieved within the 25-year threshold or, even sooner, if desired. The following two sections examine the  $\Delta V$  requirement as a function of area-to-mass ratio (AMR) for a microsattellite in circular orbits with altitude ranges of (1) 450 - 650 km and (2) 650 - 2,000 km.

### $\Delta V$ Requirement for Altitude Range 450 - 650 km

This altitude range is common for small satellite missions launched as either the primary or secondary (rideshare) manifest. Within this range, AMR plays a significant role in orbital lifetime. Within this altitude range we consider two deorbiting strategies for five AMR values that represent

---

<sup>23</sup> The radius of the Earth is 6,378 km so a 500 km circular orbit has a constant radius of 6,878 km.

typical levels for 1U to 6U cubesats: 0.005, 0.0075, 0.01, 0.015 and 0.02 m<sup>2</sup>/kg. The satellite altitude at the end of the mission is first determined through STK LOP (Long-term Orbit Propagator) simulations. Two de-orbiting strategies are then evaluated using equations in Vallado [1]. The first strategy is to ensure the satellite altitude to be 600 km or lower at the end of the mission. Two maneuver burns are assumed to execute the Hohmann transfer from higher altitude to the lower altitude. In this case, the results are presented in Table 5-1.

**Table 5-1** The  $\Delta V$  requirement for circularizing 625 km and 650 km orbits to 600 km versus AMR shows that an object with a smaller AMR requires a greater propulsive maneuver.

Initial Satellite Altitude (km)	$\Delta V$ Requirement (m/s)				
	AMR = 0.005 m <sup>2</sup> /kg	AMR = 0.0075 m <sup>2</sup> /kg	AMR = 0.01 m <sup>2</sup> /kg	AMR = 0.015 m <sup>2</sup> /kg	AMR = 0.02 m <sup>2</sup> /kg
625	13.50	10.81	10.27	8.11	6.49
650	26.93	25.33	24.79	23.18	22.11

In the second strategy, the perigee is dropped to 400 km through one burn. The ensuing orbit will be elliptical. The reader should note that for circular orbits below 600-625 km there is no need to reduce the perigee to 400 km to be compliant with the 25-year rule; a circular orbit below 600-625 km is likely already compliant. However, this exercise helps to identify means to reduce an object's orbital lifetime to even less than 25 years. The  $\Delta V$  requirement is summarized in Table 5-2 for various AMR values.

**Table 5-2** The  $\Delta V$  requirement to drop a satellite's perigee to 400 km versus AMR is not highly dependent on AMR.

Initial Satellite Altitude (km)	$\Delta V$ Requirement (m/s)				
	AMR = 0.005 m <sup>2</sup> /kg	AMR = 0.0075 m <sup>2</sup> /kg	AMR = 0.01 m <sup>2</sup> /kg	AMR = 0.015 m <sup>2</sup> /kg	AMR = 0.02 m <sup>2</sup> /kg
450	12.65	N/R	N/R	N/R	N/R
475	20.18	N/R	N/R	N/R	N/R
500	27.37	15.73	8.73	N/R	N/R
525	34.52	28.20	25.16	16.56	N/R
550	41.35	37.53	35.89	32.05	27.37
575	48.13	45.70	44.61	42.44	39.99
600	55.14	53.26	52.72	51.37	49.76
625	61.84	60.51	60.24	59.17	58.36
650	68.50	67.70	67.44	66.64	66.11

N/R = Not Required

Note that there officially is no need to drop the perigee of a satellite from a 625 km orbit (or lower) to meet the 25-year threshold. However, it is useful to see the propulsive requirements to even further reduce a satellite's orbital lifetime to shorter than 25 yr.

The results for both Table 5-1 and Table 5-2 are presented in Figure 5.1; Table 5-1 data are the two clumps of points to the lower right of the figure while the Table 5-2 results are the color-coded contours shown running diagonally in the figure.

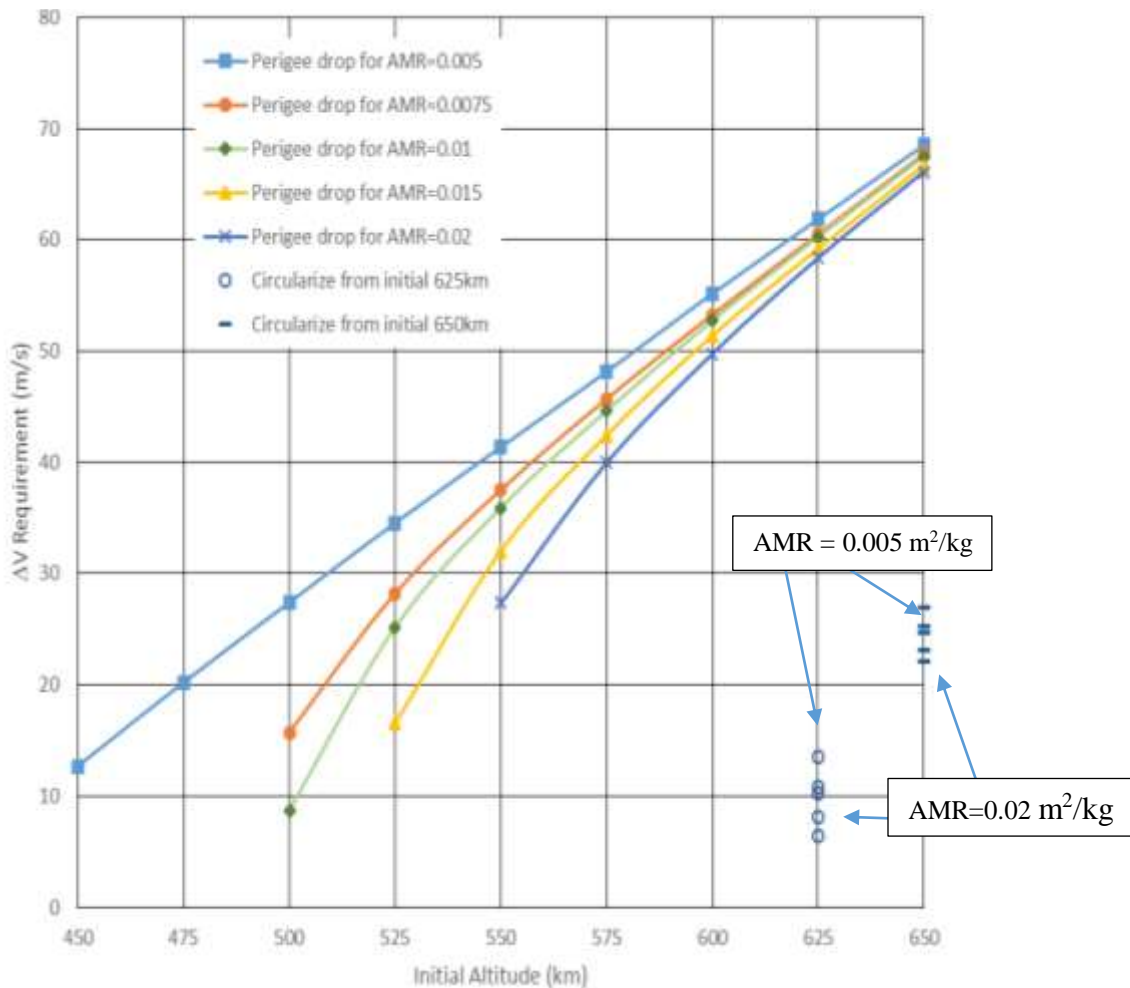


**Figure 5.1** The plot of estimated braking  $\Delta V$  (m/s) required vs initial orbital altitude highlights the different challenges of orbit circularization to 600 km (i.e., diagonal lines) rather than dropping the perigee to 400 km (i.e., data points in lower right quadrant) to accelerate re-entry.

Figure 5.1 illustrates that the  $\Delta V$  is considerably lower for circularizing the orbit to 600 km versus lowering the perigee. For instance, at an initial satellite altitude of 650 km, a satellite with  $AMR = 0.005 \text{ m}^2/\text{kg}$  will require almost 42 m/s more in  $\Delta V$  if the perigee drop strategy is chosen.

### ΔV Requirement for Altitude Range of 650 km to 2,000 km

As illustrated in Figure 5.1, the curves for satellites with different AMR values converge as the initial satellite altitude increases. This is due to the diminishing atmosphere with altitude and as such, the AMR has less effect at higher altitudes. This means that the AMR parameter can be neglected in estimating the ΔV requirement for altitude from 650-2,000 km. Again, two de-orbiting strategies are considered. The first one is to circularize the orbit to 600 km and the second is to drop the perigee to 400 km. Results are presented in Table 5-3 and Figure 5.2.

**Table 5-3** The comparison of ΔV (m/s) for the two de-orbiting strategies highlights the utility of dropping the perigee to 400 km for the higher altitude LEO orbits.

Initial Satellite Altitude (km)	ΔV (m/s)		Initial Satellite Altitude (km)	ΔV (m/s)	
	Circularizing Strategy	Perigee Drop Strategy		Circularizing Strategy	Perigee Drop Strategy
650	26.93	68.50	1350	375.86	239.15
700	53.58	81.68	1400	398.93	250.28
750	79.94	94.71	1450	421.78	261.27
800	106.03	107.57	1500	444.40	272.14
850	131.85	120.27	1550	466.80	282.89
900	157.39	132.82	1600	488.98	293.51
950	182.67	145.21	1650	510.95	304.00
1000	207.69	157.46	1700	532.70	314.38
1050	232.46	169.55	1750	554.25	324.64
1100	256.97	181.50	1800	575.59	334.79
1150	281.23	193.31	1850	596.73	344.82
1200	305.25	204.97	1900	617.66	354.73
1250	329.02	216.50	1950	638.41	364.54
1300	352.56	227.89	2000	658.95	374.24

A general trend can be observed in Figure 5.2. The circularizing the orbit strategy is more advantageous when the initial satellite altitude is below 800 km. However, from 800 km upward, it is better to execute the perigee drop maneuver.

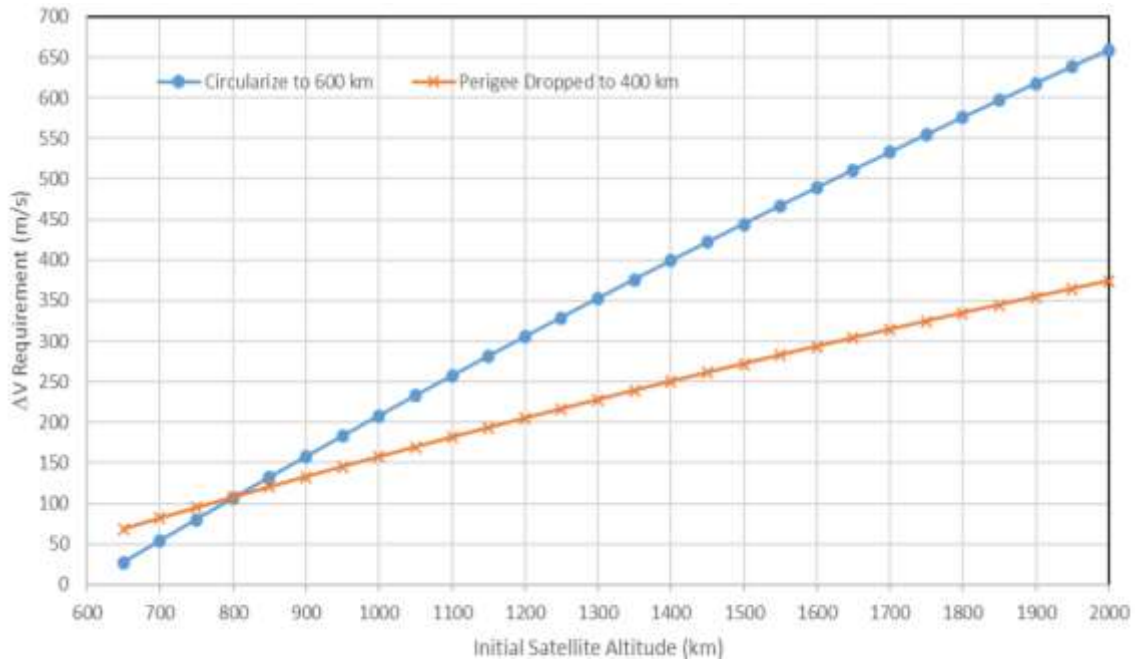


**Figure 5.2** The point at where perigee drop to 400 km is superior to circularizing an orbit to 600 km is about 800 km altitude.

### Challenges of propulsion system

Propulsion systems are a very well-established technology and many devices are commercially available for small satellites, even those as small as 1U cubesats. Though there are some challenges in implementing a propulsion system that may affect satellite system design and operations, it is important to point out that a propulsion system cannot be thought of as a “stand-alone” system which will de-orbit the satellite. This is because the propulsion system requires a functioning attitude determination and control capability for two reasons. First, the direction in which the thrust is to be oriented needs to be measured on-board and a pointing capability of the spacecraft is needed. Second, direction of the thrust needs to be maintained and controlled during the propulsive maneuver against the (often high) torque generated by the thrust itself. In addition, the propulsion system typically contributes to the overall spacecraft mass and power budgets plus adding complexity and volume depending on the propulsion system technology and required  $\Delta V$ .

A detailed description of propulsion systems is beyond the scope of this book. However, the reader is referred to references 24-26, if more detail is desired.

## Drag Augmentation

Drag augmentation for post-mission disposal (PMD) of LEO satellites is nothing new – the concept has been studied since the late 1980’s. An early publication by Petro [1] discussed the use of deployable balloons as an effective mechanism for de-orbiting “objects” below an altitude of 800 km. Since then, there has been a plethora of studies exploring the merits and challenges of drag-augmentation devices for PMD of LEO satellites. Reference [2] provides a summary of some of these activities.

In addition to the studies, flight demonstrations of satellites equipped with devices that can be utilized for drag augmentation during PMD have been attempted. The NanoSail-D mission [3] was conceived as solar sail technology demonstrator by NASA to be flown in LEO where it would operate as a drag sail. The satellite was lost during launch in 2008 but its replacement, NanoSail-D2, was successfully flown in 2010, see Figure 5.3.

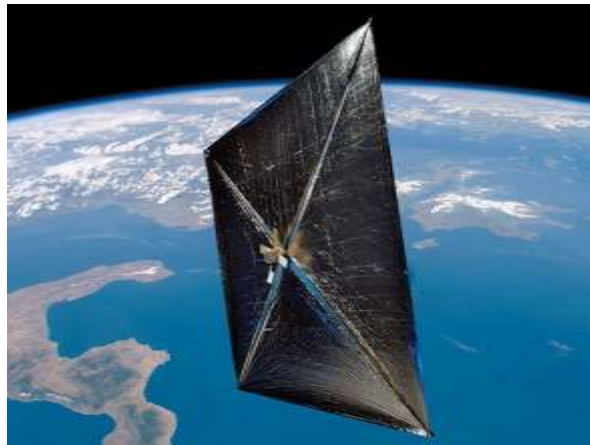


**Figure 5.3** NanoSail-D2 [http://www.nasa.gov/mission\\_pages/smallsats/11-010.html](http://www.nasa.gov/mission_pages/smallsats/11-010.html)

Nanosail-D2 deployed a 9 m<sup>2</sup> sail from a 3U cubesat, and managed to deorbit from an initial altitude of 650 km in only 240 days. [17] A typical cubesat with area-to-mass ratio of 0.01 m<sup>2</sup>/kg would have taken around 25 yr to deorbit unassisted from this altitude, as per Chapter 3 .

A 1U cubesat FREEDOM, released from ISS on Jan 16, 2017, successfully deployed its 1.5 m<sup>2</sup> sail and re-entered atmosphere after three weeks on Feb. 5. It was jointly developed by a Japanese steelwork company, Nakashimada Engineering Works and Tohoku University. It aimed at demonstrating a deployable deorbit device for application in future missions. [20]

InflateSail was another successful demonstrator of drag-augmented deorbiting; the altitude profile with and without the sail is shown in Figure 5.4. The 3U cubesat deployed a 10 m<sup>2</sup> sail that was extended from the cubesat bus using a 1 m inflatable mast [18]. InflateSail was deployed from an initial 518 km x 494 km orbit, and stayed in orbit for only 72 days (blue line) but it would have stayed in orbit for over six years without the drag sail deployment. [19] The analysis of this

demonstration implies that a 100 kg spacecraft can comply with the 25-year rule from an altitude of 800 km under average solar activity and active attitude control that points the sail into the RAM direction. [20] Note that by using active attitude control to direct the solar radiation pressure it is possible to achieve an even shorter deorbit duration from higher initial orbits. This will be discussed further in Chapter 6 .

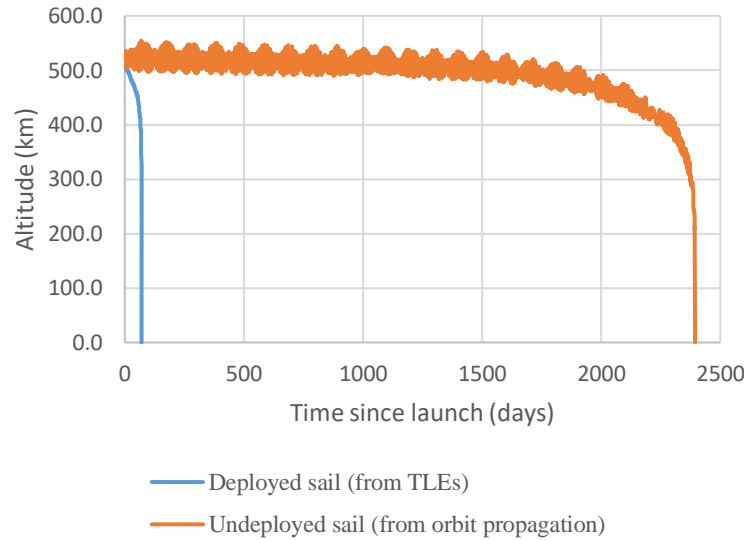


**Figure 5.4** InflateSail comparison of deployed vs. undeployed decay profile: the deployed sail profile from actual TLEs is depicted versus the undeployed decay profile from orbit propagation. [19]

Drag-augmentation devices rely on the force exerted by the atmosphere on the larger exposed area to reduce the orbital lifetime of the satellite. The two most promising drag-augmentation designs are flat drag sails (as shown in Figure 5.3) and inflatable gossamer devices (see Figure 5.5-Figure 5.7). On the one hand, a drag sail typically utilizes structural member(s) to provide support to the sail area, which is usually constructed from lightweight film material. Gossamer drag-augmentation devices are effectively large balloons either inflated or using a deployable shell to significantly increase the satellite’s cross-sectional area.

Examples of successful inflatable space structure missions include the NASA Echo balloons (Figure 5.5), Global Aerospace GOLD balloon (Figure 5.6), and the Inflatable Antenna Experiment (Figure 5.7). Although only the GOLD system was designed to demonstrate drag de-orbiting, it was also the only one that did not fly in space.

One reason why an inflatable structure might be preferred is because of the three-dimensional nature of the structure - the orientation of the satellite becomes less important in ensuring a consistently maximum drag force. An inflatable sphere has the same cross-section regardless of orientation, but a flat sail has the potential to create very little drag if the orientation of the satellite is unfavorable. Concerns regarding attitude stability of a drag sail are addressed later in this chapter.



**Figure 5.5** Echo II undergoing stress test (image credit NASA)



**Figure 5.6** Global Aerospace GOLD inflatable balloon (Global Aerospace Corporation)



**Figure 5.7** Inflatable Antenna Experiment (image credit NASA)

Since the aerodynamic drag force is directly proportional to the cross-sectional area of the satellite, an increase in cross-sectional area is beneficial in terms of the magnitude of the generated drag force. Figure 5.8 demonstrates how the de-orbit duration is impacted by varying the area-to-mass ratio. The figure was created by running Monte Carlo simulations with varying initial orbit and start epoch relative to the solar cycle. It shows the altitude range from which a satellite can be de-orbited, for a target deorbit duration of 5, 15, and 25 yr.

As mentioned before, a “typical” satellite (i.e., AMR of  $0.01 \text{ m}^2/\text{kg}$ ) will de-orbit in 25 yr from an altitude of around 625 km. Figure 5.8 can be used to find the AMR required in order to meet deorbiting duration requirements. Conversely, one can use it to look up the maximum altitude into which a satellite with a given AMR can be launched and still comply with the target deorbit duration.

### Challenges of Drag Augmentation

While drag augmentation is a credible alternative for de-orbiting, there are many challenges, both in the design of the deorbit device, and the mission itself, that have to be overcome. First and foremost, this approach can only be used if the casualty risk has been proven to not exceed the threshold of  $10^{-4}$  probability of a casualty on the ground. If that criterion is not met then one must do a controlled re-entry with the assistance of a propulsive system. Next, a drag-augmentation approach will invariably require a deployable element. If the deorbiting device is an inflatable then there must be a way to insure that it retains its shape even after penetration by a micrometeoroid or space debris particle. The drag-augmentation effect should preferably not be active while the satellite performs its normal operations. Only towards the end of its life will the drag-augmentation device be deployed; this has some concerns as the device needs to be designed as to still function even if the spacecraft has lost its ability to operate. Many of the challenges of this approach can be attributed to the deployable nature of drag-augmentation strategies and the reliability of in-space deployable devices potentially years after a satellite has been launched. Other challenges are due to material choices and effects of long-term exposure to storage and the LEO space environment.

Lastly, some devices that may be used for drag augmentation will also encounter perturbations from solar radiation pressure that are detailed in Chapter 6 .

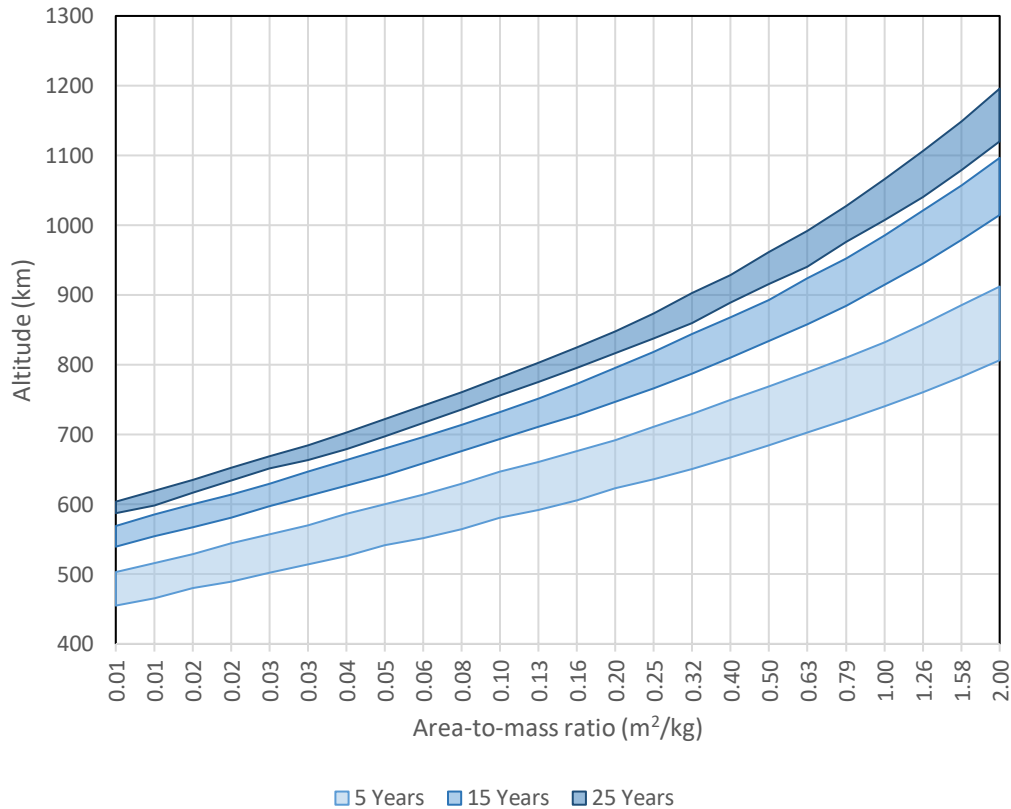


**Figure 5.8** The altitude range from which a satellite can be deorbited through aerodynamic drag forces when targeting 5, 15, and 25 yr deorbit time, is shown as a function of area-to-mass ratio.

### Effect of Impacts

A larger drag surface area will lead to a shorter orbital decay duration in LEO, which is desirable from a debris mitigation point of view, however, the larger surface area will also increase the likelihood of a collision. Large structures, such as drag-augmentation devices will be susceptible to particulate impacts from objects in LEO. While the probability of collision with a “large” object of 10 cm or more (which can lead to a catastrophic<sup>24</sup> collision) is manageable, there are many more, smaller particles which have a greater probability of impact that could still disrupt the drag augmentation significantly. The Area-Time-Product (ATP) is often used as a relative measure of how many particulates a satellite may encounter. It is simply the collision cross-sectional area of the satellite multiplied by the time spent in orbit, however, the area to take into account is not always obvious.

<sup>24</sup> Catastrophic means that the satellite will be completely fragmented as a result of the encounter with typically 1-3 trackable fragments per kg of mass of the satellite.

As stated earlier, it is imperative that an inflatable be able to retain its shape after an impact of a small particle. It should be noted that it is unlikely that an impact with a drag-augmentation device would create any significant amount of debris due to the low mass structures used. Table 5-4 outlines issues related to particulate impacts on a satellite augmented with a drag sail.

**Table 5-4** The collision scenarios for parts of a drag sail satellite are speculated to highlight potential operational considerations for such PMD options; the actual damage is very difficult to determine without significant testing.

Target constituents	Impacting object	Collision type	What happens to drag sail satellite?	What happens to impacting object?
Sail membrane (7 µm Aluminized Kapton)	Micro-meteoroid	Potentially mission-degrading	Hole and micro-cracks in sail. Part of impacted sail membrane turned to vapour and dust	Vaporized (dust produced)
	Small object (10 cm spacecraft fragment)	Mission-degrading	Small hole in sail. Impacted sail membrane turned to dust/vapour	Pass through
	Large object (100 kg satellite)	Mission-terminating	Large hole in sail. Loss of deorbiting function	Pass through, damage to operational satellite
Boom (18-49 g/m)	Micro-meteoroid	Potentially mission-degrading	Very small (<1mm) objects are less likely to damage boom.	Vaporized (dust produced)
	Small object (10 cm fragment)	Mission-terminating	Fragmentation. Several large fragments produced	
	Large object (100 kg satellite)	Catastrophic	Fragmentation. Many large fragments produced.	
Hard-body satellite	Micro-meteoroid	Potentially mission-degrading	Component of the satellite may be disrupted	Vaporized (dust produced)
	Small object (10 cm spacecraft fragment)	Mission-terminating or Catastrophic	Fragmentation. Several large fragments produced	
	Large object (100 kg satellite)	Catastrophic	Fragmentation. Hundreds of large fragments produced.	

The area to use for a three-dimensional shape will have to be evaluated differently because in this case the collision probability varies by direction. For a drag-augmentation strategy, the ATP should be balanced with the reduction in orbital lifetime.

Debris in space comes from two sources, natural and human-made. Both can have similar impact effects on spacecraft; they collectively are called micrometeoroids and orbital debris (MMOD). Micrometeoroids are small sub-millimeter particles that intersect the Earth's orbit and are remnants of comets, asteroids, and other primordial material left over from the formation of the solar system. They are in orbit around the Sun, not the Earth. In contrast, human-made orbital debris may be due to defunct satellites, mission-related debris, fragments produced by past explosions and collisions, or slag from solid rocket motor firings. The human-made debris does indeed orbit the Earth. Micrometeoroids and small orbital debris can cause degradation and erosion of satellite surfaces, puncture solar panels, and even penetrate exterior-mounted components. For payloads, it might be possible to shield against such particles to some extent, but for deployable structures, particulate impacts may cause rips in the membrane and leaks in inflatable structures. Figure 5.9 shows some typical results from small particulate impacts on space systems.

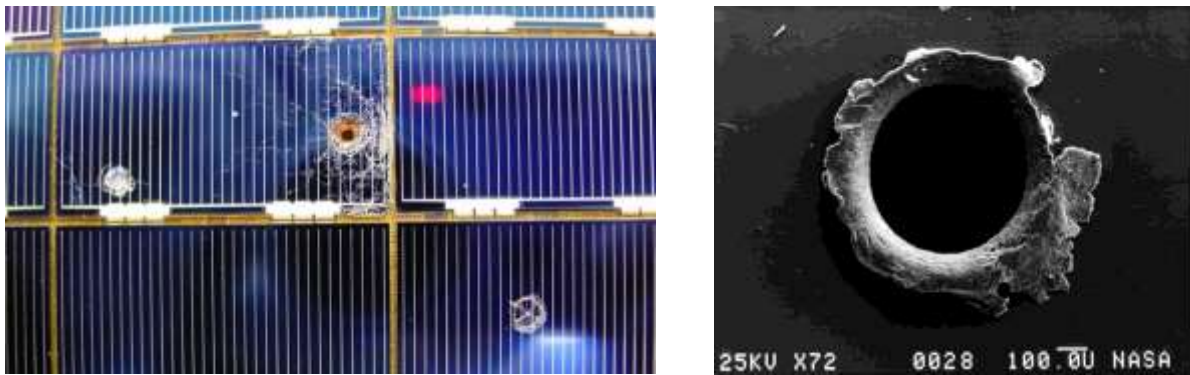


**Figure 5.9** Examples of non-catastrophic micrometeoroid impacts accentuates the need to consider the debris environment when considering the use of drag-augmentation devices. The left panel shows a returned solar array from the Hubble telescope. (image credit ESA). The right panel shows an impact on satellite component retrieved during the STS-41C Solar Max repair mission. (image credit NASA)

ESA has developed a software tool called MASTER<sup>25</sup> (Meteoroid and Space Debris Terrestrial Environment Reference) that can estimate the space debris flux and spatial density for any orbit for epochs ranging from 1957 to 2060. The debris sources used in the model extends past the list of catalogued objects to include explosion and collision fragments, rocket motor slag, NaK droplets (sodium-potassium alloy used as coolant in Russian radar satellites with nuclear reactors), various ejecta, and micrometeoroids down to one-micron size.

---

<sup>25</sup> MASTER is freely available at <https://sdup.esoc.esa.int>

Using MASTER, or the MIDAS tool in the DRAMA suite which uses the MASTER population, one can determine the number of impacts of certain object types one can expect for a de-orbiting satellite. While collisions with 10 cm and larger fragments are unlikely, it is very much a certainty that the drag sail or inflated structure will experience micrometeoroid and small orbital debris impacts. It is thus important to design the structure with such impacts in mind. For drag sails, the common solution is to make use of strengthening cords such as Kevlar or additional layers of Kapton tape to provide barriers for rips. This will prevent small holes made by micrometeoroids from propagating to form large holes. Inflatable structures will either have to be rigidized after inflation, so that inflation pressure is no longer needed, or the inflation system should be capable of dealing with small leaks over the duration of the de-orbiting phase.

#### Materials – mass, strength, and long-term space exposure effects

Another important design aspect of a drag-augmentation device is that of materials. The intent is to use lightweight materials, otherwise the mass of the de-orbiting device will negate the drag-enhancement benefit. The membrane of a drag sail usually consists of a thin polymer film substrate with coating to achieve the desired thermal and optical properties. The most common substrate materials used are Mylar, Kapton, and CP-1. Membranes as thin as 2  $\mu\text{m}$  have been produced, but for such thin membranes, handling and folding becomes problematic. Atomic oxygen causes erosion of Kapton and aluminum-coated Kapton for exposed materials on space systems operated below 650 km altitude. If the sail has to remain intact for as long as 25 yr, it is essential to apply an atomic oxygen-resistant coating.

Materials from which supporting booms are manufactured include various metal alloys and carbon fibre. Carbon fibre booms can typically be made lighter than metal counterparts, while being able to withstand the same load. An important consideration that remains to be investigated is the effect of long-term storage on coiled carbon-fibre booms, such as the ones shown in Figure 5.10. The strained carbon fibre is susceptible to “creep” effects which may ultimately cause it to lose its deployed shape.

#### Mass and Volume

The mass and stowed volume of the deployable structure will typically scale with the size of the host satellite, in order to satisfy deorbit requirements. When considering a scaling law for the deorbiting system, the properties of existing sail and inflatable designs can be used with an assumed scale range.

The ESA Gossamer Deorbiter (Figure 5.10) deploys a sail up to 25  $\text{m}^2$ , using a lightweight open section carbon fibre reinforced polymer (CFRP) booms, that results in a low mass system. The ESA Gossamer booms have a mass per unit length of 15 g/m and a deployment mechanism with a mass of 0.3 kg with dimensions 12 cm  $\times$  12 cm  $\times$  8 cm. [23] A sail thickness of 7.5  $\mu\text{m}$  is used for all sail sizes, as this is the average thickness including edge reinforcements and rip-stops. The

sail material, Kapton or CP-1, has a volumetric density of  $1.4 \text{ g/cm}^3$  and an areal density of  $10.7 \text{ g/cm}^2$ .<sup>26</sup> These parameters allow us to find the mass of a sail with area anywhere between  $1 \text{ m}^2$  and  $25 \text{ m}^2$  by calculating the amount of material required.

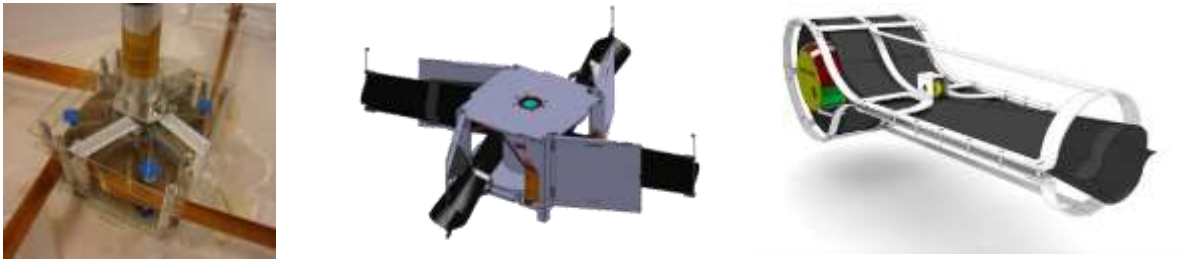


**Figure 5.10** Various deployment mechanisms with coiled booms are shown to highlight the engineering considerations for using such PMD options. Left: Deployment mechanism of the ESA Gossamer Deorbiter (metal boom version), Middle: DeOrbitSail deployment mechanism (image credit DLR), Right: DLR Boom Deployer that travels along with boom as it extends (image credit DLR)

The open section CFRP booms and deployment mechanism are not suitable for larger sails. For sail sizes up to  $80 \text{ m}^2$  the concept designs for the Near Earth Asteroid (NEA) Scout and Lunar Flashlight missions can be used (see Figure 5.11 and Figure 5.12). These will deploy square sails up to  $80 \text{ m}^2$  using TRAC (Triangular Rollable and Collapsible) booms, from two side-by-side NanoSail-D deployment mechanisms. The booms have a mass per unit length of  $50 \text{ g/m}$ , and the deployment mechanism will have a volume of  $2,000 \text{ cm}^3$  with a mass of  $1 \text{ kg}$ .

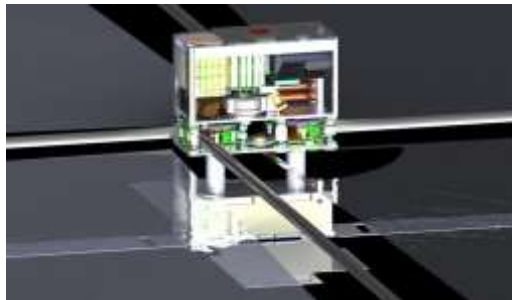


**Figure 5.11** Lunar Flashlight concept design (Complements of NASA)

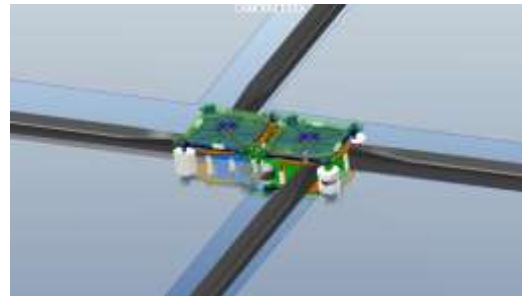


**Figure 5.12** Lunar Flashlight and NEA Scout sail sub-system (Complements of NASA)

Note that Figure 5.13-Figure 5.18 plot the ESA Gossamer Deorbiter for  $0\text{-}25 \text{ m}^2$  sails and the Lunar Flashlight from  $25\text{-}80 \text{ m}^2$  on the same plot; that is why there is a discontinuity along the sail area axis at  $25 \text{ m}^2$ .

These parameters allow us to derive a plot of sail system mass as a function of sail area, as in Figure 5.13. It is then further useful to plot the percentage mass of the sail sub-system relative to the satellite mass, as in Figure 5.14. The figure shows that if deorbiting requirements can be met

<sup>26</sup> New materials are being developed for these applications; these values are likely to continue to drop over time.

with a  $0.1 \text{ m}^2/\text{kg}$  AMR, then the sail subsystem mass will be less than 1% of the satellite mass. An AMR of  $0.5 \text{ m}^2/\text{kg}$  can be achieved with only 2 to 4% mass increase.

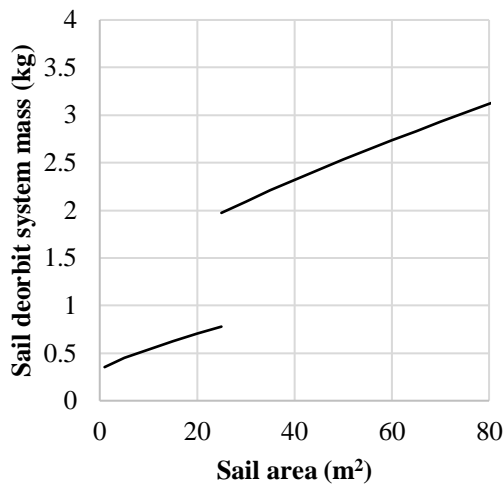


**Figure 5.13** Sail deorbit system mass increases linearly as a function of sail area.

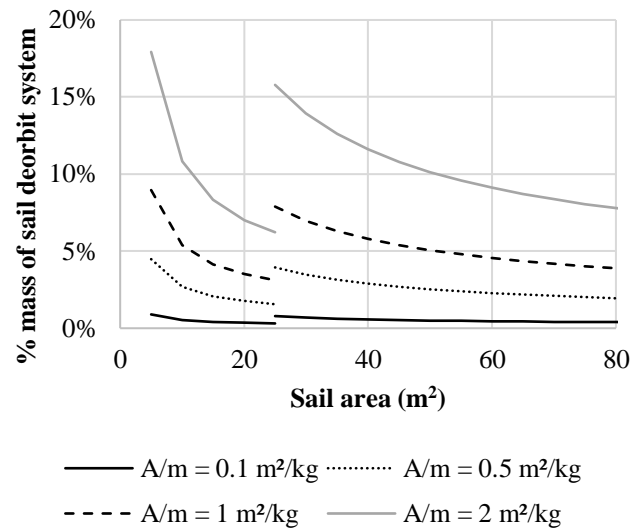


**Figure 5.14** Sail deorbit system mass decreases as a percentage of total satellite mass, as sail area increases.

In order to do the same for the stowed volume, a sail packing efficiency of 20% is assumed based on previous missions. This yields a plot of stowed sail deorbit system volume as a function of sail area as in Figure 5.15 and Figure 5.16.

This process can also be applied to inflatable structures, by considering parameters from the Echo balloons. We will consider both rigidizable envelopes, where a laminate membrane is strain rigidized due to the initial inflation pressure, and a thinner membrane that requires maintained pressure throughout deorbiting.

Echo 1 and 1A used  $12.5 \text{ }\mu\text{m}$  thick Mylar with areal density of  $17.5 \text{ g/m}^2$ . It is anticipated that newer inflatable structures will attempt to make use of thinner material and  $7 \text{ }\mu\text{m}$  Mylar is assumed for the inflation-maintained envelope material. The rigidizable membrane of Echo II used a Mylar-Aluminum laminate. An areal density of  $45 \text{ g/m}^2$  is assumed for the  $4.5 \text{ }\mu\text{m}$  Al –  $9 \text{ }\mu\text{m}$  Mylar –  $4.5 \text{ }\mu\text{m}$  Al membrane including adhesives.

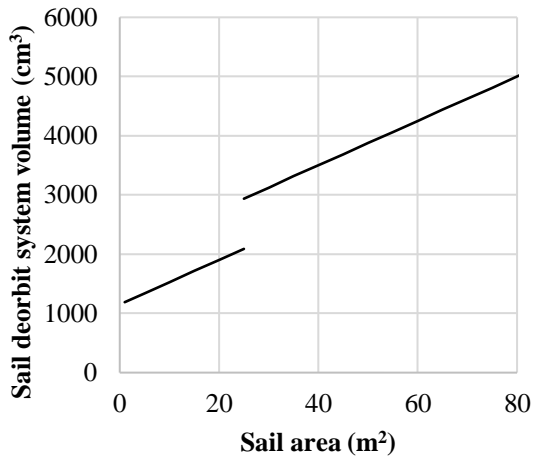


**Figure 5.15** Sail deorbit system stowed volume increases linearly with increasing sail area.

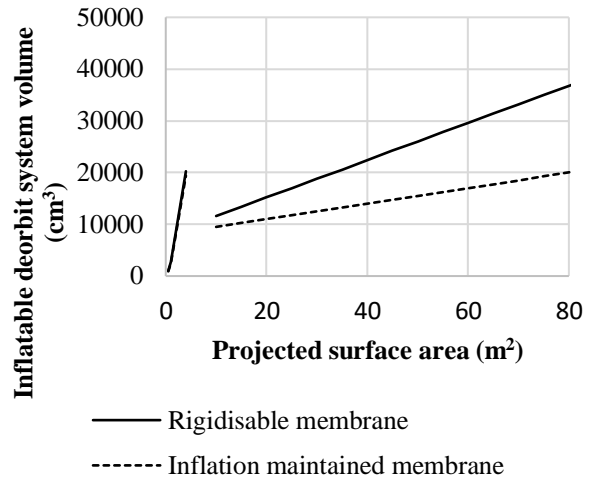


**Figure 5.16** The inflatable sphere stowed volume as a function of projected surface area varies by technology solution.

The mass of the canister carrying the inflation chemicals and the mass of the chemicals themselves on Echo I totaled 32 kg. Such an inflation system is appropriate for large diameter spheres. Cool Gas Generators (CGGs) provide a compact alternative for providing inflation pressure with lower volume requirements and can safely be used on cubesats.

The InflateSail CGG can deliver 3.2 l of nitrogen gas at 1 bar (100 kPa) and mass of 35 g. For the inflatable sphere scaling law, it is assumed that the CGG mass scales linearly with gas delivered. For the rigidizable sphere, an inflation pressure of 0.5 bar (50 kPa) is required. [20]

For the inflation-maintained membrane, it is assumed that a pressure of 0.1 bar (10 kPa) is sufficient, but that five times the gas volume is required to maintain the pressure for the deorbit duration. The amount of gas required is thus the same for both types of membrane.

The expected mass and percentage of host satellite mass of the inflatable deorbit system, as a function of projected surface area, is shown in Figure 5.17 and Figure 5.18. One can see that the mass of the CGG quickly becomes unrealistic for sphere sizes in excess of 1 m<sup>2</sup> projected surface area and that the larger inflation system has too much of a mass penalty.

### Attitude Stability

A good PMD strategy will work even in the case of a damaged or failed satellite. Such a fail-safe de-orbiting strategy will ensure the satellite de-orbits even if it experiences a failure of its normal subsystems.

An inactive satellite would, however, not be able to control its attitude, and so may not present the largest possible projected drag surface area. A tumbling sail will take longer to de-orbit than one that is stabilized so that the sail continually faces the ram direction. This is another benefit of

spherical inflatables; the drag area stays fairly constant no matter the attitude of the spacecraft. However, using a drag sail, it is possible to achieve such stability even without active attitude control, as long as the sail center of pressure trails behind the center of mass of the satellite. If the sail has a non-zero angle of attack, the aerodynamic force from the sail will result in a restoring torque (i.e., to rotate the sail back to a zero angle of attack).

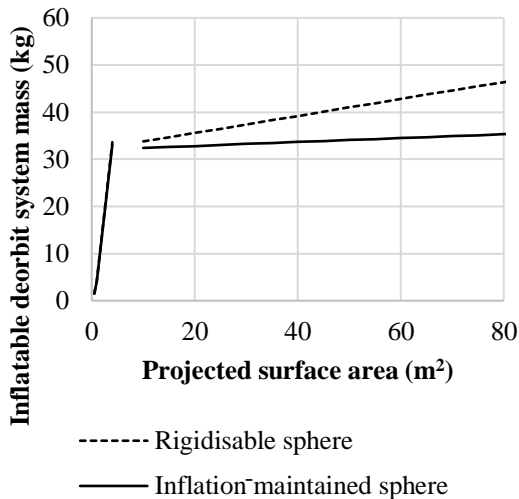


**Figure 5.17** Inflation-maintained sphere system mass increases linearly with increasing projected surface area.

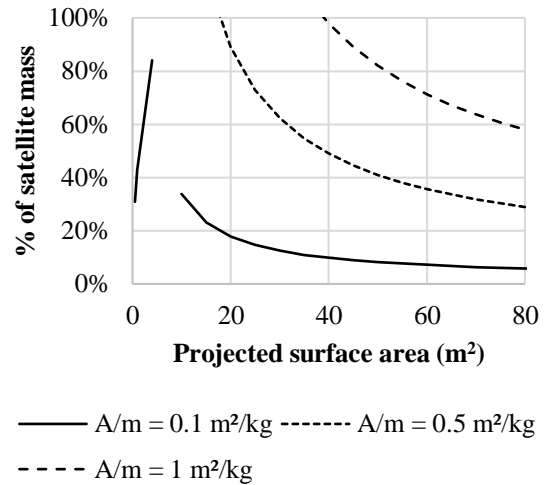


**Figure 5.18** Rigidisable sphere system mass increases linearly as a percentage of total satellite mass for a CGG inflation system and leads to an unfeasible solution for structures greater than 1 m<sup>2</sup>. Larger inflatable structures will have a mass percentage that decreases as projected area increases.

A restoring torque alone is not enough to result in a stable attitude. The restoring aerodynamic torque will rotate the satellite back to a zero angle of attack, but at the point where the angle of attack is zero, it needs a non-zero angular rate. Without damping, the attitude will not be stable, but merely oscillate around the zero angle of attack. Damping will be more pronounced with a flexible sail structure rather than a rigid configuration.

By ensuring the sail center of pressure trails behind the center of mass, passive attitude stability is possible, but only if the restoring torque is larger than other disturbance torques. The relative torque comparison in Figure 5.19 shows that it should be possible for a 100 kg satellite with a 25 m<sup>2</sup> sail to achieve passive attitude stability below 600-700 km where aerodynamic force will dominate above solar radiation pressure (SRP) and gravity gradient torque. It is, however, possible to make use of a membrane material with high transmittance and low absorptance in the solar spectrum, such as CP-1. Such a “transparent” membrane will lessen the impact that SRP has on the sail attitude, and potentially increase the upper altitude at which passive attitude stability can be maintained. This examination highlights how even a simple concept of a drag sail becomes fairly complicated when considering real-world implementation issues.

As discussed in Chapter 3 and earlier in this chapter, the time it takes to deorbit due to drag is dependent on the area-to-mass ratio. In situations where the changing satellite attitude results in changes to the area-to-mass ratio, it would be appropriate to use an average cross-sectional area based on the expected rotational movement of the satellite and sail, in order to find the effective area-to-mass ratio. An average cross-sectional area, which is defined as the average of the satellite's projected surface area when viewed equally over  $4\pi$  steradians (i.e., a full sphere) is used. For convex objects, the average cross-section area is one-fourth of the object's total surface area. [12] The CROC tool in the DRAMA suite is capable of simulating the shape of a satellite based on simple components (spheres, cubes, cylinders, etc.) and compute a more detailed cross-sectional area in different viewing perspectives, as well as in a tumbling state.

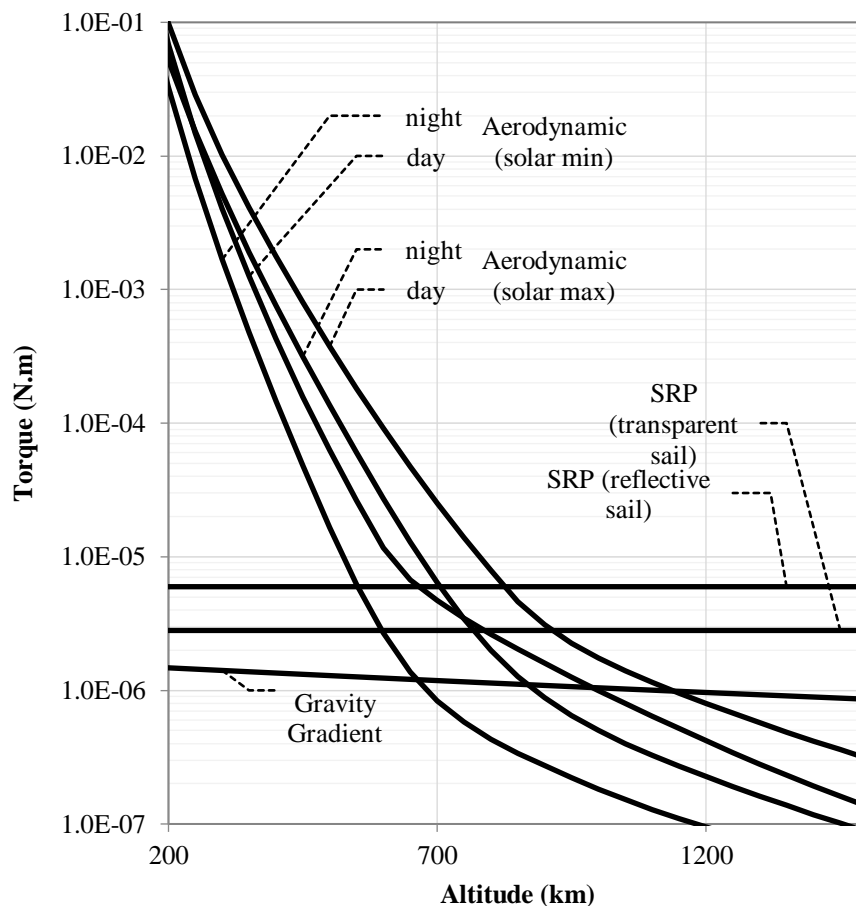


**Figure 5.19** The aerodynamic, solar, and gravity-gradient torque versus altitude for a 100 kg satellite with 25 m<sup>2</sup> sail is depicted for LEO applications.

#### Dependence on Power and Other Satellite Subsystems

As mentioned earlier, an advantage of a drag-augmentation deorbiting strategy is the fact that the host satellite does not necessarily have to be active for the entire de-orbiting phase. Figure 5.20 depicts how the drag sail may be implemented in a fail-safe deployment mode. The deployment actuation itself, however, may require power or an active host satellite. One way to implement a

fail-safe strategy is to make use of a battery or capacitor to store energy while the satellite remains operational. If the spacecraft power fails, a countdown timer can be triggered and unless the spacecraft power is restored in a certain time, the deployment actuation will occur and the de-orbiting phase will begin. This functionality can exist alongside a normal commanded deployment. Such a command interface should also allow for first arming the device before triggering the deployment, again to prevent accidental deployment commands.

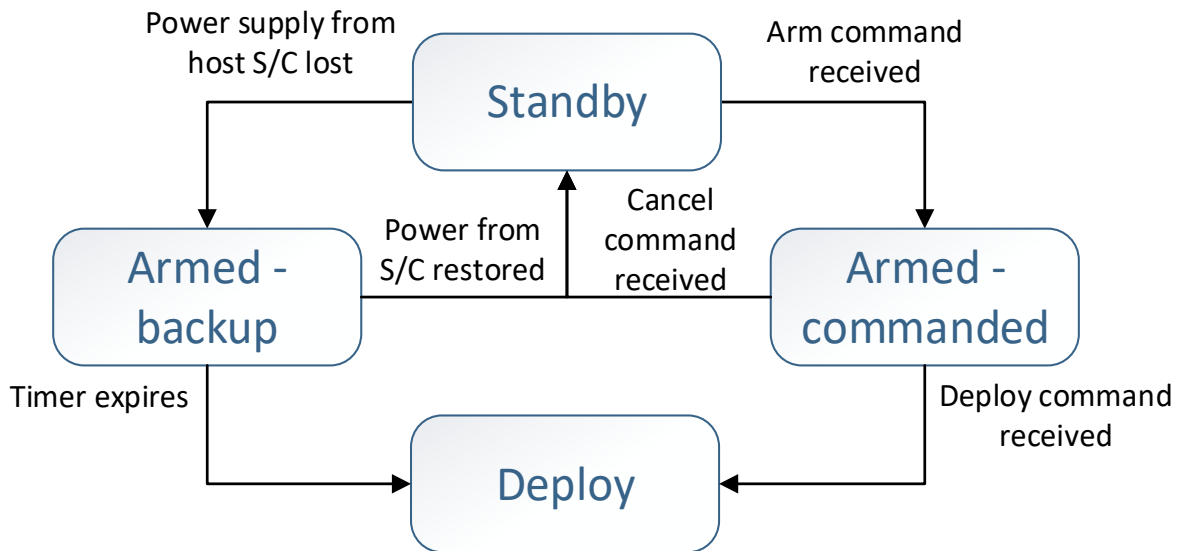


**Figure 5.20** The deployment activation state diagram identifies the key operational activities required for fail-safe deployment of a drag sail.

The actual power requirement to actuate the deployment can be quite low. The deployments for InflateSail and NanoSail-D2 were driven by electric motors, powered through a typical cubesat Electric Power System (EPS). Miniature CGGs also have relatively low power requirements. Both CGGs and deployment motors can be actuated with less than 10 W power. In all cases, except for the inflation-maintained sphere, the duration for which electrical power is required is also relatively short (i.e., on the order of minutes or even seconds).

### Mechanical Deployment Reliability

Mechanical deployment in space remains a challenging task. Mechanical parts are susceptible to cold-welding. Friction in bearings and between other moving mechanical parts can increase with extreme temperatures and lack of atmosphere causes lubricants to become less effective. Cold temperatures can also inhibit “thermal knife” actuators.

It is difficult to test deployable devices on the ground, because of their large size and fragile construction. It makes it difficult to fit the entire device into a vacuum chamber and to perform deployments in thermal vacuum conditions. The effect of Earth gravity is also a nuisance when it

comes to testing deployable elements. The structures that maintain the shape of the drag device, such as the booms and cables, are designed to withstand aerodynamic forces, but tend to fail under Earth gravity. Gravity off-loading methods, such as suspending booms from gantries or helium-filled balloons, are typically employed in deployment tests. An example of such a setup can be seen in Figure 5.21.



**Figure 5.21** Surrey Space Centre’s InflateSail: carbon-fibre boom tips are suspended from sliding gantry. (Image Credit: Surrey Space Center)

### Cost

The availability of lightweight materials used in gossamer structures influences the cost of manufacturing them. Deployable structures remain a relatively expensive component, however, the advent of COTS deployable deorbiting devices should lead to a cost reduction, similar to how other commercially-available cubesat hardware has influenced the market. The complexity of inflatable systems can also be expected to increase cost.

### Active Drag Augmentation

Some spacecraft may be able to use their own components to increase drag on their spacecraft in order to measurably reduce its orbital lifetime. For example, turning solar arrays into the ram direction, orienting the satellite to maximize cross-sectional area, or opening up battery casing covers all provide ways to potentially decrease orbital lifetime. Planning in satellite design in advance to leverage embedded features may either reduce or eliminate the need to apply PMD devices. However, this might also introduce significant additional design and/or operational complexity, thus increasing overall mission risk.

### Summary

Successful sail deployments from NanoSail-D2, LightSail-1, InflateSail, and other missions have demonstrated that drag sail de-orbiting is indeed feasible for microsatellites. It is important for the

technology to become more reliable so that deployment failures do not hamper the success of the de-orbiting goals.

Advances in materials and the availability of ultra-thin membranes enable gossamer structures that can drastically increase a satellite's AMR with minimal parasitic mass. Such a strategy can be used to comply with debris mitigation requirements. Even a slight increase in AMR will lead to a shorter deorbit duration or increase the altitude from which the satellite can start deorbiting.

Drag augmentation, however, is limited operationally to orbits below 800-1000 km. At higher altitudes the required AMR becomes problematic, such that the deployable structure will be too large and heavy for the satellite. Drag augmentation can also only be applied to situations where an uncontrolled re-entry is acceptable.

Although drag augmentation can be achieved by both deployable sails and inflatable structures, sails remain the more competitive choice for smaller satellites, due to the small mass and volume impact, and undesirable complexity of an inflatable system. Drag sails still have challenges. These include guaranteeing reliable deployment, attitude stability, and integration complexity with the host satellite.

## References

1. Petro, A. J., "Techniques for Orbital Debris Control," AIAA PAPER 90-1364 presented at the AIAA, NASA, and DOD, Orbital Debris Conference: Technical Issues and Future Directions, Baltimore, MD, Apr. 16-19, 1990.
2. Macdonald, M., McInnes, C., Bewick, C., Visagie, L., Lappas, V., and Erb, S., "Concept-of-Operations Disposal Analysis of Spacecraft by Gossamer Structure", *Journal of Spacecraft and Rockets*, Vol. 52, No. 2 (2015), pp. 517-525
3. Johnson, L., Whorton, M., Heaton, A., Pinson, R., Laue, G., and Adams, C., "NanoSail-D: A Solar Sail Demonstration Mission," *Acta Astronautica*, Vol. 68, No. 5, 2011, pp. 571–575.
4. Lappas, V., Adeli, N., Visagie, L., Fernandez, J., Theodorou, T., Steyn, W., and Perren, M., "CubeSail: A Low Cost CubeSat Based Solar Sail Demonstration Mission," *Advances in Space Research*, Vol. 48, No. 11, 2011, pp.1890–1901.
5. L.G. Jacchia, "Atmospheric Models in the Region from 110 to 2000 km," *COSPAR International Reference Atmosphere 1972*, International Council of Scientific Unions (Akademie-Verlag, Berlin, 1972), p 227.
6. L.G. Jacchia, "Thermospheric Temperature, Density and Composition: New Models: S.A.O. *Special Report No.375* (Smithsonian Astrophysical Observatory, Cambridge. MA,1977).
7. F. Barlier. C. Berger, J.L. Falin, G. Kockarts, and G. Thuillier, "A Thermospheric Model Based on Satellite Drag Data: *Ann. Geophys.* 34, 9 (1978).
8. A.E. Hedin. "A Revised Thermospheric Model Based on Mass Spectrometer and Incoherent Scatter Data: MSIS83," *J. Geophys. Res. A* 88, 10,170 (1983).

9. De Pater, Imke and Lissauer, Jack, Planetary Sciences, 2<sup>nd</sup> Ed., Cambridge University Press, 2010
10. G.E. Cook, "Satellite Drag Coefficients," Planet. Space Sci. 13. 929 (1965).
11. FA Herrero, "The Drag Coefficient of Cylindrical Spacecraft in Orbit at Altitudes Greater Than 150 km: NASA, Technical Memorandum 85043 (Goddard Space Flight Center. Greenbelt, MD. 1983).
12. Slepian, Z., The Average Projected Area Theorem – Generalized to Higher Dimensions, 2011. [arXiv:1109.0595](https://arxiv.org/abs/1109.0595)
13. Vallado, D. A., "Special Perturbation Techniques," *Fundamentals of Astrodynamics and Applications*, 2nd ed., Microcosm Press, El Segundo, CA, 2001, Chap. 8.
14. Battin, R. H., "Variation of Parameters," *An Introduction to the Mathematics and Methods of Astrodynamics, Revised Edition*, Revised ed., American Institute of Aeronautics and Astronautics, Inc., Reston, VA, 1999, Chap. 10.
15. Wertz, J. R., and Larson, W. J., *Space Mission Analysis and Design*, 3rd ed., Microcosm Press, Torrance, CA, 1999, pp 144-145.
16. L.G. Jacchia and J.W. Slowey, "Analysis of Data for the Development of Density and Composition Models of the Upper Atmosphere: AFGL-TR-81-0230 (Air Force Geophysics Laboratory. Hanscom Air Force Base. MA. 1981), AD-A-100420.
17. "NASA's Nanosail-D 'Sails' Home -- Mission Complete," NASA, Nov. 29, 2011, URL: [http://www.nasa.gov/mission\\_pages/smallsats/11-148.html](http://www.nasa.gov/mission_pages/smallsats/11-148.html)
18. A. Viquerat, M. Schenk and V. Lappas, "Functional and Qualification Testing of the InflateSail Technology Demonstrator," 2nd AIAA Spacecraft Structures Conference, AIAA SciTech Forum. doi:10.2514/6.2015-1627
19. Underwood, C, Viquerat, A, Schenk, M, Fellowes, S, Taylor, B, Massimiani, C, Duke, R, Stewart, B, Bridges, C, Masutti, D & Denis, A 2017, "The InflateSail CubeSat Mission: The First European Demonstration of Drag-Sail De-Orbiting," in 4<sup>th</sup> IAA Conference on University Satellite Missions and CubeSat Workshop., IAA-AAS-CU-17-04-05, Univelt Inc
20. Taylor, B., Underwood, C., et al, "Flight Results of the InflateSail Spacecraft and Future Applications of Drag Sails," Smallsat Conference, Logan, Utah, August 2018.
21. RocketLab: Rocket Lab confirms new 'It's Business Time' launch window and bolsters manifest, 25 May 2018, URL: <https://www.rocketlabusa.com/news/updates/rocket-lab-confirms-new-its-business-time-launch-window-and-bolsters-manifest>
22. A. Viquerat, M. Schenk, B. Sanders, V. Lappas, "Inflatable Rigidisable Mast for End-of-Life Deorbiting System," Proceedings of the 13th European Conference on Spacecraft Structures, Materials & Environmental Testing, held 1-4 April, 2014 in Braunschweig, Germany
23. Fernandez, J. M., Visagie, L., Schenk, M., Stohlman, O. R., Aglietti, G. S., Lappas, V. J. & Erb, S., 2014. Design and development of a gossamer sail system for deorbiting in low earth orbit. Acta Astronautica, 103(0), pp. 204-225.
24. Charles D. Brown, Spacecraft Propulsion, AIAA Education Series, 1996

25. A.Tummala, A.Dutta, “An Overview of Cube-Satellite Propulsion Technologies and Trends,” MDPI Aerospace 2017, 4(4), 58, pp. 1–30
26. J.Mueller, R.Hofer, M.Parker, and J.Ziemer, “Survey Of Propulsion Options For Cubesats“, JANNAF-1425, 57<sup>th</sup> JANNAF Propulsion Meeting, May 3-7, 2010, Colorado Springs, CO.
27. S. Trofimov, M. Ovchinnikov, Performance Scalability of Square Solar Sails, Journal of Spacecraft and Rockets, 2018, Vol. 55, No. 1, pp. 241-245.

## CHAPTER 6 USING OTHER RETARDING FORCES

---

### KEY POINTS

Retarding-drag forces of sunlight and the Earth's magnetic field can be leveraged via a solar sail and electrodynamic tether, respectively, to deorbit a LEO microsatellite.

A solar sail requires very little mass or complex circuitry and leverages a freely available fuel source (i.e., sunlight). However, the large collision cross-section of the sail, the small accelerations available, dynamic direction of the forces, space environmental effects, and the requirement to maintain attitude control create a combination of engineering issues that must be understood and managed.

An electrodynamic tether (EDT) typically has a smaller volume and lower mass than a chemical propellant system but is typically larger, more massive, and more complicated than an electric thruster. An EDT also loses some effectiveness at higher inclinations ( $>60^\circ$ ) and higher altitudes ( $>1000$  km). The EDT solution has limited operational experience relative to either type of propulsion system but has the potential for significant performance as a PMD device.

---

### Introduction

For LEO satellites in orbits higher than 800-1,000 km, it is impractical to use atmospheric drag to deorbit. Propulsive systems, while effective from any altitude, do require fuel and an onboard propulsion system. Two possible PMD device alternatives to propulsion and drag augmentation are covered in this chapter: exploiting either the solar radiation pressure (SRP) force or the Lorentz force. Both forces can be leveraged through a solar sail or an electrodynamic tether (EDT), respectively. The following two sections of this chapter will describe both options, including the corresponding operational constraints, requirements, and performance.

### Solar Sail

It is well known, since J. Maxwell and P. Lebedev, that electromagnetic radiation exerts a force upon any physical body. The value of solar radiation pressure varies with distance to the Sun according to an inverse square law and equals approximately  $4.56 \mu\text{N}/\text{m}^2$  at the distance of 1 astronomical unit (approximately  $150 \times 10^6$  km) from the Sun (i.e., at the Earth). For an arbitrary flat panel, the SRP force can be decomposed into two parts, one being aligned with the panel normal and the other being opposite to the sun vector (see Figure 6.1). [1] The SRP force attains the maximum magnitude when the panel is totally specular reflective.<sup>27</sup> In this case, the force

---

<sup>27</sup> This means that all energy reflects from the panel at the same angle, relative to the panel's normal, as the incident energy.

created is in the panel's anti-normal direction. Conversely, if the panel is totally absorptive, the SRP force is directed opposite to the Sun. Any natural or artificial celestial body with a more complex shape can be approximated by a series of flat polygons, which makes it possible to calculate the net SRP force and torque through superposition of individual polygon-based forces.

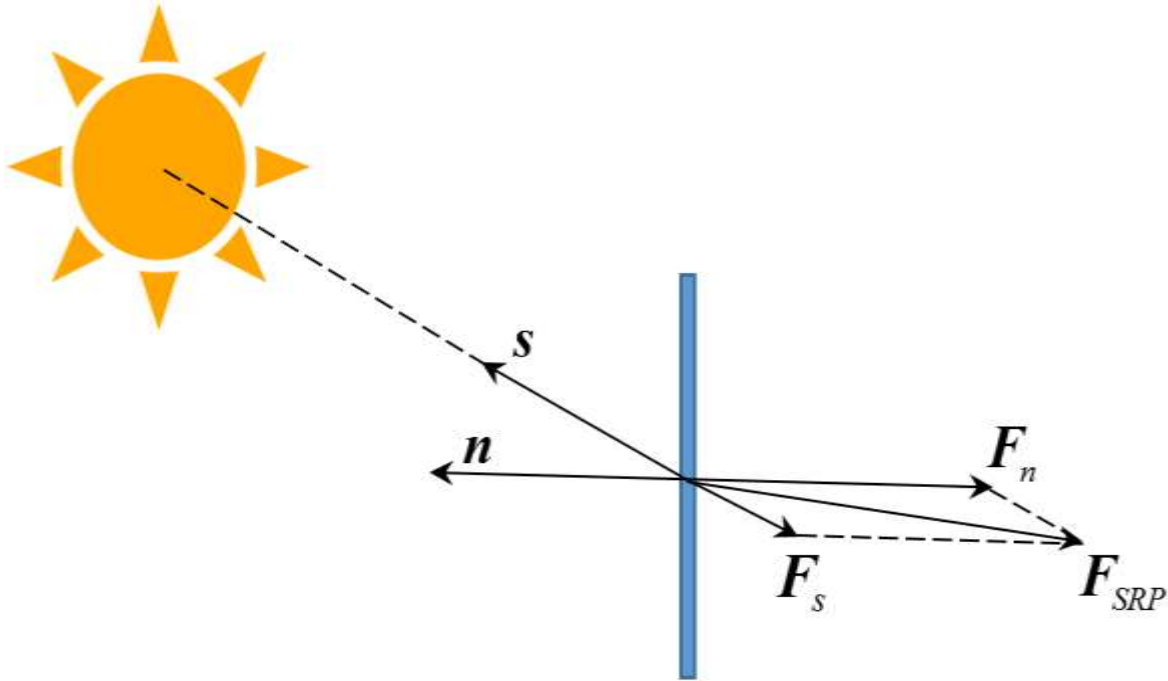


**Figure 6.1** The decomposition of the solar radiation pressure force,  $F_{SRP}$ , into the anti-normal,  $F_n$ , and anti-sun,  $F_s$ , parts shows that the more light-absorptive the surface, the larger the anti-sun component of the SRP force.

To increase the SRP force acting upon a satellite, one can deploy a large, but lightweight, highly reflective membrane. Such a membrane, along with its mounting system, is called a solar sail. The sail membrane is typically made of some light plastic, such as Mylar or Kapton, and covered with an aluminum layer on one or both sides. [1] Though the shape of sail-like deployable space structure is not necessarily flat, this configuration is the most common and the only one discussed in this chapter.

There are two main classes of flat sails depending on whether a sail system includes quasi-rigid deployable booms holding membrane petals. The square sail consisting of four booms with four triangular petals is a typical configuration of the first class [2]; examples of this type were shown in Chapter 5.

Solar sails may also be spin-stabilized to exploit the centrifugal force during the deployment process and for keeping the membrane stable. Spin-stabilized sails are considered Class 2 sails. As a result, solar sails of the first class—mostly of square form—are used most often despite their three-axis stabilization constraint and higher operating reliability (than spin-stabilized sails). Since

the SRP force is directed close to the normal of the mirror-like solar sail, three-axis attitude control of the sailcraft is required to provide controllability of the orbital motion.

Several sailcraft have been successfully operated in space, with the first completely successful deployment being the Japanese interplanetary mission IKAROS in 2010 [3].<sup>28</sup> Considering the growing number of near-future missions involving the use of solar sails, we can say that the space sailing is an emerging trend in propulsion for small spacecraft. However, past successes of solar sails have primarily been on interplanetary missions.

Is a solar sail suitable for LEO?

Using a sail as a tool for SRP force augmentation is commonly believed to be acceptable for medium and high Earth orbits as well as interplanetary trajectories. [4] A closer look reveals that the upper segment of LEO is also potentially suitable for this purpose. It is important to note that both the atmospheric drag force and the SRP force depend in a similar way on the area-to-mass ratio (AMR) of a satellite: the magnitude of either acceleration is proportional to AMR. However, the direction of the projected area is typically different for the drag augmentation and solar sail applications.

Solar radiation pressure magnitude is obviously almost constant for satellites in LEO, whereas the drag force rapidly decreases with increases in altitude. However, the solar sail goes in and out of the Sun during an orbit and has to be re-oriented to maintain a large area pointing toward the Sun. At altitudes above about 700-800 km, the maximum SRP force can surpass the drag force. The absolute values of these two forces for a 3U cubesat with a 5 m x 5 m square sail are shown in Figure 6.2.

The behavior of the two main perturbation forces, excluding the  $J_2$  effect (i.e., Earth not being a perfect sphere) which is irrelevant for deorbiting, allows us to come up with an idea of using a sail in the solar mode when the satellite just begins the deorbiting process from a higher LEO orbit (from 800-2,000 km) and switching it to the drag mode when the satellite's orbit drops below approximately 700-800 km. The main challenge here is to properly and efficiently control the solar sail attitude to ensure an SRP-induced secular decrease in the semi-major axis.

---

<sup>28</sup> The Russians deployed the sail Znamya in 1993 but it was partly torn-out during deployment <https://www.smithsonianmag.com/smart-news/how-russian-space-mirror-briefly-lit-night-180957894/> . The Japanese also deployed a successful one in 2004 <https://www.space.com/25800-ikaros-solar-sail.html> .

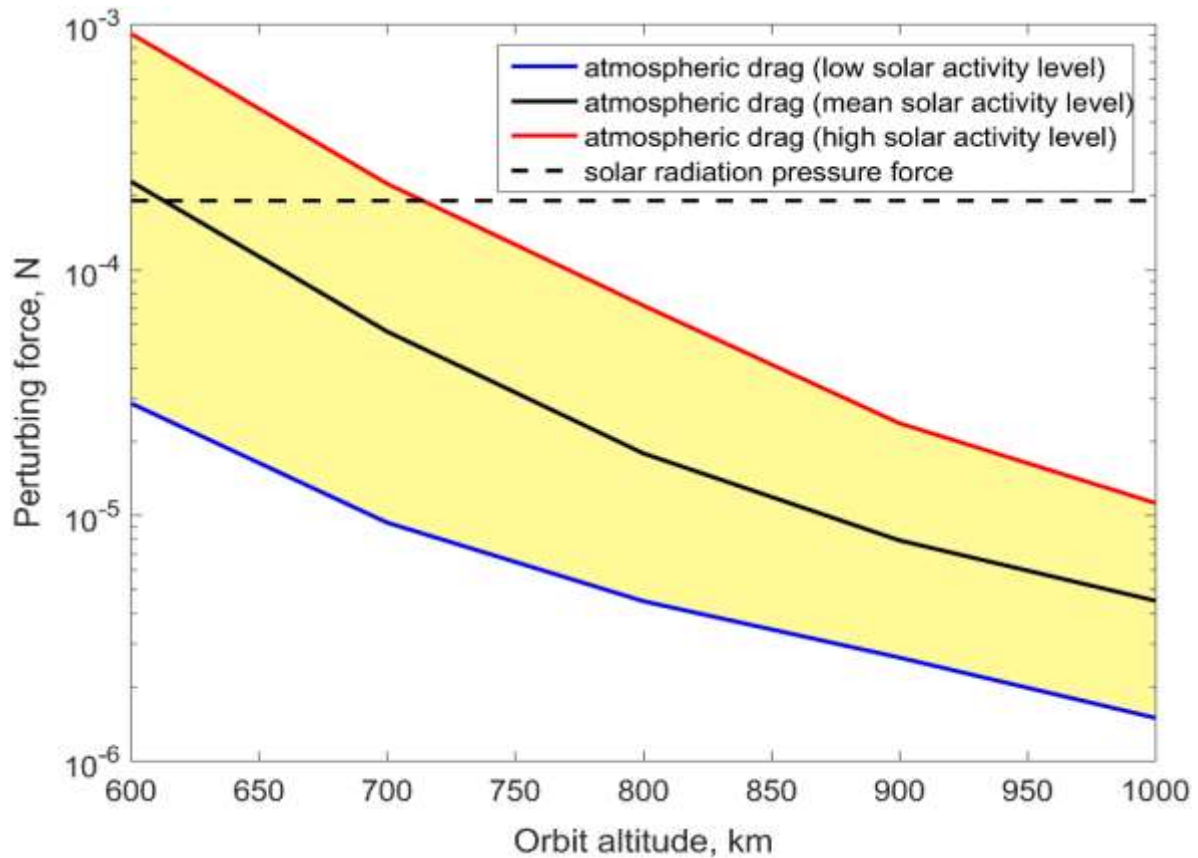


**Figure 6.2** Perturbing forces of atmospheric drag and solar radiation pressure acting on a 5 kg satellite with a 25 m<sup>2</sup> solar sail are depicted. The qualitative behavior observed is AMR-independent and would be the same for any spacecraft with any sail as long as the sail is kept ram-facing or Sun-facing.

#### Apparent Sun motion in the orbital frame

In the orbital frame centered in the satellite's center of mass and rotating almost uniformly as the satellite revolves around the Earth in a near-circular orbit, the sun vector revolves around the orbit plane normal at the orbital rate sweeping out a conical surface (see Figure 6.3).

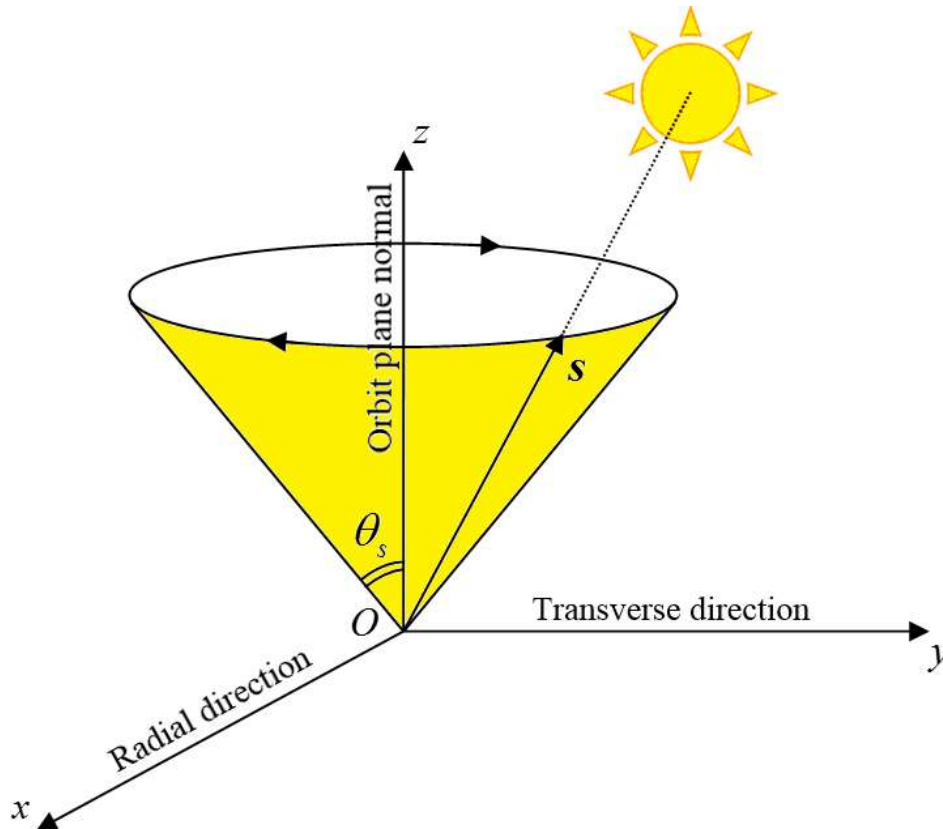


**Figure 6.3** The apparent Sun motion in the orbital frame is depicted with the  $O_z$ -axis as the orbit plane normal; the  $O_x$ -axis is along the geocentric radius vector. For a near-circular orbit, the satellite velocity is aligned approximately with the transverse direction (the  $O_y$ -axis).

The solar cone angle  $\theta_s$  depends on the orbit plane orientation with respect to the sun vector and can change over time due to the  $J_2$ -induced nodal precession and the annual apparent Sun motion along the ecliptic.

The sail normal attitude primarily matters, not the sun direction. Further, the greatest stability in  $\theta_s$  can be achieved for sun-synchronous orbits whose plane precesses at the same rate as the Earth's annual path around the Sun (i.e., about 1 deg/day).

#### Solar sail orientation favorable for deorbiting

If we assume, without loss of generality, that the Sun is the  $z$ -positive hemisphere with respect to the orbit plane, then the SRP force would slow the satellite down provided the sail normal is near the first quadrant of the  $y$ - $z$  plane of the orbital frame. This case corresponds to the clock angle of the solar sail normal  $\psi \approx 180^\circ$  (see Figure 6.4), while the optimal value of its cone angle  $\phi$  depends on the solar cone angle  $\theta_s$ .

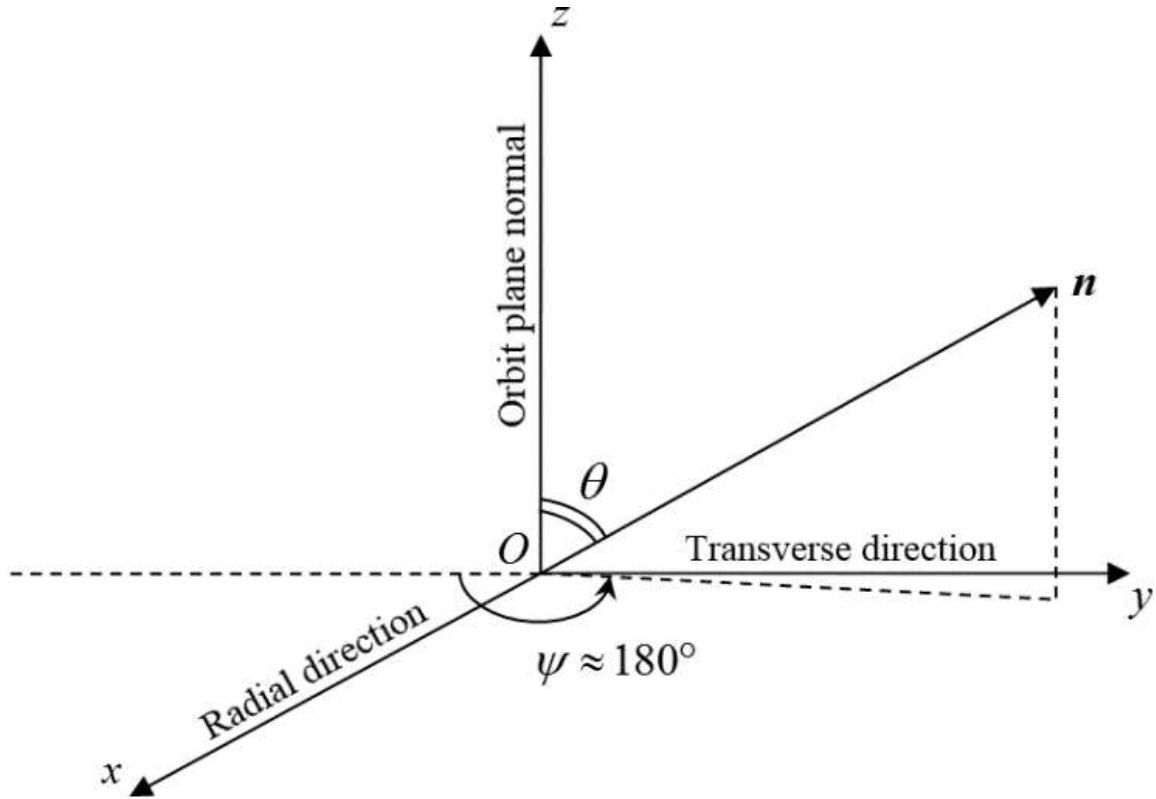


**Figure 6.4** The orientation of the solar sail normal favorable for SRP-based deorbiting is shown.

One may introduce the useful concept of SRP force deorbit efficiency: for a near-circular orbit, this is defined as the orbit-averaged transverse component of the SRP force divided by the maximum magnitude of the SRP force. Considering the square sail ideal (i.e., with total specular reflection) and taking into account that LEO objects are in Earth's shadow about half of the time, one can plot a series of curves  $\eta_{SRP} = \eta_{SRP}(\bar{\theta})$  for different values of the solar cone angle  $\theta_s$ . Here  $\eta_{SRP}$  is average SRP force deorbit efficiency and  $\bar{\theta}$  is the orbit-averaged cone angle of the sail normal (the clock angle is assumed to be equal  $180^\circ$ ). Such curves are shown in Figure 6.5. For example, if the Sun sweeps out a conical surface with the cone angle  $\theta_s = 45^\circ$ , we can attain the maximum decrease rate in the semi-major axis by keeping the average attitude angles of the solar sail normal close to  $\bar{\psi} = 180^\circ$ ,  $\bar{\theta} = 50^\circ$ .

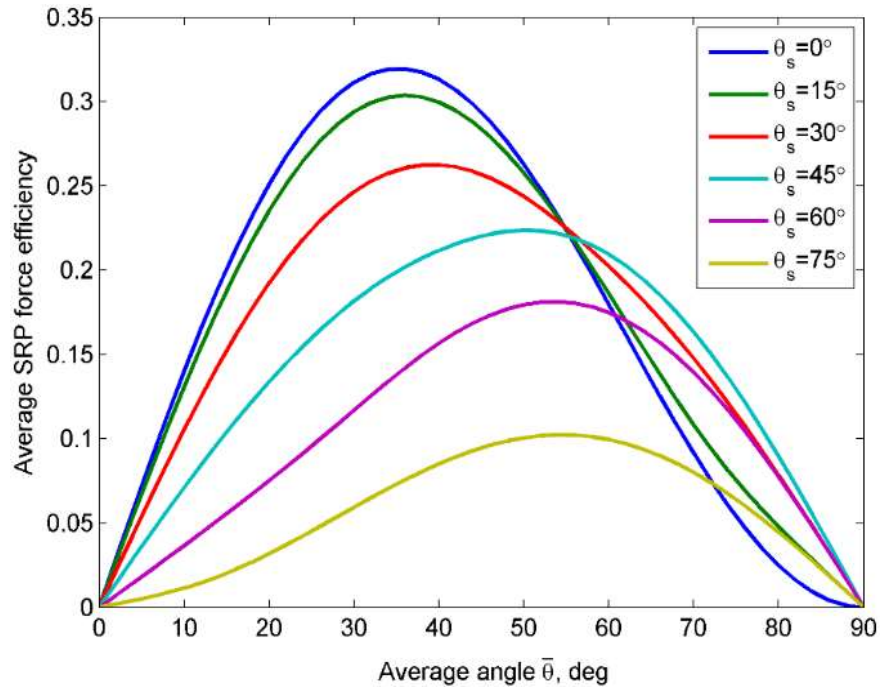


**Figure 6.5** SRP force efficiency as a function of the average sail normal cone angle shows the importance of the proper orientation of the sail to achieve desired results.

#### Solar sail attitude dynamics and control

A microsatellite with the deployed square sail has typically an oblate ellipsoid of inertia, with the largest principal axis of inertia being directed approximately along the sail normal. The desired sail normal attitude in the  $y$ - $z$  plane resembles the hyperbolic relative equilibrium, one of the three relative equilibria of an axisymmetric rigid body in the orbital frame under the action of the gravity-gradient torque discovered independently by V. Beletsky [5], P.W. Likins [6], and R. Pringle [7]. The single necessary condition of hyperbolic equilibrium stability consists in keeping the sailcraft spin rate (the absolute value of the angular velocity component along the sail normal) smaller than the orbital rate. However, the problem is much more complicated when we talk about small spacecraft with a solar sail of significant size. For instance, for a 3U cubesat with a 5 m x 5 m square sail, the aerodynamic and solar torques have the same order of magnitude as the gravity-gradient torque at altitudes within a range of 700-900 km (see Figure 6.6), which leads to substantially different attitude dynamics. [8, 9]

Note that even at those altitudes where the SRP force already dominates over the drag force, the corresponding torques are still comparable: the solar torque is generated mostly due to the relatively small anti-sun absorption component, whereas the major anti-normal component does not produce any torque because the shift between the center of pressure (CoP) and the center of mass (CoM) is also aligned (or almost aligned) with the sail normal.

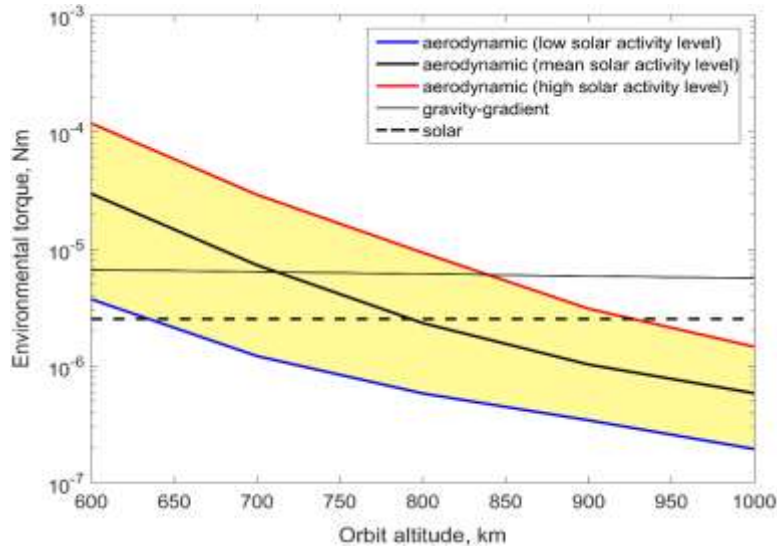


**Figure 6.6** The external torques acting upon a 3 kg satellite with a 25 m<sup>2</sup> solar sail are shown with the assumption of a 13 cm distance between the center of pressure and the center of mass.

In spite of more complicated dynamical environment, recent studies [10, 11] show that it is possible to stabilize the desired “hyperbolic” attitude (no longer an equilibrium in the complex dynamics) of the solar sail normal. Stabilization can be attained even when using a simple active magnetic attitude control system. The control law is generally composed of three parts: the damping control, the spin rate control, and the potential control. [10, 11] The first one damps the angular velocity of the sail normal relative to the orbital frame. This control component is critical and should be applied at any time. The spin rate, the component of the sailcraft angular velocity along the sail normal  $\omega_n$ , is nominally the integral of motion, but under the conditions of a real flight the control should be periodically switched on to keep the spin rate close to the desired small value. Finally, in some cases the potential control is required for stabilization. It tends to align the sail normal to the desired orientation. What is important is that all of the control components are of the same order of magnitude as the environmental torques and, therefore, affordable for small satellites.

The resulting EOL disposal duration, as can be observed from Figure 6.7a-b, is considerably lower than for the traditional velocity-pointing sail attitude (Figure 6.7c) or especially the uncontrolled rotation regime (Figure 6.7d). Furthermore, the lower the solar activity level, the greater the difference in performance. The key role is played by the SRP force ensuring the rapid decrease in altitude at the start of the deorbit process.

It is worth emphasizing that the correct choice of the nominal spin rate can significantly speed up the disposal. This fact is convincingly demonstrated by Figure 6.7a and Figure 6.7b: the initial orbit decay rate can be more than doubled. The reason consists in the refined tuning of the orbit-averaged cone angle of the sail normal. It becomes closer to the optimal value, which boosts SRP force deorbit efficiency. The hyperbolic regime, being effective in the solar mode of functioning,

gradually transforms to the aerostabilized regime as the orbit altitude drops and the atmospheric drag increases. Thus, it can be viewed as a natural high-altitude complement to the drag sail deorbit strategy.

In general, the solar torque tends to destabilize the hyperbolic attitude. Hence, one should avoid large values of the CoP-CoM distance. It is especially important considering the sail membrane degradation, which increases absorption and, as a result, the solar torque. Modern telescopic sail deployment mechanisms with an adjustable arm length could help solve this problem.

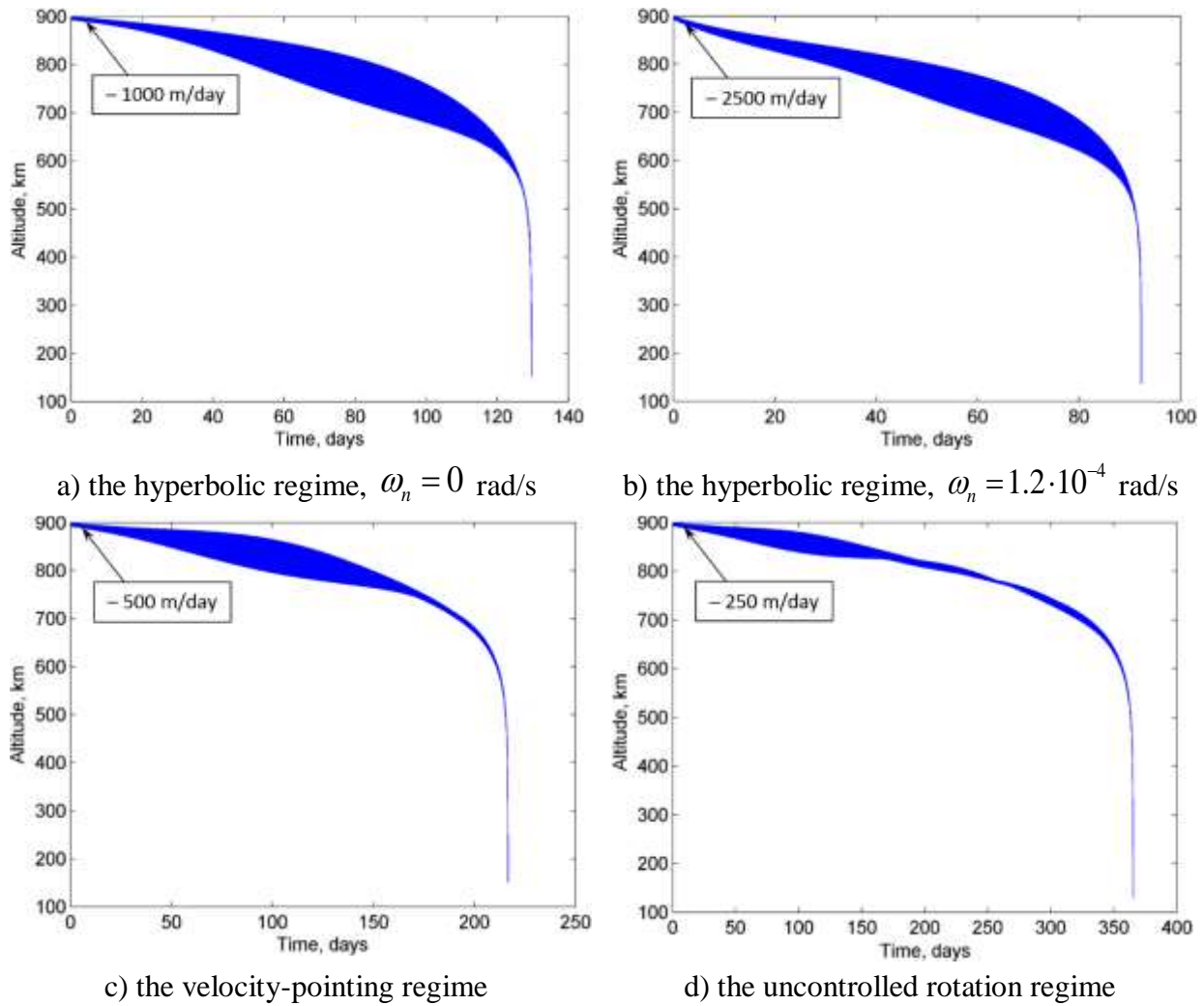


**Figure 6.7** The evolution of the orbit altitude for the 900 km dusk-dawn sun-synchronous orbit at mean solar activity is depicted for a 3 kg satellite with a 25 m<sup>2</sup> solar sail.

It can be seen that the effectiveness of a solar sail can vary by an order of magnitude based on the stability of the satellite using the solar sail. However, even the worst-case situation shows that a 3 kg satellite can be easily deorbited within the 25-year threshold if equipped with a 5m x 5m sail. Such a size is larger than is needed for a 3U cubesat. With this size of sail, one can afford a non-

optimal attitude control (e.g., no control at all, just chaotic rotations) while still complying with the 25-year rule. However, for more challenging cases (e.g., higher altitude or larger mass), active attitude control becomes critical.

Table 6-1 collects the deorbit time ranges calculated in the numerical simulations for a series of sun-synchronous orbits with different local times of the ascending node. A 25 m<sup>2</sup> sail appears to be suitable for the end-of-life disposal of a 30 kg satellite in any low Earth orbit and even for a 100 kg satellite in an orbit below 1,000 km.

In some cases, performance can be increased by applying an additional control torque. In the performed simulations, this has not been done, unless necessary for the attitude stabilization. It is interesting to note that the stability of the hyperbolic attitude regime is ensured even for a 100 kg satellite in a 1,200 km or 2,000 km orbit, but the decay rate is too low to satisfy the 25 yr requirement. Consequently, a larger sail is needed in these cases.

**Table 6-1** The deorbit time for sun-synchronous orbits of different altitudes are determined assuming a 5 m x 5 m sail at high, mean, or low solar activity (SA) levels. The ranges reflect the variation of the deorbit time across the orbits with different local times of the ascending node.

Deorbit Time						
	Satellite mass					
Orbital altitude	3 kg		30 kg		100 kg	
700 km	high SA	~1 week	high SA	~8-9 week	high SA	~6-7 month
	mean SA	~3-4 week	mean SA	~7-9 month	mean SA	~2-2.5 yr
	low SA	~2-3 month	low SA	~2.5-3 yr	low SA	~11-11.5 yr
900 km	high SA	~8 week	high SA	~1.5-2 yr	high SA	~5-6 yr
	mean SA	~4-6 month	mean SA	~3-4 yr	mean SA	~14-15 yr
	low SA	~5-14 month	low SA	~4-6 yr	low SA	>25 yr
1200 km	high SA	~5-13 month	high SA	~4-6 yr	>25 yr	
	mean SA	~0.5-1.5 yr	mean SA	~6.5-7 yr		
	low SA	~0.6-1.8 yr	low SA	~9-13 yr		
2000 km	high SA	~1-1.8 yr	high SA	~20-28 yr	>25 yr	
	mean SA	~1.2-2 yr	mean SA	~23-31 yr		
	low SA	~1.7-2 yr	low SA	>25 yr		

It should be noted that there is a trade-off for a mission operator between installing a larger (and, hence, more costly and complex) solar sail and supervising the longer deorbit process: the strategy

of exploiting the SRP force is not fully passive although it can be made autonomous or semi-autonomous.

The additional costs for utilizing ground stations and personnel during the deorbiting phase should be taken into account, which often makes targeting the 25 yr deorbit period to be non-optimal. Moreover, the risk of fatal membrane damage and/or failure of some control actuators rapidly rises for a mission lasting longer than 5-10 yrs.

As a rule of thumb, one can recommend to choose a sail providing the area-to-mass ratio of about  $1 \text{ m}^2/\text{kg}$ . For an altitude above 1,200 km, this value is advised to be upgraded to  $2 \text{ m}^2/\text{kg}$ . As modern solar sails weigh about  $50 \text{ g/m}^2$  (including booms and the deployment mechanism), the solar sail system mass ratio can be estimated as being in the region of 5-10% of total spacecraft mass.

### **Electrodynamic Tether (EDT)**

An EDT is a propulsion system which utilizes electromagnetic force as thrust. [12-14] In contrast to conventional chemical and electric thrusters, the EDT does not use propellant for thrust generation but creates force by the interaction between an electric current on the spacecraft and the Earth's geomagnetic field. In this section, the principle of EDT, required components, advantages & disadvantages, and performance levels are introduced.

#### Principles of Operation

The principle of EDT thrust is shown in Figure 6.8. When an end-mass connected with a tether is ejected from a microsatellite, the tether is stabilized in the vertical direction by a gravity-gradient force. An electromotive force is set up within a conductive tether as it moves through Earth's geomagnetic field.

If a pair of plasma contactors at either end of the tether emits and collects electrons, an electric current flows through the tether by closing the circuit via the ambient plasma. The tether then generates a Lorentz force that acts opposite to the direction of flight via interaction between the current and the geomagnetic field. Therefore, an EDT can provide deceleration without the need for propellant or high electrical power. EDT shows promise as a PMD device. An EDT stabilizes with gravity-gradient force and so it can be installed almost any place on the spacecraft without considering the center of mass.

A bare tether (a conductive wire without insulation) can collect electrons and ions directly from the ambient plasma by the electromotive force [15]. Electrons are collected at a positive electrical potential part of the tether, and ions are collected at a negative electrical potential part. However, ions are hard to collect as they are heavier than electrons and so an electron emitter can be installed on the satellite in order to get larger electric current (active EDT). A passive EDT, without an electron emitter, can deorbit a microsatellite as high as 800-1,000 km depending on its orbital

inclination, and tether configuration such as tether length and width. Alternatively, an active EDT is required for microsattellites at a higher altitude and inclination. The passive EDT is simpler and more cost-effective because no operation is required after the tether is deployed. A low-work-function electrodynamic tether which emits electrons from the tether itself utilizing a special coating is possible. [16]

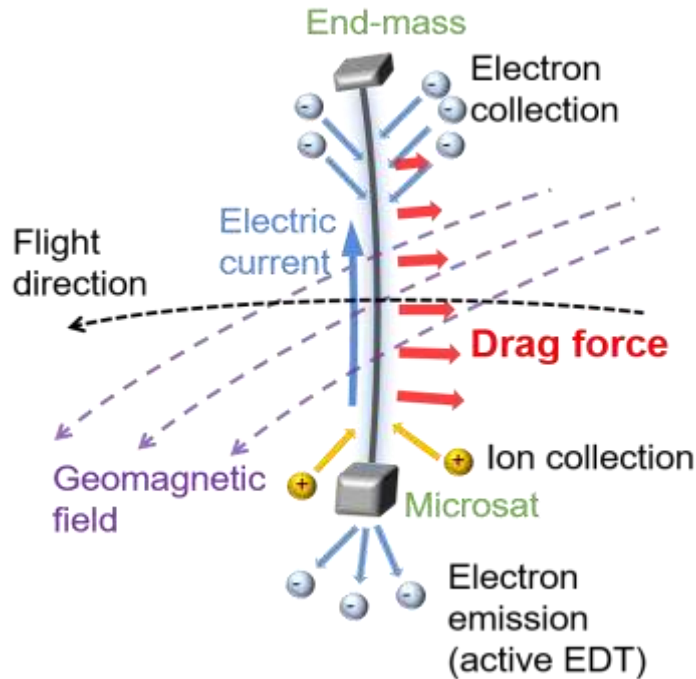


**Figure 6.8** The principle of operation of an electrodynamic tether (EDT) leverages Earth’s magnetic field.

A single-line tether would be susceptible to being severed by collisions with even very small debris objects and micrometeoroids, and could be severed within a short period of time in crowded orbits, [17] so alternatives such as a braided tether, net tether, or tape tether are proposed. [18, 19] Those tethers also have larger electron/ion collection capability but larger air drag. Braided (or knitted) tethers also provide a damping effect of the potential libration of the tethered system.

The tether can be deployed from storage by ejecting an end-mass by a spring. There are several types of reel mechanisms such as (a) drum type, (b) spool type from the outside (outside spool reel), and (c) spool type from the inside (inside spool reel). A folded storage mechanism is proposed for a tape tether. In order to stop tether deployment smoothly, a braking mechanism may be required.

#### EDT - Advantages and Disadvantages

The advantages and disadvantages of an EDT for PMD compared with other propulsion technologies are summarized in Table 6-2.

**Table 6-2** The advantages and disadvantages of EDT provide insights into the utility of an EDT as a viable PMD option.

ADVANTAGES	
High efficiency	EDT can generate sufficient thrust for orbital transfers without the need for propellant by utilizing interactions with Earth’s magnetic field. Because of this, required electric power is lower than that for general electric propulsions.
Simplicity	EDT does not require propellant tanks, valves, and pipes for main deorbit thrust generation.
No requirement for installation place	EDT components can be installed anywhere without considering the center of mass, because the tether will be stabilized by the gravity-gradient force.
No requirement for thrust vector control	Thrust vector control for debris deorbit is not required because the EDT thrust is automatically directed towards lowering the altitude.
DISADVANTAGES	
Mission – less efficient at higher inclination and higher altitude	EDT thrust depends on its orbit and tether configurations such as tether length and diameter; thrust is reduced for high inclination and high altitude where geomagnetic field component and plasma density becomes small.
Possibility of tether being severed	The tether may be severed by impacts from small debris objects or micrometeoroids, prematurely ending the mission. This risk can be minimized by adopting a shorter tether and using a net or a braided or tape tether.
Collision risk with other operational satellites	The risk of collision with operational satellites is a function of the exposed area of the tether. Collision avoidance can be achieved by switching the electric current on and off by shifting the orbital phase of the tether which could possibly serve to control re-entry trajectory. In case of a malfunction or severed tether, a “converging” tether is proposed which would autonomously converge if gravity gradient force is lost. [20]
Difficulty of controlled re-entry	EDT cannot be used to conduct controlled re-entry because of the small thrust generated; this is true for all PMD approaches other than chemical propulsion.
Complexity and reliability of the system	A passive EDT is very simple while an active EDT requires several systems to work together. Once the tether is successfully deployed, the primary concern is impact hazard, like most PMD options.

### Typical EDT performance

The performance of an EDT varies depending on solar activity, tether length, tether diameter, tether material, available electron emitter, and satellite orbit. Figure 6.9 shows deorbit time with EDT for various spacecraft masses and altitudes using one specific EDT solution: nanoTerminator

Tape™, as seen in Figure 6.10. [21] It enables 3U cubesats to comply with the 25-year rule in orbits up to 1000 km. However, it should be noted that actual orbital transfer by EDT has not been confirmed, and an on-orbit demonstration is needed.

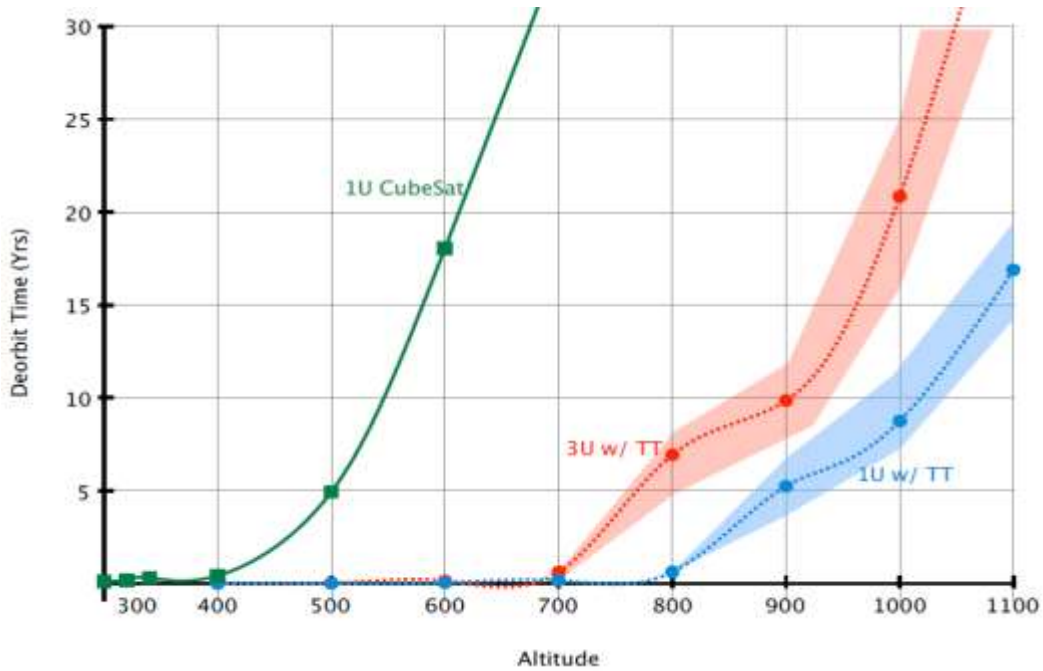


**Figure 6.9** The deorbit profile for 3U and 1U cubesats using nanoTerminator Tape™ (i.e., TT) follow similar general trends. [21]

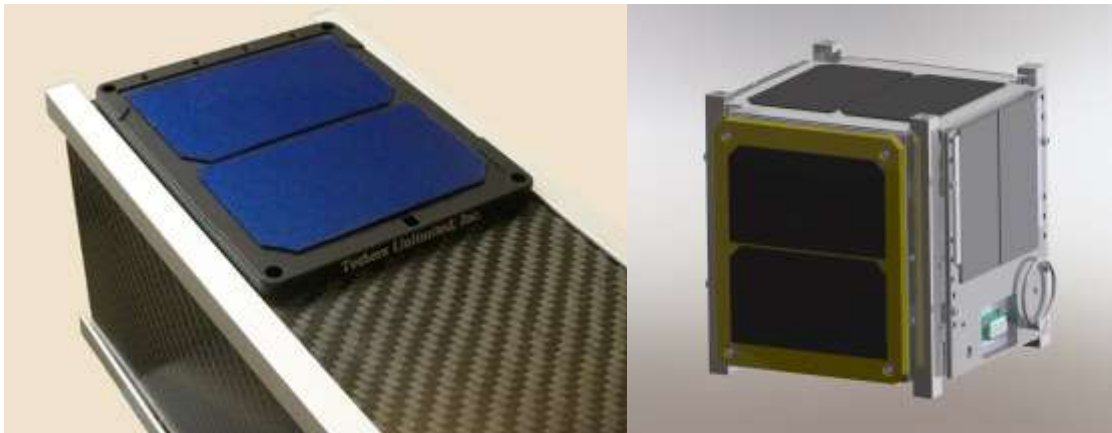


**Figure 6.10** CubeSat nanoTerminator Tape is shown mounted on a 3U cubesat structure (left) [13] and a 1U cubesat (right). [21]

EDT performance changes significantly depending on the orbit. The Lorentz force becomes smaller for high inclination ( $> 60^\circ$ ) and high altitude ( $> 1,000$  km) orbits. To evaluate the available thrust, precise numerical simulations are needed due to variations in the geomagnetic field and plasma density. [18]

Figure 6.11-6.13 depict results of numerical simulations. [22]

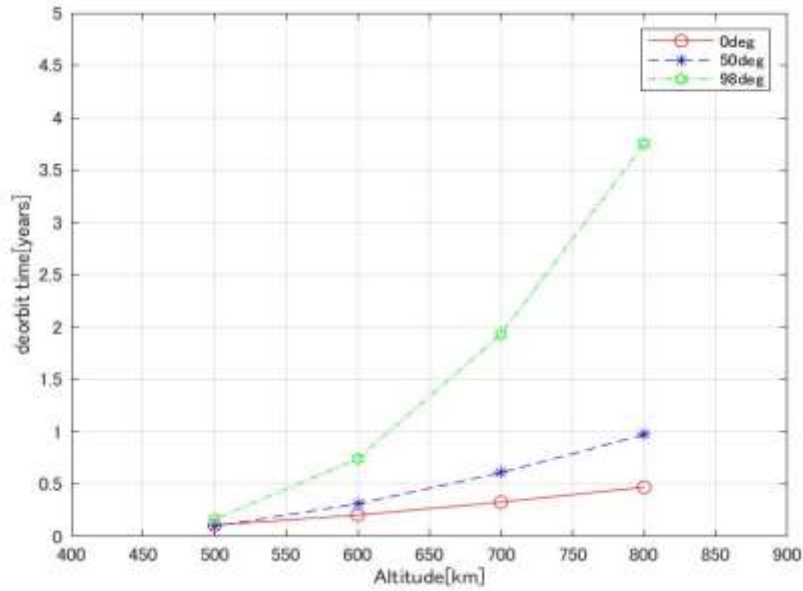


**Figure 6.11** Required deorbit time as a function of altitude are shown for a 70 kg satellite at various orbital inclinations with a tape tether of 900 m in length and 25 mm in width, and an electron emitter of 0.04 A. [22]

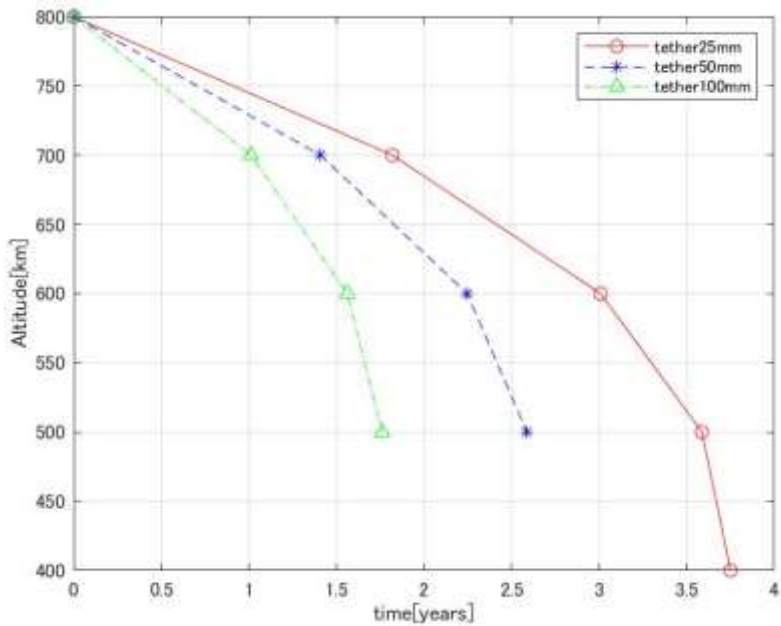


**Figure 6.12** The deorbit time profile for a 70 kg satellite in 800 km SSO with a 900 m tether and electron emitter of 0.04 A.

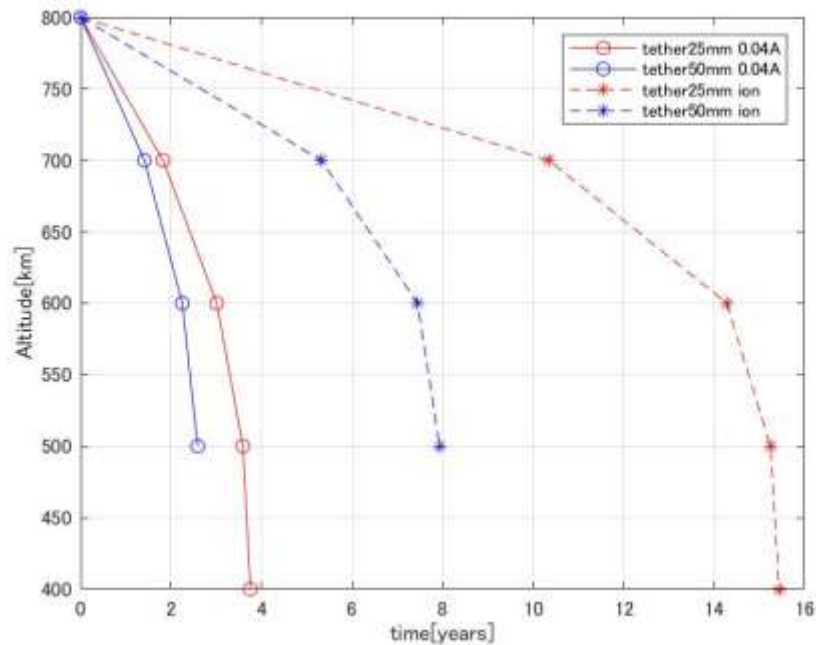


**Figure 6.13** The deorbit time profile for a 70 kg satellite in 800 km SSO with a 900 m tether, with and without electron emitter of 0.04 A.

#### Past Missions and Plans of EDT

Nonconductive tethers up to 20–30 km in length have been successfully deployed in the past on SEDS-1, SEDS-2, and YES2 missions. For the TiPS mission, a 4 km tether survived for more than 10 yrs and showed that the tether, with appropriate characteristics, can have long lifetime. EDTs such as PMG and TSS-1R showed that electric current can flow through the tether. [12]

In STARS-II, two nanosats connected by a 300 m conductive bare tether, were launched in 2014. Although tether deployment could not be confirmed because of a communications issue, its deorbit rate derived from TLE data was much faster than those of the other cubesats deployed from the same rocket, as shown in Figure 6.14. [23] KITE showed that Field Emission Cathodes (FEC) can emit electrons to the space plasma, although a 700 m bare tether could not be deployed because of a malfunction of the holding mechanism. [24]

For deorbiting a microsatellite, nanoTerminator tape is available from Tethers Unlimited, Inc. [13, 21] It is installed in Aerocube-5 launched in 2013 but details have not been reported though it is described as TRL 8/9. [25]

TEPCE consists of two 1.5U cubesats with 1 km tether; it will be launched on the second Falcon Heavy launch in early 2019, expecting orbit change rate of ~1 km/day. [19, 26]

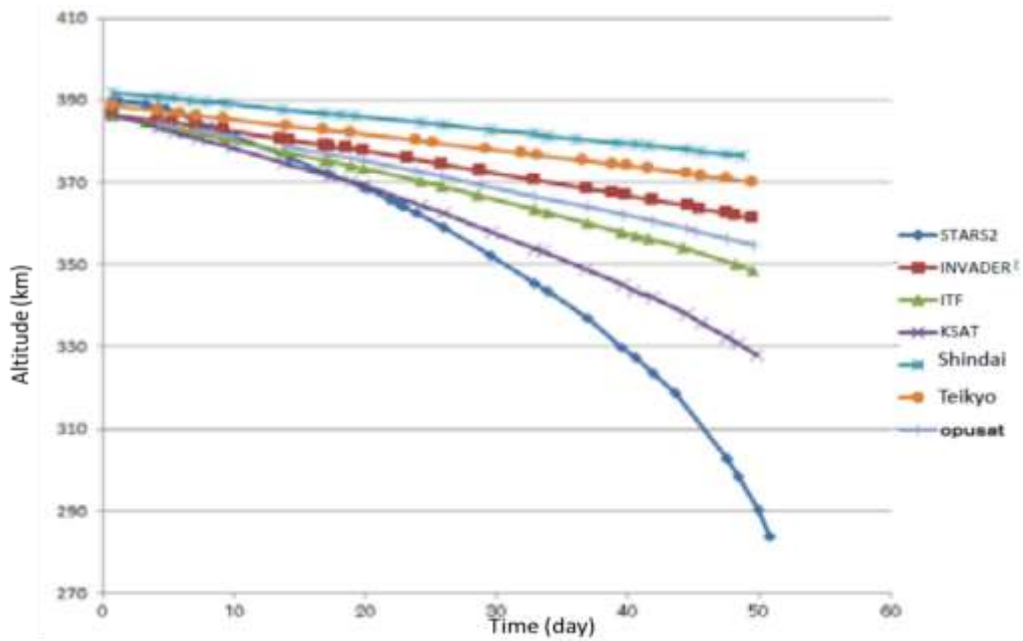


**Figure 6.14** The orbital altitude evolution of seven microsattellites after deployment is depicted highlighting the potential effectiveness of an EDT system. [23]

## Summary

Solar sails and EDTs have the potential for providing viable PMD options for microsattellites. They characteristically may be effective for a wide variety of relevant missions with conceptually low cost to include price, size, mass, and power required. However, these options have limited operational maturity but several ongoing and planned on-orbit technology demonstrations may advance the viability of these options in the near future.

More specifically, a passive EDT would be sufficient for a low inclination orbit, but a 100 kg satellite in Sun Synchronous Orbit would require a longer (heavier) tether for passive EDT so an active EDT with a small electron emitter may make more sense as it would impose a smaller mass penalty and provide a quicker de-orbit time. However, the emitter for the active EDT requires electric power and operation; this is a classic tradeoff that depends on what a microsattellite designer and operator have available for their specific mission. These are the exact issues that will be dealt with in the next chapter covering specific tradeoffs for all PMD options.

## References

1. McInnes, C.R., *Solar Sailing: Technology, Dynamics and Mission Applications*, Praxis Publishing, Chichester, England, U.K., 1999.
2. Fernandez, J.M., Visagie, L., Schenk, M., Stohlman, O.R., Aglietti, G.S., Lappas, V.J., and Erb, S., "Design and Development of a Gossamer Sail System for Deorbiting in Low Earth Orbit," *Acta Astronautica*, Vol. 103, 2014, pp. 204–225. doi:10.1016/j.actaastro.2014.06.018

3. Shirasawa, Y., Mori, O., Okuizumi, N., Satou, Y., Yamasaki, A., Furuya, H., Nishizawa, T., Sakamoto, H., and Ono, G., "Evaluation of Sail Mechanics of IKAROS on its Slow-Spin and Reverse-Spin Operation," *Advances in Solar Sailing*, edited by Macdonald, M., Springer-Verlag, Berlin, 2014, pp. 57–74.
4. Macdonald, M., McInnes, C., Bewick, C., Visagie, L., Lappas, V., and Erb, S., "Concept-of-Operations Disposal Analysis of Spacecraft by Gossamer Structure," *Journal of Spacecraft and Rockets*, Vol. 52, No. 2, 2015, pp. 517–525. doi: 10.2514/1.A32919
5. Beletsky, V.V., *Motion of an Artificial Satellite About its Center of Mass*, Israel Program for Scientific Translation, Jerusalem, 1966.
6. Likins, P.W., "Stability of a Symmetrical Satellite in Attitudes Fixed in an Orbiting Reference Frame," *Journal of Astronautical Sciences*, Vol. 12, No. 1, 1965, pp. 18–24.
7. Pringle, R., "Bounds on the Libration of a Symmetrical Satellite," *AIAA Journal*, Vol. 2, No. 5, 1964, pp. 908–912. doi: 10.2514/3.2436
8. Lawrence, D.A., and Whorton, M.S., "Solar Sail Dynamics and Coning Control in Circular Orbits," *Journal of Guidance, Control, and Dynamics*, Vol. 32, No. 3, 2009, pp. 974–985. doi: 10.2514/1.35970
9. Lawrence, D.A., and Whorton, M.S., "Coning Control of Solar Sails Using Magnetic Momentum Error Reduction," *Journal of Spacecraft and Rockets*, Vol. 46, No. 6, 2009, pp. 1298–1308. doi: 10.2514/1.43088
10. Trofimov, S., and Ovchinnikov, M., "Sail-Assisted End-of-Life Disposal of Low-Earth Orbit Satellites," *Journal of Guidance, Control, and Dynamics*, 2017, Vol. 40, No. 7, pp. 1794–1803. doi: 10.2514/1.G002300
11. Trofimov, S., Tkachev, S., and Roldugin, D., "Sail-Assisted End-of-Life Disposal of High-LEO Satellites," *4<sup>th</sup> International Symposium on Solar Sailing*, Kyoto, Japan, January 17-20, 2017, 7 p. The paper can be accessed via link [http://www.jsforum.or.jp/ISSS2017/papers/paper/17031\\_Paper\\_Dr.%20Sergey%20Trofimo%20v.pdf](http://www.jsforum.or.jp/ISSS2017/papers/paper/17031_Paper_Dr.%20Sergey%20Trofimo%20v.pdf).
12. Cosmo, M.L., Lorenzini, E. C.: *Tether in space handbook*, Third edition, NASA Marshall Space Flight Center, 1997.  
<https://ntrs.nasa.gov/archive/nasa/casi.ntrs.nasa.gov/19980018321.pdf>
13. <http://www.tethers.com/TT.html>
14. <http://www.thebetsproject.com/>
15. J.R. Sanmartin, M. Martinez-Sanchez, and E. Ahedo, "Bare wire anodes for electrodynamic tethers", *J. of Propulsion, Power*, pp.353-360, 1993.
16. Sanchez-Arriaga, G. and Chen, X.: *MODELING AND PERSPECTIVES OF LOW-WORK-FUNCTION ELECTRODYNAMIC TETHERS TO DEORBIT SPACE DEBRIS*, 7TH EUROPEAN CONFERENCE ON SPACE DEBRIS, 2017.
17. C. Pardini, L. Anselmo, T. Hanada, H. Hirayama, "Assessing the Vulnerability to Debris Impacts of Electrodynamic Tethers during Typical De-Orbiting Missions", 4<sup>th</sup> European Conference on Space Debris, 2005.

18. Kawamoto, S., Makida, T., Sasaki, F., Ohkawa, Y., Nishida, S.: Precise Numerical Simulations of Electrodynamic Tethers for an Active Debris Removal System, *Acta Astronautica*, 59 (2006) pp.139-148.
19. Pearson, J., Carroll, J., and Levin, E.: Space Test of LEO Debris Removal, 1st IAA Conference on Space Situational Awareness (ICSSA), Orlando, FL, USA, 13-15 November 2017.
20. Kawamoto, S., Ohkawa, Y., Okumura, T., Iki, K., and Okamoto, H.: Performance of Electrodynamic Tether System for Debris Deorbiting: Re-evaluation Based on the Results of KITE Experiments, IAC-18- A6.6.5, 69<sup>th</sup> International Astronautical Congress (IAC), 2018.
21. Hoyt, R., Barnes, I., Voronka, N., Slostad, J.: The Terminator Tape<sup>TM</sup>: A Cost-Effective De-Orbit Module for End-of-Life Disposal of LEO Satellites, AIAA Paper 2009-6733, Space 2009 Conference, Sept 2009.
22. Watanabe, T., Sato, T., Sakamoto, H., Kawamoto, S., Ohkawa, Y., Kamachi, K., and Okajima, L.: A Study on Post-Mission Disposal Device for Microsatellite Using Electrodynamic Tape Tether Technology, 8<sup>th</sup> JAXA space debris workshop, 2018.
23. Nohmi, M.: Planned Mission and Operation Result of Nano-Satellite STARS-II, *AEROSPACE TECHNOLOGY JAPAN*, Vol. 14, pp. 53-58, 2015.
24. Ohkawa, Y., Okumura, T., Horikawa, Y., Miura, Y., Kawamoto, S., Inoue, K.: Field Emission Cathodes for an Electrodynamic Tether Experiment on the H-II Transfer Vehicle, *Trans. JSASS Space Tech. Japan*, Vol. 16 (2018) Issue 1 63-68.
25. NASA, State of the Art of Small Spacecraft Technology, <https://sst-soa.arc.nasa.gov/>, Last modified: 12. Passive Deorbit Systems (Last modified: March 28, 2018)
26. <https://www.nrl.navy.mil/sed/programs/tepce>

## CHAPTER 7 EVALUATING TRADEOFFS BETWEEN PMD OPTIONS

---

### KEY POINTS

This chapter summarizes a trade study for PMD options outlined in Chapters 5 and 6 to guide the selection of the best approach for a given satellite to comply with the debris mitigation guidelines. The potential capability of PMD options assessed have to be considered in tandem with their previous operational usage (i.e., technology readiness level) due to the 90% PMD success rate requirement.

A propulsive maneuver strategy is the only option that works reliably for all LEO orbits but it carries with it a large size, weight, and power (SWAP) burden.

Drag-augmentation devices are only viable below 800-1,000 km altitude and they impose a low to moderate SWAP penalty.

Solar sails provide a slow deorbiting capability above 1,000 km and below 800 km behave like a drag sail. Solar sails have proven useful for interplanetary applications but require attitude determination and control to function optimally in low Earth orbit (LEO).

Electrodynamic tethers (EDT), while having limited operational experience for deorbiting, hold promise for deorbiting effectiveness up to 1,000 km.

If a microsatellite is deemed to require a controlled re-entry then only a propulsion system has proven experience in this application.

---

### Introduction

Previous chapters provide a clear picture of engineering and performance characteristics for four major families of PMD options for microsatellites. As can be seen from the detailed reading of previous chapters, the determination of the best PMD strategies is affected by:

- mission orbit and requirements,
- satellite capabilities and physical characteristics such as size, weight, and power (SWAP),
- operational paradigms,
- cost and SWAP requirements,
- technology readiness level,
- operational complexity, and
- vulnerability of the PMD options to space environmental effects, to include orbital debris.

The interaction of mission parameters and PMD options will vary over time as technology and its implementation advances and regulations evolve.

### Pros and Cons of PMD Options

A summary of the post-mission disposal methods discussed in this document is given in Table 7-1 below. It lists general methods by category and sub-category, detailing implementation pros and cons.

**Table 7-1** The pros and cons of potential PMD strategies highlight the key issues a microsatellite designer/operator must address.

Disposal method	Pros	Cons
<b>1. Propulsion (chemical and electric)</b>	<ul style="list-style-type: none"> <li>- Direct control of disposal</li> <li>- Technically straightforward; high Technology Readiness Level (TRL)</li> <li>- Can perform collision avoidance and controlled re-entry</li> </ul>	<ul style="list-style-type: none"> <li>- Requires propulsion system on the satellite or additional propellant if a propulsion system was part of the design</li> <li>- Requires high reliability of propulsion system and attitude control (to end of mission or beyond)</li> </ul>
1.a Single-burn to lower perigee (chemical propulsion)	<ul style="list-style-type: none"> <li>- Less operationally complex than 2-burn disposal</li> <li>- Transiting populated altitudes can reduce collision probability over near-circular transit though those altitudes</li> </ul>	<ul style="list-style-type: none"> <li>- Satellite traverses a wider range of altitudes</li> <li>- Less efficient if thruster firing is prolonged</li> </ul>
1.b Two-burn Hohmann transfer to lower circular orbit (chemical propulsion)	<ul style="list-style-type: none"> <li>- Can quickly traverse populated or sensitive altitudes</li> </ul>	<ul style="list-style-type: none"> <li>- More operationally complex than single burn</li> </ul>
1.c Electric Propulsion spiral	<ul style="list-style-type: none"> <li>- Reduces deorbit time over multi-burn approach</li> </ul>	<ul style="list-style-type: none"> <li>- Must maintain control of system for extended post-mission maneuvering time</li> </ul>
1.d Electric Propulsion multi-burn	<ul style="list-style-type: none"> <li>- Can reduce <math>\Delta V</math> requirements relative to spiral deorbit</li> </ul>	<ul style="list-style-type: none"> <li>- Must maintain control of system for extended post-mission maneuvering time</li> </ul>

Disposal method	Pros	Cons
<b>2. Drag-Augmentation</b>	<ul style="list-style-type: none"> <li>- Satellite does not need to be active for much, if any, of the post-mission decay</li> <li>- Can be designed to automatically deploy if a satellite failure occurs</li> </ul>	<ul style="list-style-type: none"> <li>- Requires a deployment mechanism sufficiently reliable to function at end of mission</li> <li>- Materials of device must survive extended exposure to space environment</li> <li>- Increases collision probability once device is deployed (may be more than compensated for by shorter lifetime)</li> <li>- Must be able to survive increased probability of debris impacts</li> <li>- Cannot perform controlled re-entry</li> </ul>
2.a Flat drag sail	<ul style="list-style-type: none"> <li>- Generally, have lower mass and stowed volume than inflatables</li> <li>- Generally, less mechanically complex than inflatables</li> </ul>	<ul style="list-style-type: none"> <li>- Effectiveness is dependent on orientation</li> </ul>
2.b Three-dimensional drag sail	<ul style="list-style-type: none"> <li>- Effectiveness of independent satellite orientation</li> </ul>	<ul style="list-style-type: none"> <li>- Potentially, more complex engineering</li> </ul>
2.c Inflatable gossamer devices (balloons)	<ul style="list-style-type: none"> <li>- Effectiveness independent of satellite orientation</li> </ul>	<ul style="list-style-type: none"> <li>- Must have technique to maintain shape over entire decay period</li> <li>- Generally, have greater mass and stowed volume than sails</li> </ul>
2.d Use existing satellite structures as drag-augmentation devices	<ul style="list-style-type: none"> <li>- Does not require separate device</li> </ul>	<ul style="list-style-type: none"> <li>- May cause significant additional design complexity</li> </ul>
<b>3. Solar sail</b>	<ul style="list-style-type: none"> <li>- Lightweight structure</li> <li>- Can be employed at higher LEO altitudes</li> </ul>	<ul style="list-style-type: none"> <li>- Small force available per area</li> <li>- Requires attitude control throughout post-mission decay</li> <li>- Cannot perform controlled re-entry</li> </ul>
3.a Class 1: quasi-rigid booms	<ul style="list-style-type: none"> <li>- Higher operational reliability</li> <li>- Can maintain 3-axis stabilization</li> </ul>	

Disposal method	Pros	Cons
3.b Class 2: spin stabilized	- Better stability from external torques	- Requires power to maintain spin
<b>4. Electrodynamic tether (EDT)</b>	<ul style="list-style-type: none"> <li>- Tends to stabilize orientation via gravity-gradient so location of device on satellite not important, however, this is subject to some constraints such as disturbing torques</li> <li>- Potential for limited controlled re-entry</li> </ul>	<ul style="list-style-type: none"> <li>- Inefficient at high inclinations (&gt;60 °) and altitudes (&gt;1,000 km)</li> <li>- Vulnerable to debris impacts (possible mitigation with tether design)</li> <li>- Can increase collision risk (may be compensated for by decreased lifetime)</li> <li>- Complexity of mechanical system</li> <li>- Low operational maturity</li> </ul>
4.a Passive EDT	<ul style="list-style-type: none"> <li>- Simpler and, therefore more reliable since no need of electron emitter.</li> <li>- Lighter than active EDT</li> </ul>	- Most effective for smaller than 100 kg satellites in low inclination orbits
4.b Active EDT	<ul style="list-style-type: none"> <li>- Able to deorbit faster than passive EDT</li> <li>- Able to de-orbit heavier satellites on higher inclination orbits</li> </ul>	<ul style="list-style-type: none"> <li>- Heavier than passive EDT</li> <li>- Need of small electron emitter that requires electric power and operation</li> </ul>

The most technically developed solutions are those associated with the use of propulsion systems and provide a number of advantages if a propulsion system is already a part of the spacecraft design. Depending on the mission orbit and propulsion system technology, there may be penalties in terms of required fuel. The effectiveness of the other PMD options is more strongly dependent on mission orbits (i.e., altitude and inclination). The availability of commercially-produced and space-tested hardware will affect both cost and reliability and will change over time.

### Engineering Tradeoffs of PMD Options

Table 7-1 quantifies some of the characteristics for the disposal options listed in Table 7-1. The results use a baseline set of characteristics to facilitate the comparison between PMD options for four specific, but diverse, mission scenarios. The integrated collision risk is important as this represents the collision hazard posed by the microsatellite during the de-orbiting process. While collision risk is not explicitly part of the debris mitigation guidelines, it is important to consider this on a final decision for a PMD selection.

For the scenarios in Table 7-1, the drag sails act as solar sails above 800 km. All propulsive maneuver scenarios drop the perigee to 400 km to attain an orbit compliant to the 25-year rule.

**Table 7-1** A quantitative comparison of PMD approaches for four representative mission scenarios shows that there is not a single perfect one-size-fits-all PMD solution.

		3U / 5 kg @700 km, 65° inclination	100 kg/ 1 m <sup>2</sup> @700 km SSO	100 kg/ 1 m <sup>2</sup> @800 km SSO	100 kg / 1 m <sup>2</sup> @1,000 km, 90° inclination
No deorbit	Lifetime	80 yr	~50 yr	>150 yr	>800 yr
	Integrated Collision Risk	1.70E-05	4.00E-04	2.30E-03	1.00E-02
Cold Gas <i>Lower Perigee Specific Impulse = 60 s</i>	Lifetime	25 yr	25 yr	25 yr	25 yr
	$\Delta V$ [m/s]	42	28	67	133
	Consumed Mass [kg]	0.35	4.7	11	20
	Integrated Collision Risk	3.00E-06	1.60E-04	1.80E-04	2.20E-04
Electric Propulsion <i>Specific Impulse = 1600 s Total Thrust = 40 mN</i>	Lifetime	25 yr	25 yr	25 yr	25 yr
	$\Delta V$ [m/s]	47	30	82	182
	Thrust Duration [h]	1.63	21	56	125
	Consumed Mass [kg]	0.015	0.20	0.52	1.15
	Integrated Collision Risk	3.00E-06	1.60E-04	1.70E-04	2.00E-04
Drag-Augmentation Device <i>Gossamer Device</i>	Lifetime	25 yr	25 yr	25 yr	25 yr
	Cross sectional surface [m <sup>2</sup> ]	0.1	2	6	40
	Integrated Collision Risk	1.60E-05	4.00E-04	8.00E-04	1.30E-02
Drag-Augmentation Device <i>Stabilized Drag Sail</i>	Lifetime	25 yr	25 yr	25 yr	25 yr
	Cross sectional surface [m <sup>2</sup> ]	0.1	2	6	40
	Integrated Collision Risk	1.60E-05	4.00E-04	8.00E-04	1.30E-02
Drag-Augmentation Device <i>Tumbling Drag Sail</i>	Lifetime	25 yr	25 yr	25 yr	25 yr
	Cross sectional surface [m <sup>2</sup> ]	0.1	2	6	40
	Drag sail surface [m <sup>2</sup> ]	0.25	4	12	81
	Integrated Collision Risk	1.60E-05	4.00E-04	8.00E-04	1.30E-02
Passive EDT	Lifetime	25 yr	25 yr	25 yr	25 yr
	Tether length [m]	12	120	320	340
	Tether width [mm]	10	25	25	100
	Increment of drag surface [m <sup>2</sup> ]	0.12	3	8	34
	Integrated Collision Risk	2.46E-05	8.43E-04	1.19E-03	1.14E-02

The integrated collision risk considers both the original body and the increased cross-sectional area of the PMD devices. The way to consider the increment of cross-sectional area will depend on the de-orbit device used (i.e., replacing the original area for drag sail and gossamer device and increasing original area for tethers). The collision risks in the table do not consider the size of the impacting debris; this simplification may result in an underestimation of the integrated collision risk. The increased exposed area of the drag-augmentation devices, solar sails, and tethers will contribute to decreasing PMD reliability. However, there would likely not be much debris created from a debris impact since the drag-augmentation, solar sails, and tether devices have very low mass interacting with the debris hazard. As a result, the risk of a catastrophic debris collision with the original satellite, that could create a large amount of debris, will indeed be decreased with these devices decreasing the orbital lifetime of the primary satellite.

A debris impact on a PMD device, however, might degrade its effectiveness or render it useless. Thus, the reliability of a PMD option should be examined carefully.

The performance described in the tradeoff study summarized in Table 7-1 and Table 7-1 highlights several general observations:

- Satellite missions below 800 km have more available PMD options since drag can help removal and the altitude needed to move the system is less (i.e., closer to 615 km altitude).
- Between 800-1,000 km altitudes, there are several PMD approaches that can assist in the reduction of orbital lifetime with varying SWAP and operational complexity burdens. Note how any option other than propulsion poses significant integrated collision risk when trying to deorbit from above 800 km.
- Above 1,000 km altitude, only propulsive systems and solar sails are viable.
- While there have not been any detailed reliability discussions in the tradeoff analysis it may be reasonably assessed that approaches that have been used often and reliably in the past will be more reliable. The “most used” to “least used” for orbit moving are: first propulsion, then drag-augmentation, then solar sail, and lastly EDT.

### **Criteria for Assessing PMD Options**

The pros/cons of PMD options in Table 7-1 and the four mission scenarios detailed on Table 7-1 highlight five major issues that must be addressed by any PMD option:

- **EFFECTIVE:** Is it effective? Can the change in altitude be made by the approach selected? The higher the altitude, the more change is needed.
- **SWAP:** What size, weight, and power (SWAP) is required to implement a given PMD approach? Certain approaches have greater engineering requirements that require additional hardware, software, and controls to be deployed. Clearly, the smaller your satellite, the more likely that these requirements will be demanding.
- **RELIABILITY:** How reliable is the PMD option? The reliability required for PMD execution is at least 90% but evolving discussions are pushing likely reliability levels to 95% and even to 99%. This may limit PMD options for your use even further. This metric is even more challenging when it is likely that many of these PMD devices will be activated after having been on-orbit for many years.

- **ORBITAL RISK:** Does executing a given PMD strategy actually create more risk? This is examined as the area-time-product for collision risk but also includes issues of potential debris generation during a PMD device deployment (e.g., tether release or deployment of a drag-augmentation device).
- **GROUND RISK:** Does the given satellite pose a hazard above the accepted  $10^{-4}$  probability of casualty on the ground? If you have to execute a controlled re-entry due to the potential of some of your hardware posing an impact risk to people on the ground, this will likely limit your PMD option to a propulsive system with assured attitude control until re-entry.

## References

1. Palla, C. and Kingston, J., "Forecast analysis on satellites that need de-orbit technologies: future scenarios for passive de-orbit devices," CEAS Space J (2016) 8:191-200.
2. Kerr, E., Macdonald, M., and Voigt, P., "Taxonomy and Analysis of Issues Facing Post Mission Disposal Concept," 68<sup>th</sup> International Astronautical Congress (IAC), Adelaide, Australia, 25-29 September, 2017.

## **APPENDICES**

- A. Tools to Assist in Debris Mitigation Guideline Compliance
- B. List of Acronyms

## Appendix A. Tools to Assist in Debris Mitigation Guideline Compliance

**DAS (Debris Assessment Software):** <https://orbitaldebris.jsc.nasa.gov/mitigation/das.html>

DAS is designed to assist NASA programs in performing orbital debris assessments, as described in NASA Technical Standard 8719.14, *Process for Limiting Orbital Debris*.

**DRAMA (Debris Risk Assessment and Mitigation Analysis):** <https://sdup.esoc.esa.int>

DRAMA (Debris Risk Assessment and Mitigation Analysis) is a comprehensive tool for the compliance analysis of a space mission with space debris mitigation standards. For a given space mission, DRAMA allows analysis of:

- Debris and meteoroid impact flux levels (at user-defined size regimes)
- Collision avoidance manoeuvre frequencies for a given spacecraft and a project-specific accepted risk level
- Re-orbit and de-orbit fuel requirements for a given initial orbit and disposal scenario
- Geometric cross-section computations
- Re-entry survival predictions for a given object of user-defined components
- The associated risk on ground for at the resulting impact ground swath

The suite consists of five tools, which are integrated into a graphical user interface. The tools are

- ARES: *Assessment of Risk Event Statistics* (developed by DEIMOS Space S.L.U),
- MIDAS: *MASTER(-based) Impact Flux and Damage Assessment* (developed by Space Systems),
- OSCAR: *Orbital Spacecraft Active Removal* (developed by Space Systems),
- CROC: *Cross Section of Complex Bodies* (developed by DEIMOS Space S.L.U),
- SARA: *Bodies (Re-Entry) Survival and Risk Analysis* (maintained by ESOC/ESA).

**STELA (Semi-analytic Tool for End of Life Analysis):** <https://logiciels.cnes.fr/en/content/stela>

The Semi-analytic Tool for End of Life Analysis (STELA) has been procured by *CNES* (The French Space Agency) to support the *French Space Operations Act*. It reflects the standard concerning the protection of *LEO* and *GEO* regions (lifetime and protected regions crossing of disposal orbits) and provides the user with tools to assess compliance with the requirements. The software allows efficient long-term propagation of *LEO*, *GEO*, and *GTO* based on a semi-analytical models and assessment of protected regions criteria. **STELA** produces a report file that summarizes the computation (spacecraft characteristics, initial and final orbits, computation parameters, criteria status) and optionally an ephemeris file.

**STK (Systems Toolkit):** <https://www.agi.com/products/engineering-tools>

Systems Tool Kit (STK) is a commercial software application for providing four-dimensional modeling, simulation, and analysis of objects from land, sea, air, and space in order to evaluate system performance in real or simulated-time.

**ORSAT (Object Re-entry Survival Analysis Tool):**

<https://orbitaldebris.jsc.nasa.gov/reentry/orsat.html>

The Object Reentry Survival Analysis Tool (ORSAT) is the primary NASA computer code for predicting the re-entry survivability of satellite and launch vehicle upper stage components entering from orbital decay or from controlled entry. The prediction of survivability is required in order to determine the risk to humans on the ground.

**ORDEM (Orbital Debris Engineering Model):**

<https://orbitaldebris.jsc.nasa.gov/modeling/engrmodeling.html>

ORDEM 3.0 incorporates significant improvements over its predecessor, ORDEM2.0, which was released in 2001. For the first time, ORDEM includes uncertainties in the flux estimates. The model includes material density classes. It has also been extended to describe the orbital debris environment from low Earth orbit past geosynchronous orbit (100 to 40,000 km altitude). Incorporated in ORDEM 3.0 is a large set of observational data (both in-situ and ground-based) that reflect the current debris environment. These data cover the object size range from 10  $\mu\text{m}$  to 1 m. Analytical techniques (such as maximum likelihood estimation and Bayesian statistics) are employed to determine the orbit populations used to calculate population fluxes and their uncertainties. The model output lists fluxes of debris in half-decade size bins by distinct material characteristics (i.e., intact objects, high-, medium-, or low-material density objects, and NaK droplets) either by direction and velocity for an encompassing 'igloo' (for spacecraft) or by range bins (for a sensor beam on the Earth's surface), depending on the user's chosen operational mode.

**MASTER (Meteoroid and Space Debris Terrestrial Environment Reference):**

<https://sdup.esoc.esoc.esa.int>

MASTER (Meteoroid and Space Debris Terrestrial Environment Reference) has been developed for ESA and permits assessment of the debris or meteoroid flux imparted on a spacecraft on an arbitrary Earth orbit. The purpose of the ESA MASTER model is the realistic description of the natural and the man-made particulate environment of the Earth and the risk assessment via flux predictions on user defined target orbits. The incident flux due to the particulate environment of the Earth on user-defined target orbits is described down to impactor diameters of 1  $\mu\text{m}$ . Computer models have been used to simulate the generation of objects due to all known debris sources and their orbit evolution with time

**SCARAB (Spacecraft Atmospheric Re-Entry and Aerothermal Break-Up):**

<https://www.htg-gmbh.com/en/htg-gmbh/software/scarab/>

SCARAB was developed under ESA/ESOC contracts with support from other European and international partners. It is considered as operational software. SCARAB is a software tool allowing the analysis of mechanical and thermal destruction of spacecraft and other objects during re-entry (controlled or uncontrolled). The software development has evolved over time, based on lessons learned from preceding software versions, upgrades and specific requests on re-entry analysis performed for various spacecraft (ATV, ROSAT, BeppoSAX, TerraSAR-X, GOCE, Sentinel-1/2/3/5P, SWARM, Jason-CS, EnMAP, Cluster-II, Integral, Envisat, EarthCare, ISS, Tandem-L), and for the European launcher programs. Typical launch vehicle (or similar) re-entry applications have been: Ariane 5 cryogenic main stage EPC, Ariane 5 upper stage EPS/VEB, Ariane 5 upper stage ESC-A, VEGA Zefiro 9 and AVUM.

Source: Lips, Tobias, et al., “Re-entry Risk Assessment for Launchers – Development of the New SCARAB 3.1L”, in Proceedings of the 2<sup>nd</sup> IAASS Conference, ESA SP-645, July 2007

**DEBRISK:** <https://logiciels.cnes.fr/fr/content/debrisk>

The DEBRISK software is a tool of analysis of the ablation of the fragments of a spacecraft after its destruction in the entry into the atmosphere. It is based on a directed approach object in which the space vehicle is represented by a set of interconnected basic geometries. A structure of type parent-child allows to define the relations between these various objects. Every object is defined by its shape, its sizes, its mass and its material.

DEBRISK calculates at first the trajectory and the kinematics conditions of the global vehicle between the altitude of departure specified by the user and the altitude of fragmentation by considering a loss of solar array. Then, DEBRISK calculates the trajectory (between the altitude of fragmentation and the ground) and the possible ablation of the fragments of the vehicle. These fragments are defined by the user and can be grouped (included) in parent / child. Finally, DEBRISK calculates the casualty area of the surviving fragments.

## Appendix B. List of Acronyms

AGI	Analytical Graphics, Inc.
AIAA	American Institute of Aeronautics and Astronautics
AMR	area-to-mass ratio
ATP	area-time-product
ATV	Automated Transfer Vehicle (spacecraft, ESA)
AVUM	Attitude Vernier Upper Module (rocket stage, ESA)
BeppoSAX	X-Ray astronomy satellite (Italy/The Netherlands)
$C_D$	coefficient of drag
CFRP	carbon fibre-reinforced plastic
CGG	Cool Gas Generator
CLAES	Cryogenic Limb Array Etalon Spectrometer
CNES	Centre National d'Etudes Spatiales (Space Agency, France)
CoM	center of mass
CoP	center of pressure
COPUOS	Committee on the Peaceful Uses of Outer Space (United Nations)
COTS	Commercial off-the-shelf
DAS	Debris Assessment Software
DLR	Deutsche Luft- und Raumfahrtagentur (Space Agency, Germany)
DRAMA	(Space) Debris Risk Assessment and Mitigation Analysis (software tool)
ECOC	European Code of Conduct for Orbital Debris
ECSS	European Cooperation for Space Standardization
EDMS	European space Debris Mitigation Standard
EDT	electrodynamic tether
EnMAP	Environmental Mapping and Analysis Programme (spacecraft, Germany)

EOL	end of operational life
EPS/VEB	Storable Propellant Stage/Vehicle Equipment Bay (Ariane 5 upper stage)
ESC-A	Etage Supérieur Cryogénique-A (Ariane 5 upper stage)
ESA	European Space Agency
ESOC	European Space Operations Centre
EVOLVE	one-dimensional software tool, NASA
FEC	field emitter cathodes
FHST	Fixed Head Star Tracker
GEO	Geostationary Earth Orbit
GOCE	Gravity field and steady-state Ocean Circulation Explorer (spacecraft, ESA)
HPS	High Performance Space Structure Systems
HTG	Hyperschall Technologie Göttingen GmbH (Germany)
IAA	International Academy of Astronautics
IADC	Inter-Agency Space Debris Coordination Committee
IKAROS	Interplanetary Kite-craft Accelerated by Radiation Of the Sun (spacecraft, Japan)
ISO	International Organization for Standardization
ISO/TS	ISO/Technical Standard
ISS	International Space Station
Jason-CS	Jason-Continuity of Service (spacecraft, NOAA/NASA/ESA/CNES and others)
K-H	King-Hele
LEO	Low Earth Orbit
MAR	mass-to-area ratio
MASTER	Meteoroid and Space Debris Terrestrial Environment Reference
MMOD	micrometeoroids and orbital debris
MMS	Multi-Mission Modular Spacecraft

MSIS	Mass Spectrometer Incoherent Scatter (atmospheric density model)
NABEO	De-Orbit Nanosystem (drag sail system, Germany)
NaK	sodium-potassium
NASDA	National Space Development Agency of Japan
NASA	National Aeronautics and Space Administration (Space Agency, United States)
NEA	Near Earth Asteroid
ORDEM	Orbital Debris Engineering Model
ORSAT	Object Reentry Survival Analysis Tool
OSCAR	Orbital SpaceCraft Active Removal
PMD	post-mission disposal
RTN	radial-transverse-normal
ROSAT	Röntgensatellit-X Rays (satellite, Germany)
SARA	Survival And Risk Analysis
S/C	spacecraft
SCARAB	Spacecraft Atmospheric Re-Entry and Aerothermal Break-Up
SRP	solar radiation pressure
SSO	sun-synchronous orbit
STARS-II	Space Tethered Autonomous Robotic Satellite (spacecraft, Japan)
STELA	Semi-analytic Tool for End of Life Analysis
STK	Systems Tool Kit
STK LOP	STK-Long-term Orbit Propagator
STS	Space Transport System (Space Shuttle, United States)
STSC	Scientific and Technical Sub-Committee (UN COPUOS)
SWAP	size, weight, and power
SWARM	name of spacecraft system (ESA)

TEPCE	Tether Electrodynamics Propulsion CubeSat Experiment
TerraSAR-X	Terra- Synthetic Aperture Radar-X Rays (Spacecraft, Germany)
TRAC	Triangular Rollable and Collapsible
TRL	Technology Readiness Level
UARS	Upper Atmosphere Research Satellite (United States)
UMA	Umbilical Mechanism Assembly
UN	United Nations
VEGA	name of ESA launch vehicle, Vettore Europeo di Generazione Avanzata